Synthesis, Characterization and Potential Applications of 4,4-Nitrophenoxyaniline based novel azo dyes and esters

Submitted

by

Samina Qamar
Reg. No.02061611009
Department of Chemistry
Quaid-i-Azam University
Islamabad
2016-18

Synthesis, Characterization and Potential Application of 4,4-Nitrophenoxyaniline based novel azo dyes and esters

A dissertation submitted to the Department of Chemistry, Quaid-i-Azam University, Islamabad, in partial fulfillment of requirements for the degree

of

Master of Philosophy

in

Inorganic/Analytical Chemistry

Submitted by

Samina Qamar
Department of Chemistry

Quaid-i-Azam University

Islamabad

2016-18


بِسْمِ اللَّهِ الرَّحْمَٰنِ الرَّحِيمِ

DEDICATED TO MY SISTER

IQRA

(Most precious gift from ALLAH)

ACKNOWLEDGEMENTS

All praises for **Allah Almighty,** for being with me all the way and giving us the perfect code of life through His beloved prophet **Hazrat Muhamad Mustafa (S.A.W).**

I consider myself very fortunate to work under the inspiring supervision of **Prof. Dr. Zareen Akhter** without her guidance, dedication and personal attention, this tedious work was not possible.

I would like to forward my depth of gratitude to **Prof. Dr.Muhammad Siddique** (Chairman of Chemistry Department) and **Prof. Dr. Amin Badshah** (Head of Inorg/Anal Chemistry) for providing necessary research facilities, nice attitude and constant support.

I am indebted to my parents for their love, encouragement and support. I am thankful to my family members my brothers **(Waqas and Junaid**) and my sisters (**Rubina, Iqra and Sawera**) for their love and moral corporation.

My special thanks to my friends **Rubab, Nimrah, Sara, Maida, Saima, Shaista** and **Javaria** for supporting me emotionally during this important phase of life.

Finally, I would like to acknowledge all the technical staff of Chemistry department during the experimental work of my research.

SAMINA QAMAR

List of schemes

List of figures

List of tables

Glossary

b.p.	Boiling point
Cp	Cyclopentadienyliron
DMSO	N,N'- Dimethylsulphoxide
DMF	N,N'-Dimethylformamide
THF	Tetrahydrofuran
M.p.	Melting point
NMR	Nuclear magnetic resonance
FT-IR	Fourier transform Infrared
UV	Ultraviolet
DPPH	2,2-Diphenyl-1-picrylhydrazyl
Fc	Ferrocene
µM	Micro molar
TLC	Thin layer chromatography

Table of Contents

ABSTRACT

Azo compounds have gained immense importance because of its preparative convenience and wide range of applications. Five azo alcohols were synthesized successfully by using diazotization coupling reaction and two series of esters were prepared by low temperature condensation method. Ferrocenyl esters were produced using 4-ferrocenyl benzoyl chloride as precursor. Physical properties of the both series of compound were studied. Further alcohol and ester linkages were confirmed using characterization techniques like IR, NMR and single crystal analysis. Chemosensing property and photoisomerization potential of the compound were also investigated. DNA binding studies were done through UV-VIS spectroscopy. Antioxidant properties of these compounds were determined by DPPH free radical and hydrogen per oxide scavenging activity. The results of these studies showed that some of these compounds can be successfully used as potential DNA –binders and antioxidant.

INTRODUCTION CHAPTER 1

Azo-dyes are versatile and highly known compounds comprise of at least one conjugated azo chromophoric (-N=N-) group in connection with one or more heterocyclic or aromatic structure, which can results in full diversity of colors.[1] A general azo containing compound is shown in Fig 1.1 where R_1 and R_2 can be same or different.

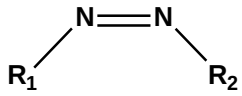

Fig 1.1: General representation of azo group

The properties of such compounds like enhanced tinctorial strength and brightness as compare to other aromatic system are responsible for their long term use as colorants.[2] Since their invention in 19^{th} century, round about 3100 different dyes are industrially being used which are enough to accommodate 50% color need of the population.[3]

Azo derivatives in which azo (-N=N-) group connects two phenyl rings are commonly termed as azo benzene. These compounds are under higher consideration in both fundamental and applied research areas. Further substitution of phenyl ring results in strong electronic absorption, that leads to fall in anywhere from UV to Visible region. The greater stability of the azo group leads to an increase in interest in the study of dyes.[4]

The azobenzene derivatives are most extensively used array of dyes regarding their diverse application in copious fields, such as in textile dyeing, food coloring industries, biomedical investigations and the most promising applications in organic synthesis. In addition to these, azo derivatives also have demands in high technical areas such as chemosensors, electro-optical devices, liquid crystalline displays, optical memory storage devices and ink jet-printers. [5]

Showing geometrical and electronical switching upon irradiation of external stimuli also let azobenzene derivative to exhibit stimulus responsive properties. They are responsive towards external stimuli by showing changes in their properties.[6] External stimuli include variation in temperature, pH, light intensity, magnetic field and variation in ionic

strength of the media. Depending upon multi responsive property of the azo compounds they are also termed as environmental responsive or smart material.[7] These materials have numerous applications in catalysis, drug delivery system and also in biotechnology.
The azo benzene having hydroxyl group at ortho position of azo group also have tendency to show tautomerism. The tautomers comprise of two different geometric form of the same chemical formula having enormous applications in various fields. Beside this arenediazonium salts also provide site for grafting of organic molecule on metallic or nonmetallic surfaces enabling them to be used in optoelectronics and nano-manipulations.[8]

1 Chemical attributes of azo dye

1.1: Photoisomerization:

Generally photoisomerization is defined as the conversion of isomers into one another upon photochemical or thermal stimulation. This phenomenon is extensively studied in azobenzene derivatives.[9]

Azobenzene has two isomeric forms which exhibit different physical and chemical attributes depending upon various spatial arrangements. Thermodynamically, trans form is 50 kJ/mol more stable than cis form. Upon irradiation of UV light, azobenzene moiety goes from its more thermally stable trans form to less meta-stable cis form as shown in Fig 1.2.Typically cis configuration relax back to thermally stable trans form after a time period which critically depends upon environmental conditions and substitutions on azo group.[10]

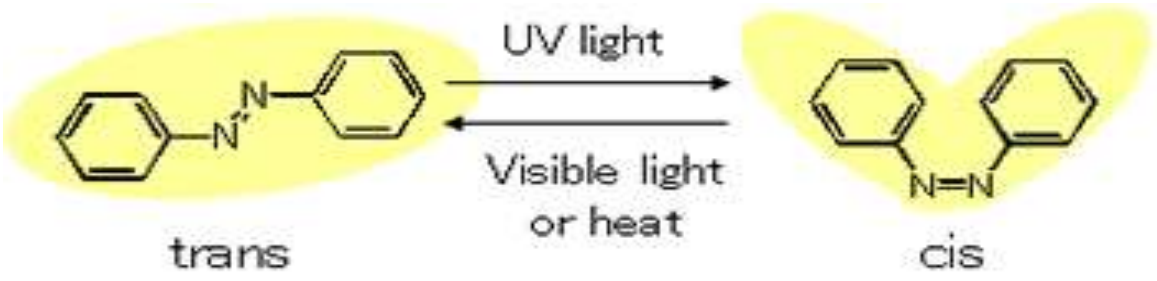

Fig 1.2 Photoisomerization of azobenzene

Significant changes in geometry and dipole of azo group have been illustrated during this phenomenon leading to enhance their potential use in photo controlling properties of the materials. Photo-switching property of azobenzene has also provoked their potent use in various biological applications. Currently this property is extensively used to study the thermal regulation of protein conformations, nucleic acid functionality and enzymatic activities.[11]

Literature studies have also revealed the fact that cis trans isomerzation property could be employed to design and manufacture novel photoactive substances based on liquid crystals and micro-displays.[12]

The transition metal if conjugated with azo group also imparts variety of new molecular functions, due to the mutual effect of photoisomerization of azo-chromophore and variation in optical, magnetic and redox properties arising from d electron of the metal. Numerous azo conjugated metal complexes and compounds have been illustrated to show some novel behavior which were not observed in pure organic moieties, such as metal ligand charge transfer photoisomerization and single light redox isomerization.[13]

1.2 Tautomerism:

Tautomerism is one of the class of structural isomerism, which involves exchange of hydrogen atom within the same molecule. Increasing number of tautomers and their potential practical applications have captured the attention of many scientists leading to large number of published articles in this period (Fig:1.3) using both theoretical and experimental approaches.[14]

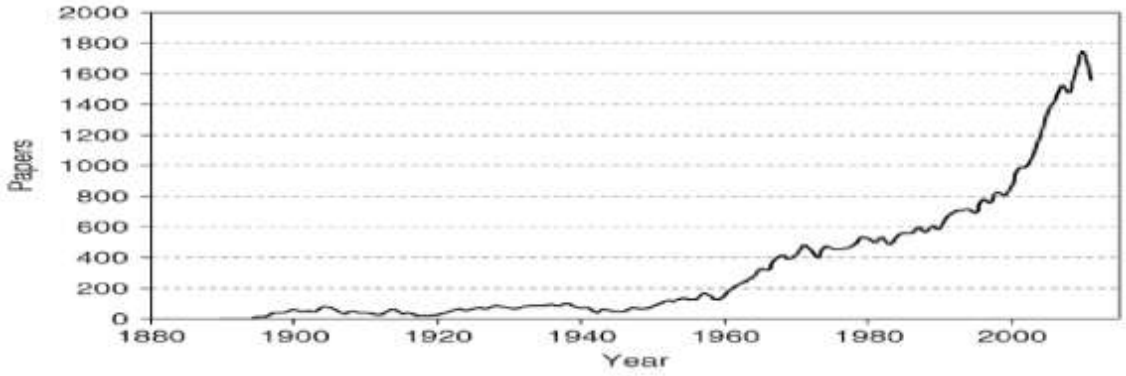

Fig 1.3: Numbers of published tautomerism articles as a function of time

This emerging trends shows that tautomers have significant technical applications in various emerging and developing fields. Azo derivatives which have hydroxyl group at ortho or para position also have capability to show the azo-hydrazone tautomerism by exchanging position of alpha proton.[15] Equilibrium established between two forms is controlled by acid or basic attribute of the species. A simple example of tautomerism in hydroxyl containing azo dye is shown in Fig 1.4

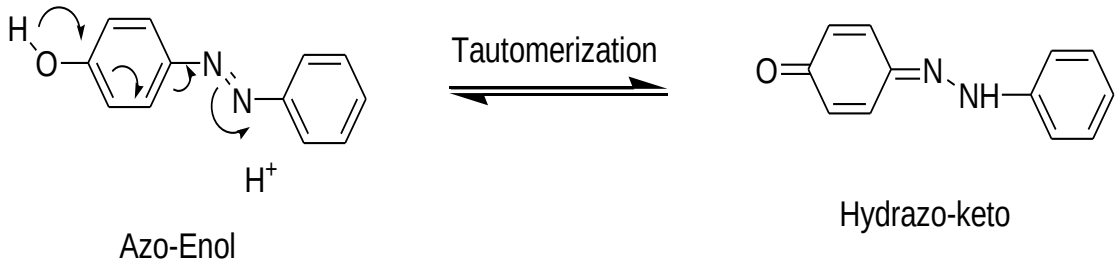

Fig 1.4 Azo-hydazone tautomerism

Tautomerism is vibrant and potentially reversible in nature; causes rearrangement of structural pattern as well as electronic density of organic dye, which lead to significant change in chemical and physical properties of the tautomers. Based on these varying property keto-enol tautomers are found to have enormous application in variety of fields such as optical signal monitoring, telecommunication, ion detectors, laser technology, optical switches molecular date processing and many biological applications.[16]

From many years determination of factors affecting azo-hydrazone tautomerism both in liquid and solid state has become a challenging point for the scientist regarding their emerging technical applications. Literature review has shown that tautomerism is not dependent only on a single entity but in actual it is controlled by many factors.

1.2.1 Hydrogen bonding:

Hydrogen boding holds very decisive role in tautomerism. As intramolecular hydrogen bonding leads to predomination of keto form by involving hydrazone proton in bonding as shown in Fig 1.5. In the given example rate of forward reaction is faster than reverse. K_f and K_r are equilibrium constant for forward or reverse reaction respectively. K_f>K

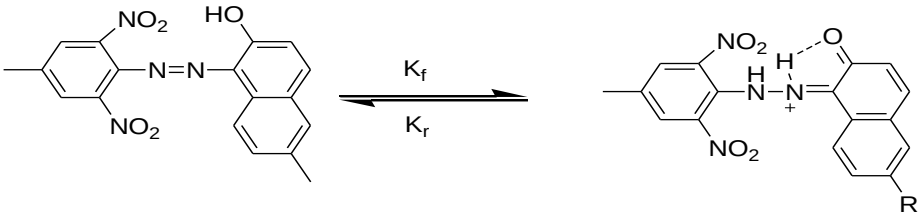

Fig 1.5 Effect of intramolecular hydrogen bonding

Whereas intermolecular hydrogen bonding favors enol form by linking complete units with one another.[17]

1.2.2 Effect of solvents:

In addition to hydrogen bonding, nature of the solvent also significantly affects the comparative stability of the tautomers. Increased polarity of the solvent leads to formation of hydrazo-keto form owing intramolecular hydrogen bonding and disturbing intermolecular hydrogen bonding. Opposite effect has been observed for non polar solvents**.**[18] Spectroscopic techniques, most commonly UV is used to illustrate the effect of solvents on the tautomerism. Red shift is observed for Keto form due to increased conjugation as depicted by the Fig 1.6

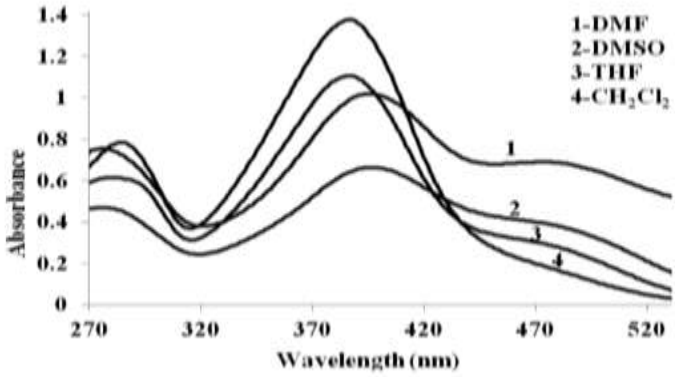

Fig 1.6: Effect of the solvent on relative stability of tautomers

1.2.3 Effect of pH:

Profound effect of pH has been observed on tautomerism as well. At increased pH higher concentration of OH^{-1} ion causes the removal of labile proton involve in intramolecular hydrogen bonding, thus favouring the enol form. However at neutral pH keto form

predominates. [19-21]

1.2.4 Effect of temperature:

Temperature has also sound effect on tautomerism[22]. As high temperature enhances the kinetic energy of the reaction, which in turn disturbs the intermolecular hydrogen bonding of azo molecules, ensuring hydrazone as dominant tautomer.

1.2.5 Effect of substituent:

Resonance and inductive effect of various substituents on the dye also have profound effect in stabilizing relative tautomeric form of dye. Electron denoting substituent favors the enol form by increasing electronic cloud in structural skeleton of azo dye whereas reverse phenomenon is observed with electron withdrawing substituent[22]

1.3 Chemosensing attributes:

Chemosensors are the class of compounds which show variation in physical and chemical attributes upon interacting with an analyte that may be ion, compound or variable hydrogen ion concentration. From previous decades azo dyes are being used as pH sensors.

Most common example is Azo violet (indicator) which shows yellow and violet color in different pH.[23]

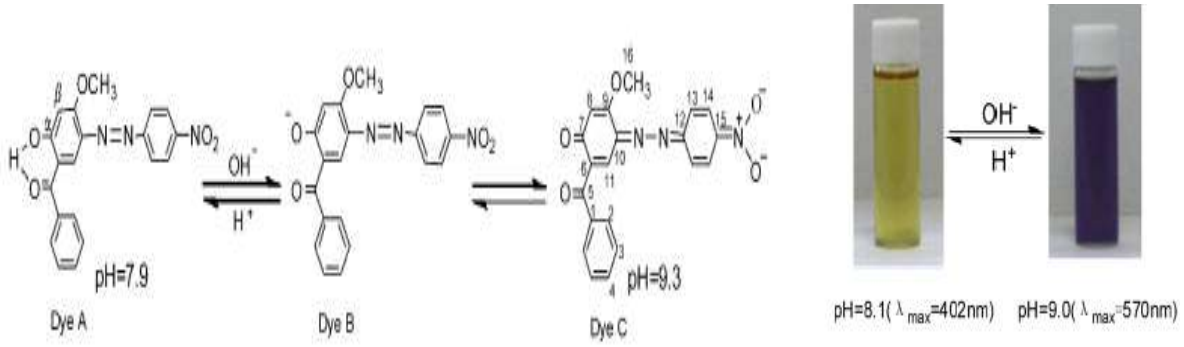

Fig 1.7 Mechanism of chemosensor having nitro group as substituent

In case of azo alcohol this chemical characteristic is attributed to the presence of OH group along with the phenyl ring and azo chromophore. Upon increasing pH, transformation between the phenol (acidic media) and phenolate (basic media) introduces new extended delocalization which results significant change in optical properties. The substituents

present in chemical structure also play a great role in the chemistry of these molecules. Electron withdrawing groups like e.g (NO_2) leads to enhancement of delocalization but reverse is observed for electron denoting substituent as shown in Fig 1.7 and 1.8.

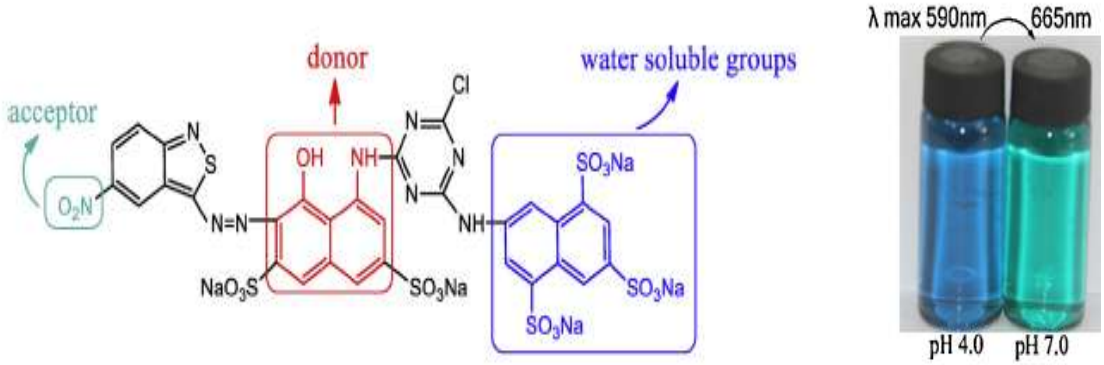

Fig 1.8 Water soluble chemosensor (sensitive in acidic media)

1.4 Synthetic procedure of azo dyes:

Dyes and pigment are usually synthesized by azo coupling reaction. Azo coupling reaction engross two essential steps, one the formation of aryldiazonium salt from aniline and second coupling with aromatic moiety.

First step:

Diazonium salt is highly unstable and a somewhat flammable in dried form, therefore it is always synthesized at 0°C. This salt comes out when aniline react with sodium nitrite under acidic condition. In actual, sodium nitrite ($NaNO_2$) react with HCl to form nitrous acid, which deprotonate to form nitrosonium ion.

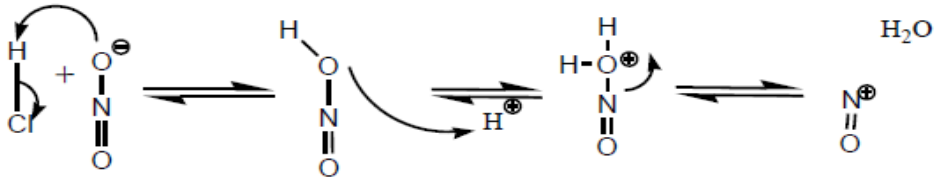

Nitrosonium ion is then attacked by nucleophilic aromatic amines and results into nitrosamine as shown in above scheme.

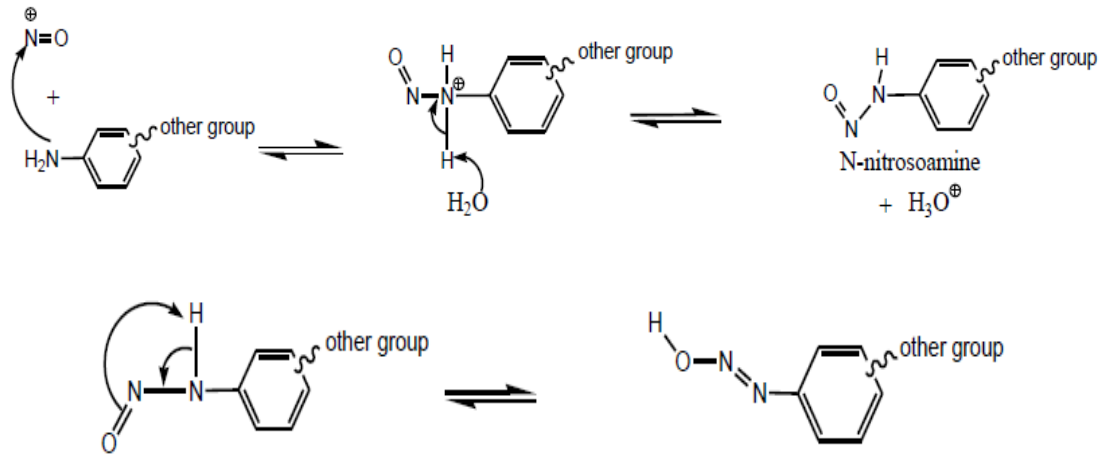

Further removal of proton occur in acidic condition which results in the production of diazonium salt which is instantly used in the second step to avoid the formation of phenol by reacting with water.

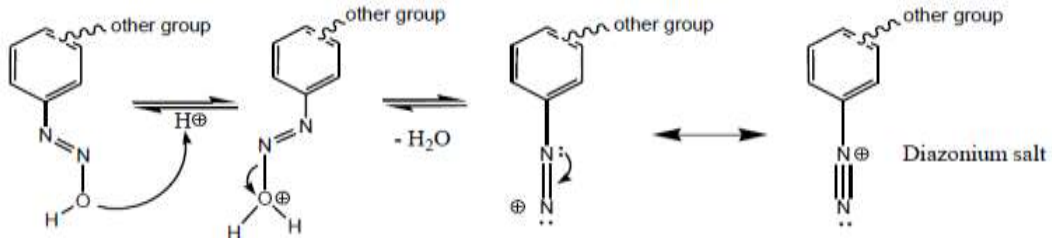

Second Step:

Second step involves the coupling of diazonium salt with electron – rich entity like phenol and napthol through aromatic substitution mechanism. Diazonium salts are mostly directed towards the para position of nucleophilic entity, unless it is occupied and not available for bonding.

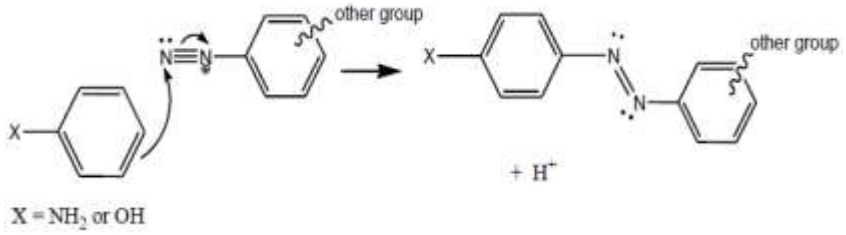

1.5 Attributes of esters:

In 19th century Leopold Gmelin first introduced the term of ester in Germany. Esters are distinctive assemblage of molecules which enclose a specific functional moiety called ester group, accompanying general formula as RCOOR′ as shown in Fig 1.9. This R can be organic or inorganic moiety.

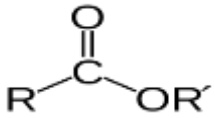

Fig 1.9: General formula of ester

Esters mostly occur naturally, but they can also be synthesized in labs artificially. Esters are generally synthesized by condensation of alcohols and carboxylic acid by using various methods depending upon conditions and availability. The word ester was designated by a common practice that the acid belongs to organic class, but esters can also be synthesized using inorganic acid. Adenosine triphosphate is typical example of inorganic ester commonly known as phosphate ester**.**

1.5.1 Physical properties:

Predominantly, esters are neutral compounds i.e they do not show any color change upon interacting litmus solution or phenophthalien indicator. Esters are more polar than ethers due to (=C=O) group in structural pattern but show less polarity than alcohols. Less polarity manifest poor chances of self assemblage in esters, as a result esters are more volatile in nature, in contrast to the acid of same molecular mass. Esters take part in hydrogen bonding residing again on the (C=O) moiety, but they act only as hydrogen bond acceptors not donors. This hydrogen bonding leads to increase in their solubility in water.

Esters mostly involve very low energy barrier toward the rotation about C-O-C bond, thus, enabling them to be flexible in nature and reduce rigidity.

1.5.2 Esterfication:

Esterfication is an important chemical reaction in organic synthesis. It simply involves the combination of two (acid and alcohols) moieties to give ester group with removal of the water. Because of excessive use of esters in fragrance, medicinel, plasticizer, micro-displays and chemical industry it is believed more than that 100 manufactures are preparing esters through esterfication. Condensation and steglich esterfication are the most common methods for ester formation

1.6 Azo esters

Depending on the fact that functional unit combinations are responsible for governing

chemical and physical properties of the molecules. Researchers have become successful in interlinking azo linkage with various functional group such as esters or methine (CH=N-) group, leading to the increase in commercial and potential application of azo-chromophore. Azo-esters have now become the most interesting research area integrating chemical and physical approaches. The involvement of double bond in structural framework increases the mesomorphic, liquid crystalline and photoisomeric properties of azo-chromophoric group. The ester group and rigid rod like structure of azo-chromophore align themselves in such a way to exhibit liquid crystalline property.

The study on ester containing azo-benzene, and their applications are focused by many researchers. In 2005 Mahmut and his coworker synthesized and characterized 4-acryloyloxy containing azo-esters and also studied their applications.[24] In **(**2010**)** Uhood and his coworkers synthesized number of azo-esters and studied the effect of substituents on their liquid crystalline property. Their studies illustrated that peripheral groups and their position have great role in controlling mesomorphic properties. One of the ester studied by this research group is shown in Fig 1.10 [25].

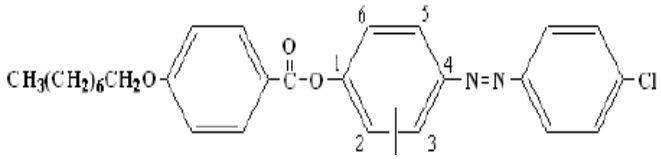

Fig 1.10 Azo-ester studied by Uhood and co workers

In 2010 a class of novel azo-ester and novel schiff bases has also been reported by B.T Thakar and his coworkers. In 2014, mesogenic azo derivatives have been synthesized and characterized by AK Parajapati in India.[26] Recently, (Fig 1.11) Jain and his coworkers also studied mesomorphic properties in newly synthesized Azo-esters and chalcone-esters [27]

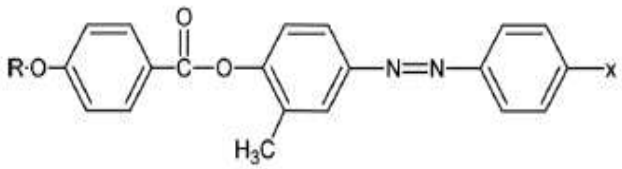

R = C_8H_{17} and $C_{16}H_{33}$, where X= -H, $-CH_3$, $-OCH_3$, -Cl, -Br, $-NO_2$

Fig 1.11: Series of azo-esters studied in 2016

1.7 Ferrocene:

Ferrocene is a stable organomettalic compound discovered in 1951 by Kaely and Pauson in an unsuccessful attempt for the formation of fulvalene. [28] (Fig 1.13) .

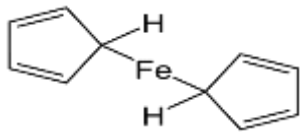

Fig 1.13 Ferrocene

Since its invention, it is being a continuous source of temptation for scientist regarding its fascinating properties. Ferrocene is orange crystalline solid in which Iron is sandwiched between two equidistant cyclopentadienyl ring providing it remarkably high stability and resistivity against moist, heat and air. It is soluble in many organic solvent e.g. dichloromethane, diethyether and benzene.

1.7.1 Structure:

Two common conformations **(Fig 1.14)** implied for ferrocene are staggered and eclipsed. X-ray diffraction studies suggest that staggered form with $D5_d$ symmetry is the more favorable. In some cases an intermediate structure having D5 symmetry has also observed showing a deviation of 9^0 from eclipsed conformation

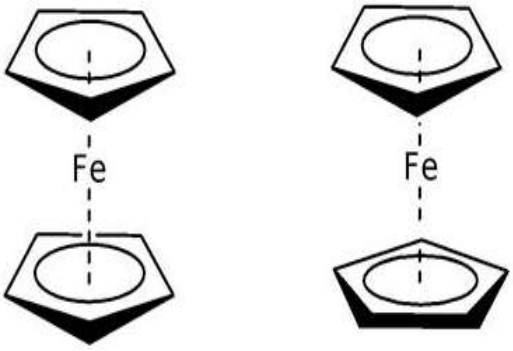

Eclipse or prismatic (D_{5h}) **Staggered or antiprismatic ($D5_d$)**

Fig 1.14 Different Conformations of Ferrocene

1.7.2 Chemical reactivity of ferrocene:

Besides high stability of ferrocene it also shows high reactivity towards number of chemical reactions. But these reactions do not disturb the aromaticity of the rings. The common reactions of which ferrocene can undergo are protonation, metallation, redox reactions and electrophilic substitution.

1.8 Ferrocenyl containing azo-esters

In recent years ferrocenyl containing azo ester have arisen as an emerging field of interest because of their mechanical and practical applications. The tremendous thermal stability and redox activity of ferrocene enhance the properties of azo-esters, enabling these compounds response electric and magnetic stimulation as well as to UV light exposure. The ferrocenyl azo esters greatly affect the liquid crystalline property of a material by affecting their mesomorphic behavior. A small variation in structural pattern, polarity, steric factors greatly affect the liquid crystalline temperature.

Very few literature on ferrocenyl liquid crystal with azo ester. Malthete and Billard have produced the preliminary series of ferrocene containing mesogens. In (2006) Apreutesei and his companions worked on the thermal stability of a number of ferrocene containing azo-ester, since as they exhibit high liquid crystalline property. [29]
Irina and his coworkers (Fig 1.15) synthesized novel ferrocene mesogens by condensation method in presence of DCC and DMAP which were mono substituted.

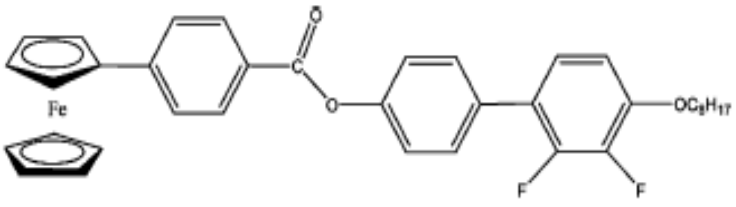

Fig 1.15: Ferrocenyl azo-ester

Roxanan and Irina synthesized two chains of ferrocene mesogens through the esterification of 4-ferrocenyl-4’-hydroxyazobenzene with substituted 4-hydroxybenzoic

acids in the presence of 4-dimethylaminopyridine and N,N'-dicyclohexylcarbodiimide as coupling agent.[30]

1.8 Applications of ferrocenyl derivatives:

1.8.1 Bioorganometallic chemistry:

The bioorganometallic chemistry of ferrocene and its derivatives is under consideration, it's actually correlates the conventional organometallic chemistry to biology, biotechnology and medicines.[31] The core feature in inducing the extraordinary characteristics to the biomolecules is accompanied by the presence of redox active metal center and extended conjugation.

Their immense role in biological field was not realized till the discovery of antitumor ferrocene derivatives. Recently large number of bio conjugates of ferrocene incorporating with aminoacids, DNA, RNA polymers have been studied and explored for many applications like catalytical, molecular sensing capability and nanolithography etc. [32]

1.8.2 Drug modification:

A large number of ferrocenyl derivatives have been screened for many biological activities due to their ease of synthesis and physiological properties. The modification of already existing drug with ferrocenyl moiety has been characterized to show up gradation in their activities. Recently, various amendments in structural pattern of drugs with ferrocene moiety have been reported

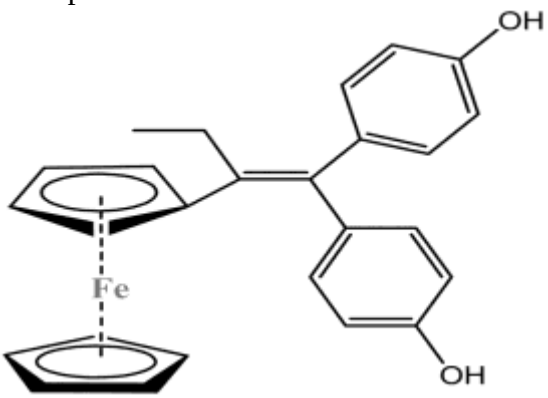

Fig 1.16 Derivative of tamixofen (Anti-cancer agent)

A common modification in structural pattern of drug is the replacement of aromatic moiety

with ferrocene as in ferrocene aspirin.[33] Ferrocifen is an anti-cancer drug commonly termed as tamixofen, as shown in Fig 1.16 Ferroquine is antimalarial drug obtained by modification in clohoroquine.[34]

1.8.3 Electrochemical devices:

The ferrocene derivative found to have tremendous applications in electrochemical devices relying on its redox properties. They are being used as sensors for the detections of anion and cations.[35] One emerging application of ferrocene is in form of self-assembled monolayer which is two dimensional aggregates showing active electrochemical property on metal surfaces.

1.8.4 Liquid crystalline property:

The aromatic moiety present in ferrocene activates the mesogenic part to enhance and tune the desired liquid crystalline property. A simple is shown in Fig 1.17

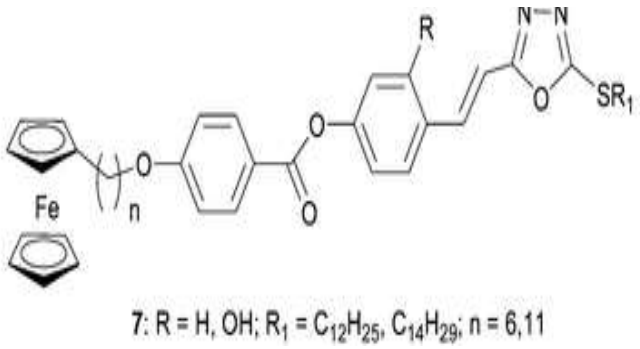

7: R = H, OH; $R_1 = C_{12}H_{25}, C_{14}H_{29}$; n = 6,11

Fig 1.17: Monosubstituted ferrocene mesogen with ester linkage

1.9 DNA interaction studies:

DNA is a building block of the entire organism without which concept of life is not even possible. It is playing role in many processes like storing and imitating of messages. Pictorial representation of DNA is shown in Fig 1.18

DNA binding studies have always been an important line of investigation for scientist relying on its significance in our life. These studies are vital to understand the mechanism of interaction of harmful chemicals with DNA and as well as to investigate and design

new site –specific drugs.

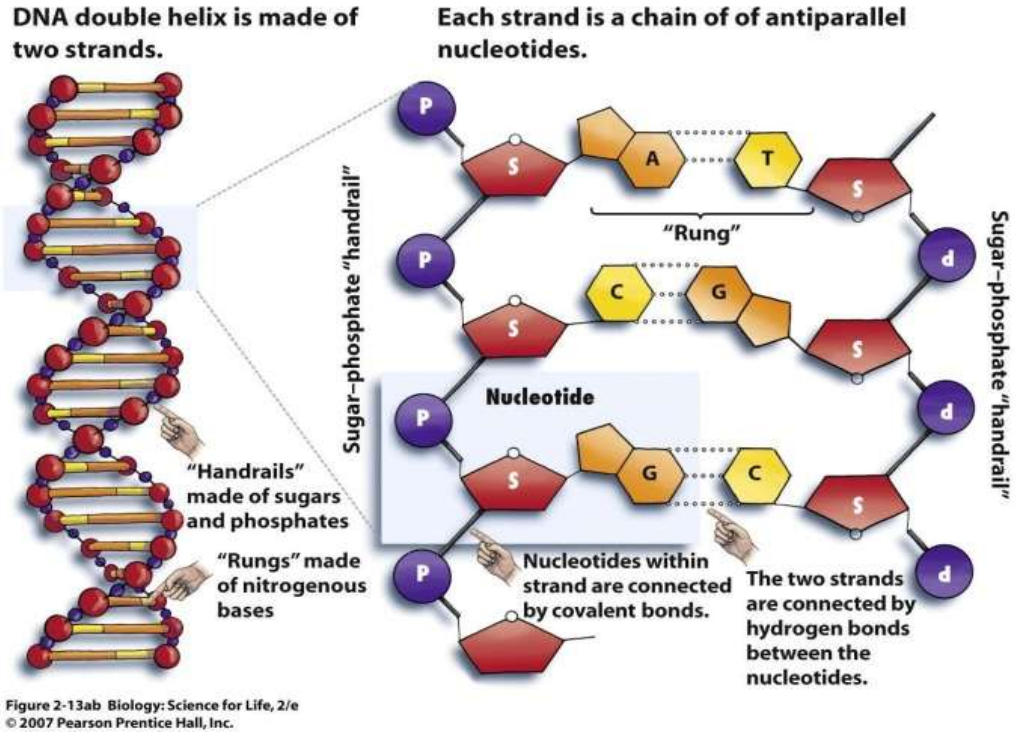

Fig 1.18 Pictorial representation of DNA

Concept of intercalative binding of DNA with molecule was first introduced by the Lermen. DNA binds with the drugs in covalent and non- covalent interaction. The non covalent mode of binding further have three types of modes

1 Intercalative

2 Groove binding

3 Electrostatic

Different spectroscopic techniques like UV – VIS and fluorescence are the most commonly used method to study the DNA-binding. Recently, electrochemical methods (Cyclic Voltametry) have also been developed to study DNA interaction**.**

1.10: Characterization methods:

1.10.1 Solubility

Solubility is the crucial factor in illustrating the applicability of the compound in variety

of useful applications. It mainly relies on various intrinsic and extrinsic factors like inter and intramolecular forces, types of functional groups present, temperature and pressure etc. It furnishes the useful information to be used in various spectroscopic techniques for solution formation of sample compound.

1.10.2 Infrared spectroscopy

Infrared spectroscopy also known as vibrational spectroscopy, that deals with the study of absorption of infrared radiation, which initiates vibrational transition in the molecule. It is frequently used in structure interpretation to determine the functional groups. The peak of specific functional groups present in corresponding region confirms the formation of the products. The wavelength range for IR is from 0.8 µm to 1000 µm which is further subdivided into three regions i.e. near IR, middle IR and far IR. Absorption of organic molecules is high in middle region that's why most of the analytical applications are limited to this region.

When IR radiations are irradiated to sample then, it produces the vibration between the atoms of the molecules. A peak is observed, when applied IR frequency becomes equal to natural frequency of vibration. As various functional groups absorb characteristic frequencies of IR radiation, so it gives individual peak value. The FTIR spectrum which comes as a result is a plot between % transmittance and wave number (cm^{-1}). FTIR spectrometers were used for trace samples without samples destruction and require least sample preparation, give high accuracy and reproducibility.[36]

1.10.3 Ultraviolet-Visible absorption spectroscopy

The UV-VIS absorption spectroscopy is concerned with the measurement of the reduction of beam of light as it passes through a sample or after reflection from a sample surface. It is can be frequently used for the detection of functional groups, impurities, drugs with chromophoric reagent, and the conjugation of the compounds without sample destruction.

The Ultraviolet region extends from 10 nm to 400 nm which is subdivided into two regions i.e. near UV region (200-400nm) and far UV region (below 200nm).[37] A

general principle of UV absorption spectroscopy is, when a sample is subjected to light energy, molecule would absorbed a fraction of this energy which causes electronic transition from lower to higher energy levels. UV absorption spectrum is a plot between absorbance and wavelength. Near ultraviolet-visible spectroscopy relates the excitation of valence electrons within an atom, where transitions between energy levels results in absorptions of energy at wavelengths below 100nm.[38]

1.10.4 Crystallography technique

Crystallography technique is used for the elucidation of the three dimensional structure of molecules at atomic resolution, including complex biological macromolecules such as proteins and nucleic acids. This technique, is frequently used for imaging of molecular structures with high resolution, when the molecules are arranged in a regular crystalline array[39]. When X-rays beam is fallen on crystal, it causes light to scattered into many specific directions. A crystallographer can produce a three dimensional picture of the density of electrons within the crystal from the angles and intensities of these scattered beams.

1.10.5 ^{1}H NMR spectroscopy

NMR spectroscopy originally developed, to investigate the different properties of atomic nuclei, Now this is frequently used to determine unique molecular structure of organic compounds after identification of carbon-hydrogen frameworks within molecules.

In the presence of applied magnetic field, the nuclei adjust themselves with or against the applied magnetic field while when there is no applied magnetic field the nuclei spins randomly. Depending on the strength of magnetic field, there are two energy states i.e. α-spin states have lower energy and are equivalent to the applied force while β –spin states have higher energy and antiparallel to the applied force.[40] The general principle of NMR spectroscopy is to fall the pulse of radio waves on sample causing resonance and when nuclei fall back to their lower energy state, the detector measures the energy released and a spectrum is recorded. Proton absorbs different frequencies in different environments which are distinguishable by NMR.

^{1}H NMR is more sensitive and has nearly 100% natural abundance. It determines the nonequivalent hydrogen in a compound. Equivalent hydrogens have same signals while nonequivalent have different signals and this may lead to additional splitting i.e. called diastereotopic effect.

1.11 Aim of research work:

The purpose of this research work was to synthesize and characterize azo alcohols and esters compounds having organic and as well as ferrocenyl moiety in their structural pattern. The biological and other practical application of reactants and products were also focus.

1.12 Outline of research work:

In a brief description complete research work consists of the following steps. First step involves the synthesis of 4-(4-nitrophenoxy) aniline according to reported method. Then formation of five hydroxyl containing azo dyes were synthesized by diazotization of 4-(4-nitrophenoxy)aniline and coupling with phenol and phenol derivatives. Furthermore these azo-ol were condensed with different acid to obtain azo-esters. Two acid chlorides i.e benzoyl chloride and 4-ferrocenyl benzoyl chloride were used for the condensation with alcohols.

1.12 PLAN OF WORK:

The objective of the present work was to accomplish the synthesis of azo functionalized dyes and their esters, and to elaborate the effect of various moieties on the properties of these compounds. In this regard, first, 4-(4-nitrophenoxy)aniline was synthesized (scheme 1) as precursor for Azo alcohols (scheme 2). Next benzoyl chloride and 4-Ferrocenyl benzoyl chloride were condensed with alcohols to get their respective esters (scheme 4 and 5)

Scheme 1 Synthesis of 4-(4-nitrophenoxy)aniline

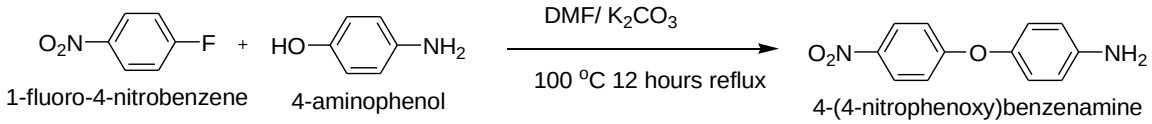

1-fluoro-4-nitrobenzene 4-aminophenol 4-(4-nitrophenoxy)benzenamine

Azo alcohols were synthesized by diazotization of 4-(4-Nitrophenoxy)anilineand then coupling with five different phenolic moieties.

Scheme 2: Synthesis of azo alcohols

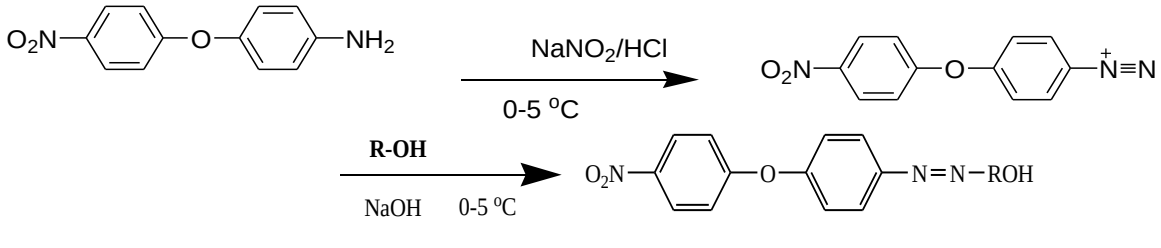

R=

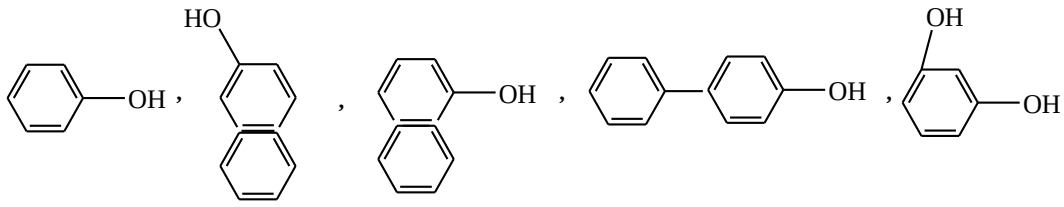

SQ1 **SQ2** **SQ3** **SQ4** **SQ5**

Scheme 2: Synthesis of azo esters

Organic esters were prepared by condensation of benzoyl chloride with azo alcohols according to the following scheme

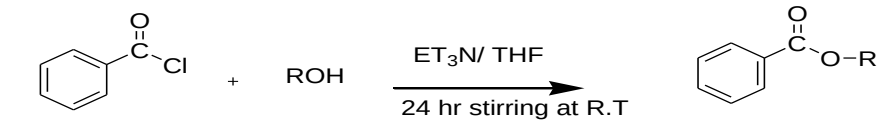

R=

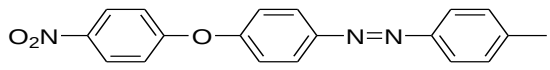

SQ1B

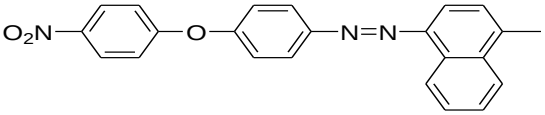

SQ3B

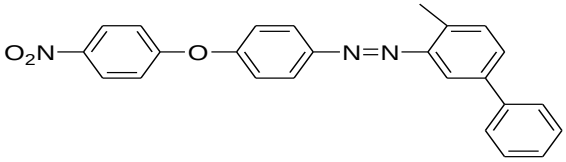

SQ4B

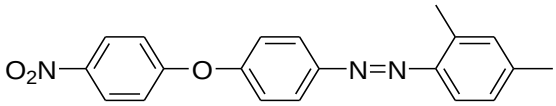

SQ5B

Scheme 3: Synthesis of 4-ferrocenyl benzoyl chloride

In order to get the ferrocene based ester, ferrocenyl benzoic acid was prepared to be use as starting material, which further reacted with $SOCl_2$ in to form 4-ferrocenyl benzoyl Chloride. Next, condensation of acid chloride with azo alcohols resulted in ferrocene based esters according to the following scheme.

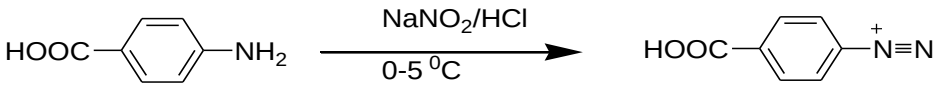

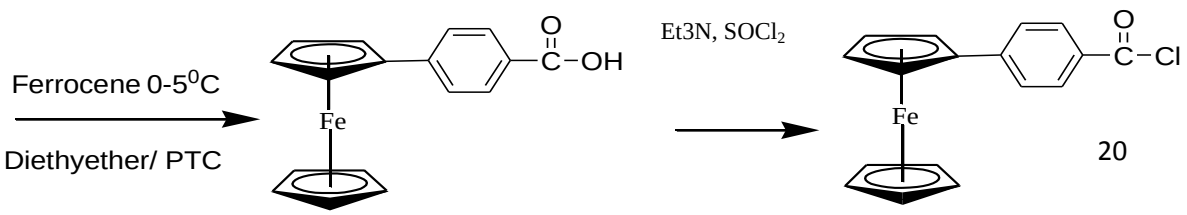

Scheme 4: Synthesis of ferrocenyl benzoates

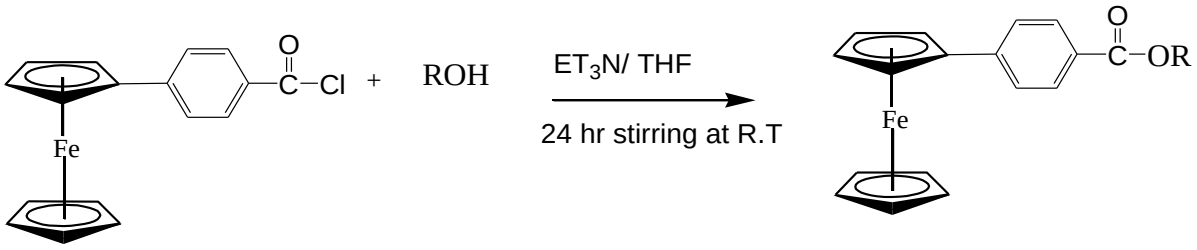

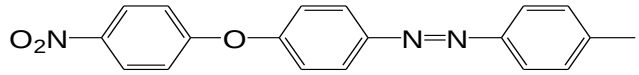

SQ1Fc

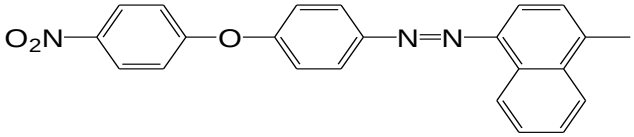

SQ3Fc

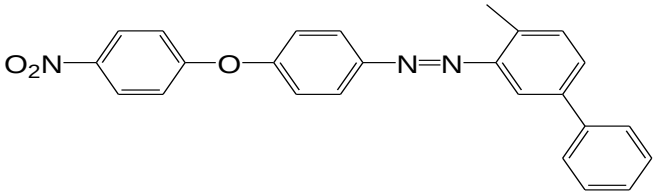

SQ4Fc

EXPERIMENTAL CHAPTER 2

Following subdivision covers the synthetic protocols for nitro terminated azo alcohols and their esters. Important precautions such as purity of reactants, drying of the solvents and reagents were kept under consideration to acquire high yield product. This chapter deliberately explains the purification of the solvents, procedure for the synthesis of dyes and their esters, in addition it also outlines the instrumentations used for characterization.

2.1 Chemical and reagents:

Highly pure chemicals and reagents were used. Chemicals 4-aminophenol, 4-floronitrobenzene, phenol, 1-napthol, 2-napthol, biphenyl-4ol, sodium nitrite, benzoyl chloride, resorcinol and ferrocene were imported from Sigma Aldrich Company, Germany and no additional purification was needed. The solvents methanol, chloroform and THF were procured in from Daejung, Korea. DMSO and HCl were obtained from Lab scan. Some solvents like ethyl acetate, acetone, dichloromethane and n-hexane were procured from Merk, Germany. The dryness of solvents was always assured before use. All the reactions were conducted under inert condition obtained using vacuum line. The success of reaction was continuously monitored using thin layer chromatography on pre coated Kieselgel-60 HF_{250} plate. Pure products were obtained by column chromatography with suitable systems.

2.2 Drying of solvents:

2.2.1 Ethyl acetate:

It was pretreated with anhydrous $MgSO_4$ for overnight. Then it refluxed round about for six hours with P_2O_5 and distilled. B.p 77.1°C.

2.2.2n-Hexane:

n-Hexane pre-dried using CaH_2 for about 12 hours then refluxed and distilled using sodium metal wire and benzophenone (indicator). Scorching blue color indicated the end point. B.p. 68.7°C.

2.2.3 Tetrahydrofuran:

Distilled and refluxed using sodium metal wire and benzophenone. B.p. 65.4°C.

2.2.4 Dichloromethane:

Dichloromethane was pretreated with anhydrous $CaCl_2$ for about 1 day then filtered and distilled using P_2O_5. B.p.40°C.

2.2.5 Ethanol:

Ethanol was predried using CaO then refluxed and distilled with Mg turnings, end point was detected using iodine crystals. B.p. 77- 78°C.

2.2.5 Methanol:

Similar method was used as described for ethanol.B.p. 65.4°C.

2.2.6 Triethylamine:

Triethylamine was dried by refluxing with CaH_2 for 2 hours then distilled and stored in dark**.** B.p 89°C.

2.3 Analytical techniques and instrumentation

2.3.1 Melting point determination:

Melting point of the reactants and products were determined by using open capillary tubes in Mel-Temp, Mitamura Riken Kogyyo, Inc Tokyo, Japan apparatus.

2.2.2 FT-IR spectroscopic studies:

Fourier transform infrared spectra were collected by BRUKER spectrophotometer in the range of 4000-400cm^{-1}.

2.2.3 NMR spectroscopic studies:

Proton (^{1}H) and Carbon (^{13}C) NMR spectra of products and reactant were recorded by

Bruker Advanced Digital (300MHz,Switzerland) NMR spectrophotometer.

2.2.4 UV-Visible spectroscopic studies:

For UV-VIS spectral studies of reactants and products, Perkin Elmer Lamda 35 UV-VIS spectrophotometer was used with appropriate solvents.

2.2.6 Single crystal X-Ray analysis:

Single-crystal X-ray analysis results were obtained on Bruker APEXII D8 Venture diffractometer in line with PHOTON 100 detector of CMOS technology. Having X-ray source of [Cu kα radiation, α =1.54178 Å] with fine focused sealed hose. Absorption correction was done by means of Multi-scan mode. Structure was resolved by using direct procedure with the help of SHELXTL program.

2.5 Synthetic procedures:

The synthetic protocols are discussed in this section.

2.5.1 Synthesis of 4-(4-Nitrophenoxy)aniline:

4-(4-Nitrophenoxy) aniline was synthesized by adding 35ml of dried DMF solvent in a mixture of 4-aminophenol (2.50 g, 25 mmol, 1eq.), 4-fluoronitrobenzene (2.51 g, 25 mmol, 1eq.) and anhydrous K_2CO_3 (3.55 g, 25 mmol, 1eq.) in fully baked three necked flask. After this addition, reaction mixture was refluxed for about 20 hours at 100°C in the under nitrogen atmosphere. The progress of reaction was constantly monitored by thin layer chromatography using ethyl acetate n-hexane (1:3) system. Reaction mixture was then cooled down to room temperature and poured in 400 ml of ice cooled water. Yellow precipitate was obtained which was filtered and recrystallized using ethanol and water (1:1). M.p.129°C.

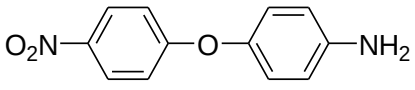

4-(4-nitrophenoxy)benzenamine

2.5.2 General procedure for synthesis of azo dyes:

In the first step, 4-(4-nitrophenoxy)aniline (0.5 g, 0.217 mmol, 1eq) was dissolved in a solution of 1.5 ml of H_2O and 1.5 ml of HCl (37%) and was ice-cooled to -5-0°C with ice salt bath. $NaNO_2$(0.149 g, 0.217 mmol, 1eq.) was dissolved in 5 ml of H_2O and added drop wise to the above solution under constant stirring for about 20 mins at 0°C.

In the next step diazonium salt of aniline was coupled with aromatic moiety (0.217mmol) in 20% solution of NaOH (1g in 5 ml) below 5°C. During coupling, pH was maintained between 5-9. After complete addition of diazonium salt, the reaction mixture was stirrered for about 2 hours to ensure the completion of reaction. Then precipitation was done with dilute HCl solution. The precipitates was filtered, dried and recrystallized using ethanol-water (1:1) solution. Organic impurities were removed by washing with small fraction of ether.

2.5.2.1 Synthesis of 4-((4-(4-nitrophenoxy)phenyl)diazenyl)phenol (SQ_1)

(0.21 g, 0.217 mmol) of phenol was treated with 3 ml of 20% NaOH solution and coupled with diazonium salt of 4-(4-nitrophenoxy)aniline, synthesized according to above mentioned procedure. Yellow colored precipitate wasobtained. M.p 216 ◦C and

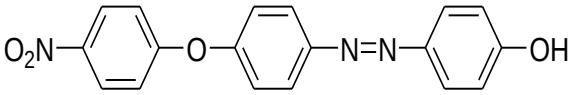

Yield was 78 %.

2.5.2.2. Synthesis of 1-((4-(4-nitrophenoxy)phenyl)diazenyl)naphthalen-2-ol (SQ_2)

0.389 g (0.217 momol) of 2-Napthol was treated with 5 ml of 20% NaOH solution and coupled with diazonium salt of 4-(4-Nitrophenoxy)aniline prepared according to above mentioned procedure. Bright red colored precipitate was obtained. M.p. 166◦C and Yield was 72 %.

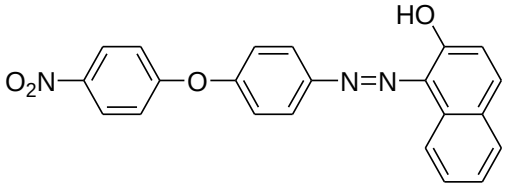

2.5.2.3. Synthesis of 1-((4-(4-nitrophenoxy)phenyl)diazenyl)naphthalen-1-ol (SQ_3)

0.389g (.217 mmol) of 1-Napthol was treated with 20% NaOH solution and coupled with diazonium salt of 4-(4-Nitrophenoxy)aniline according to above mentioned procedure. Apple red colored precipitate was obtained. M.p 174◦C and Yield was 82 %.

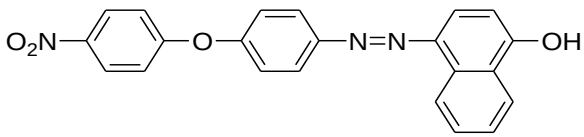

2.5.2.4 Synthesis of 1-((4-(4-nitrophenoxy)phenyl)diazenyl)biphenyl-4-ol (SQ_4)

0.36g (0.217 mmol)of biphenyl 4-ol was treated with 5ml of 10% NaOH solution and coupled with diazonium salt of 4-(4-nitrophenoxy)aniline according to above rules. Bright Yellow colored precipitate was obtained And Yield was78%.

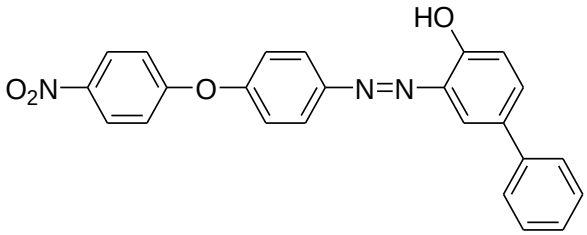

2.5.2.5 Synthesis of 4-((4-(4-nitrophenoxy)phenyl)diazenyl)benzene-1,3-diol (SQ_5)

Resorcinol (0.24 g , 0.217 mmol) was activated by using 5 ml of 10% NaOH solution and coupled with diazonium salt of 4-(4-Nitrophenoxy)aniline according to above mentioned procedure. Orange colored precipitate was obtained. M.p 215 ◦C and Yield was 79%.

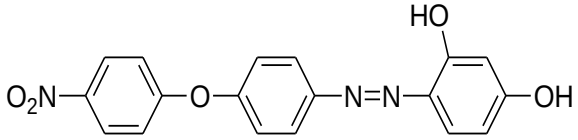

2.5.3 General procedure for synthesis of azo esters

In a pre-heated three-necked flask equipped with magnetic stirrer and condensers, the corresponding alcohol was dissolved in freshly dried 15 ml of THF, then 3 ml of

triethylamine was added dropwise at 0-5°C. In the next step, acid chloride was dissolved in 10 ml of THF and added dropwise to the reaction mixture. After complete addition, the reaction mixture was allowed to stirrer for about 24 hours at room temperature and then rotary evaporated to get the crude product. The product was further purified by washing with dried ethanol.

2.5.3.1Synthesis of 4-((4-(4-nitrophenoxy)phenyl)diazenyl)benzoate (SQ_1B):

This ester was synthesized by above mentioned procedure using 4-((4-(4-nitrophenoxy)phenyl)diazenyl)phenol (0.25 g, 0.74 mmol) and benzoyl chloride (0.085 ml, 0.74 mmol). Color; Orange yellow, Yield: 72%. M.p 166◦C.

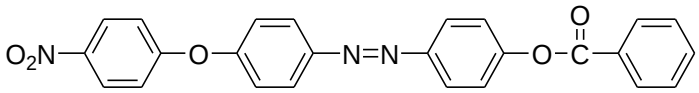

2.5.3.2Synthesis of 4-((4-(4-nitrophenoxy)phenyl)naphthalene benzoate (SQ_3B):

This ester was synthesized following above mentioned procedure using 4-((4-(4-nitrophenoxy)phenyl)diazenyl)naphthalene1-ol (0.25 g, 0.51 mmol) and benzoyl chloride (0.059ml, 0.51mmol) were used. Color; Orange red, Yield: 70%, M.p.152◦C.

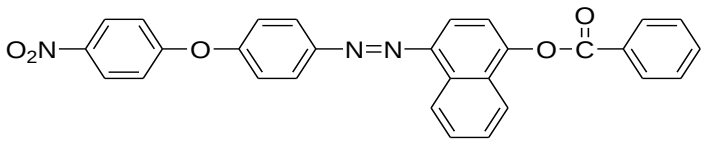

2.5.3.3 Synthesis of 1-((4-(4-nitrophenoxy)phenyl)diazenyl)biphenyl benzoate(SQ_4B)

This ester was synthesized using above mentioned procedure in the presence of 1-((4-(4-nitrophenoxy)phenyl)diazenyl)biphenyl-4-ol (0.25 g, 0.60 mmol) and benzoyl chloride (0.070 ml, 0.60 mmol) .Color : Yellow, Yield: 72%, M.p. 162 ◦C.

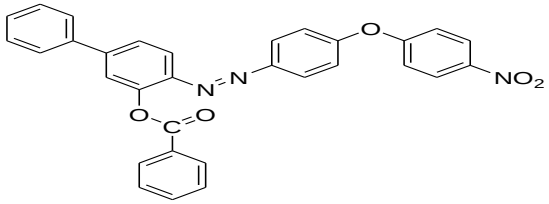

2.5.3.4 4-((4-(4-nitrophenoxy)phenyl)diazenyl)benzene-1,3-benzoate (SQ_5B)

This ester was synthesized by reacting 4-((4-(nitrophenoxy)phenyl)diazenyl)benzene-1,3-diol (0.25 g, 0.71 mmol) and bezoyl chloride (0.1654ml, 0.1.42mmol) by the above mentioned procedure. Color : Yellow, Yield: 72%, M.p 162 ◦C

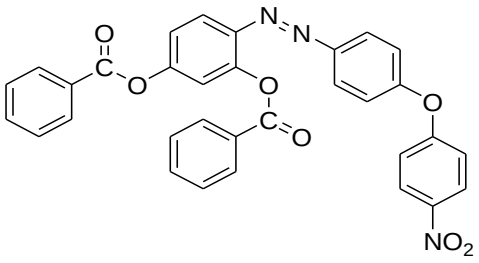

Ferrocene derivatives were synthesized via esterification reactions between ferrocenyl acid chloride and the azo alcohols the in presence of triethyl amine under inert conditions at room temperature.

2.5.4 Synthesis of ferrocenyl esters

2.5.4.1 Synthesis of 4-ferrocenyl benzoyl chloride

Step I :

4-Ferrocenyl benzoyl chloride was synthesized by the diazotization of 4–aminobenzoic acid (7 g, 50 mmol) in the presence of 12 ml of HCl and 80 ml of water .Temperature was maintained at 0-5 ◦C and sodium nitrite (3.5 g, 50 mmol) in 10 ml of water was added dropwise.

In the next step this diazonium salt was added to the 100 ml of diethyether containing ferrocene (10 g, 50 mmol) and catalytic amount of phase transfer catalyst. The reaction mixture was allowed to stirrer at room temperature for 3 hours and the rotary evaporated the diethyl ether, to get the crude product.

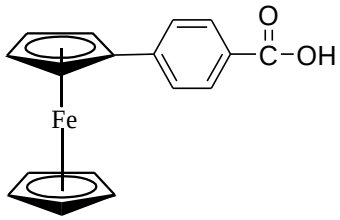

The brown colored crude product was recrystallized by using 5% NaOH and heating at 90°C and then hot saturated solution was filtered off and filtrate was precipitated with 10% dil. HCl.

Step II :

In a pre-baked 3 necked flask equipped with condensers and magnetic stirrer 4-ferrocenyl benzoic acid(1 g, 3.27 mmol) was dissolved in 20 ml of THF. Temperature of the reaction mixture was maintained at 0-5°C and thionylchloride (2 ml, 26.89 mmol) was added under inert condition after the addition of (5 ml, 35.5 mmol) of triethylamine. Then the reaction mixture was allowed to stand for about 2 hours at room temperature.

The excess of solvent was evaporated under vacuum. The residue was extracted using small amount of dried diethyl ether and then filtered using cannula filtration. The solvent was again rotary evaporated to get the red colored crystals.

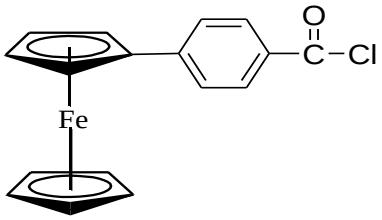

2.5.4.2Synthesis of 4-((4-(4-nitrophenoxy)phenyl)diazenyl)ferrocenyl benzoate (SQ_1-Fc)

Ferrocene containing ester was synthesized by reacting 4-ferrocenylbenzoyl chloride (0.5 g, 1.635mmol) with 4-((4-(4-nitrophenoxy)phenyl)diazenyl)phenol (0.53 g, 1.635 mmol) in the presence of triethylamine following the above mentioned procedure.

Color: Orange

Yield 64%, M.p. 141°C

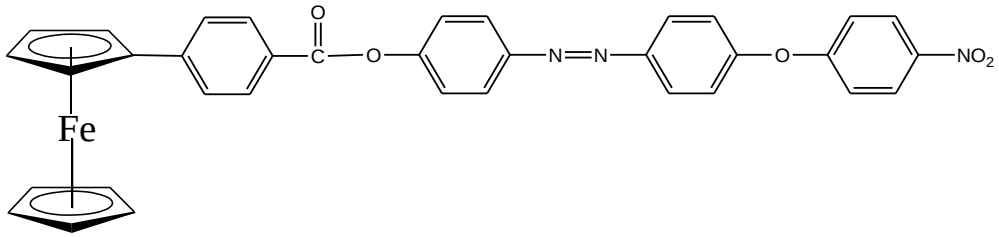

2.5.4.3 Synthesis of 1-((4-(4-nitrophenoxy)phenyl)diazenyl)napthalene ferrocenyl benzoate (SQ_3-Fc)

Ester was synthesized by reacting u1-((4-(4-nitrophenoxy)phenyl)diazenyl)napthalene 1-ol (0.46 g, 1.215 mmol) with 4-Ferroenyl benzoyl chloride (0.393 g, 1.215 mmol) in the presence of triethyl amine under inert nitrogen gas condition. Color: Brown,

Yield 63% M.p. 153◦C

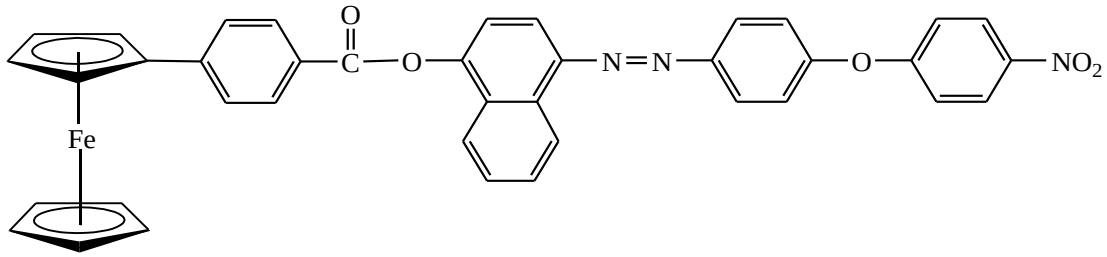

2.5.4 Synthesis of 4-((4-(4-nitrophenoxy)phenyl)biphenyl ferrocenyl benzoate (SQ_4-Fc)

This ferrocene based ester was synthesized by reacting 4-ferrocenylbenzoyl chloride (0.67 g, 1.635 mmol) and of 4-((4-(4-nitrophenoxy)phenyl)biphenyl-4)phenol (0.53g, 1.635 mmol) in presence of triethylamine accordingly above mentioned procedure. Color Brown

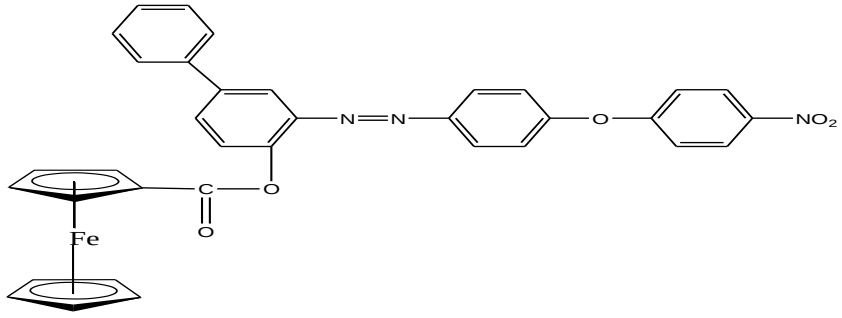

Yield 61%. M. p. 129 ◦C.

2.6 Protocols for activities:

2.6.1 Photoisomerization:

The sample solution (0.1mmol) of the entire synthesized compound was prepared in DMF solvent at room temperature. The solution were then irradiated with short wavelength UV light (365nm) for specific interval of time. UV-VIS absorption spectra were recorded after each interval of time using Perkin Elmer LAMDA 235 UV/VIS spectrophotometer.

2.6.2 Hydrogen peroxide scavenging activity:

Hydrogen peroxide scavenging activity was evaluated by preparing (4×10^{-3}mol/dm^{-3}) H_2O_2 solution in (1×10^{-1}mol/dm^{-3}) phosphate buffer of pH 7.4. In the second step 2.5 ml of above solution was added in 4 ml of (50 μg/ml) of sample and incubated for 15 mins at 310 K, and run against the blank of H_2O_2 solution. UV-Vis spectroscopy was used to monitor variation in absorption at 230 nm. Experiment was repeated thrice to reduce the chances of error.

Following formula is used to calculate the scavenging activity

$$\% \text{ Scavenging activity} = \frac{Acontrol - Asample}{Acontrol} * 100$$

Here $A_{control}$ and A_{sample} are absorbance for standard and sample respectively.

2.6.3 DPPH free radical scavenging activity:

The synthesized Azo dyes and esters were examined to assess the antioxidant capability according to the reported method. Dyes and their esters at various concentrations (1 to 5 μg/ml) were added independently to reagent solution i-e 4 ml of 0.1 mm methanol solution of DPPH and incubated in dark for 30 mins at room temperature. After incubation period the reduction of DPPH was assessed by monitoring the decrease in absorbance at 517 nm using UV-VIS spectrophotometer. Ascorbic acid was run as a standard. Each experiment was performed thrice to minimize the chances of error.

$$\% \text{ Scavenging activity} = \frac{Acontrol - Asample}{Acontrol} * 100$$

2.6.4 DNA binding investigation:

For DNA binding experiments, stock solution of Calf Thymus DNA was prepared in double distilled water and stored at 4^0C. Its concentration was monitored by UV/VIS spectrophotometer at 260nmwith 6600$M^{-1}cm^{-1}$ molar absorptivity. The confirmation of protein free DNA was endowed by the ratio of absorbance at 260/280 nm ($A_{260}/_{A280}$=1.85).[41]

Sock solution (0.1 mmol) of compounds were prepared in DMSO:H_2O system. The absorbance titrations were recorded at a fixed concentration of sample solution and titrating it against varying concentration of double standard CT-DNA.[42] For each of five experiment, DNA solution of 30 μL, 60 μL, 90 μL, 120 μL, 150μL were added to 2.5 ml of stock solution reaction mixtures and further incubated at 37 °C for 1 mins before reading the spectra.[43]

CHAPTER 3 RESULT AND DISCUSSIONS

New azo based dyes have prepared using 4,4-nitrophenoxyaniline and various aromatic groups. Further azo based ester have synthesized by following the condensation reaction between azo-alcohols with aromatic acid chlorides i.e. with benzoyl chloride and 4-ferrocenyl benzoyl chloride as mentioned in schemes 1-4- in Chapter 2. These compounds were characterized by physical parameters e.g. color, melting point, solubility and various analytical techniques including FT-IR, NMR, UV-VIS spectroscopy and single crystal analysis for the structural elucidation.

Further this chapter includes the results of chemosensing ability of azo alcohol. The DNA binding and photoisomerization studied through UV-Vis spectroscopy technique is also elaborated. In addition DPPH free radical scavenging and H_2O_2 scavenging activity of the synthesized compounds are also discussed.

3.1 Synthesis

The synthesis of azo based alcohols involves diazotization of 4,4-nitrophenoxyaninilne and coupling with phenol, 2-napthol, 1-napthol, biphenyl-4ol and resorcinol. Second step involves the formation of organic ester by reacting these azo based alcohols with benzoyl chloride in the presence of triethylamine.

Similarly the synthesis of ferrrocenyl ester includes the formation of ferrocenyl benzoic acid (precursor) according to reported method [44] which was then converted into acid chloride in the presence of excess of thionyl chloride. Further this ferrocenyl benzoyl chloride was reacted with azo alcohols to form ester

The reaction leading to ester formation is carried out under moisture free condition as ester formation is extremely vulnerable to hydrolysis resulting back into alcohols and acid. Triethylamine was used as a catalyst as well as an acid scavenger resulting into triethyl ammonium chloride which also prevents reversibility of the reaction.

3.2 Characterization:

3.2.1 Physical properties:

4,4-Nitrophenoxyanililne was characterized by melting point FT-IR and NMR spectroscopic techniques and these date are full agreement with the literature.[45] For this starting aniline the observed melting point was 129◦C.The FT-IR spectrum showed two symmetrical peaks for υNH_2 peaks at 3363.86 $cm^{-1}$and 3442.9 4cm^{-1}.The absorption band observed at 1338.60 cm^{-1} and 1585.49 cm^{-1} were due to nitro groups.

Azo alcohols and esters were characterized by melting point, solubility, FT-IR, NMR spectroscopic studies and single crystal. Their physical properties is shown in Table3.1.Single crystal of these azo alcohol and two esters were obtained by recrystallization of crude product in suitable solvent and then slow evaporation at room temperature which were subjected to X-ray crystal analysis for structural elucidation.

Table 3.1: Physical data of starting aniline and azo alcohols

Compounds	Molecular Formula	Color	Melting Point	% Yield	Molecular Weight
SQ	$C_{12}H_{12}N_2O_3$	Brown	131 ◦C	82%	230
SQ1	$C_{18}H_{13}N_3O_4$	Dirty Yellow	216◦C	78%	335
SQ2	$C_{22}H_{15}N_3O_4$	Bright Red	166◦C	72%	385
SQ3	$C_{22}H_{15}N_3O_4$	Apple red	174◦C	82%	385
SQ4	$C_{24}H_{17}N_3O_4$	Yellow	139◦C	78%	411.4
SQ5	$C_{18}H_{13}N_3O_5$	Orange	215◦C	79%	351.31

Similar to azo alcohols physical properties of azo ester is given in Table 3.2

Table 3.2: Physical data of azo esters

Compounds	Molecular Formula	Color	Melting Point	% Yield	Molecular Weight
SQ1B	$C_{19}H_{13}N_3O_5$	Yellow	166 ◦C	72%	363.32
SQ3B	$C_{29}H_{19}N_3O_5$	Orange red	152◦C	70%	489.47
SQ4B	$C_{31}H_{21}N_3O_5$	Yellow	162◦C	75%	515.51
SQ5B	$C_{32}H_{21}N_3O_7$	Dark orange	174◦C	69%	559.52
SQ1Fc	$C_{29}H_{19}N_3O_5Fe$	Orange	141◦C	64%	545.32
SQ3Fc	$C_{39}H_{25}N_3O_5Fe$	Brown	153◦C	63%	671.47
SQ4Fc	$C_{41}H_{27}N_3O_5Fe$	Brown	129◦C	69%	697.51

3.2.2 Solubility:

The solubility of all the compound was checked in various solvent and their result is tabulated in Table 3.3.and 3.4.The new azo dyes were comparatively fully soluble in polar aprotic solvent such as in DMF, DMSO, Acetone, THF etc. Good solubility was also observed in some polar protic solvent such as ethanol, methanol due to hydrogen bonding between available (OH) groups but they showed poor solubility in water because of aromatic groups present in the structure. Furthermore azo dyes were found to be insoluble in highly non-polar solvent such as n-hexane or n-heptane.

Table 3.3 Qualitative solubility data of azo alcohols

Azo Dyes	SQ1	SQ2	SQ3	SQ4	SQ5
Pet Ether	--	--	--	--	--
Hexane	--	--	--	--	--
Methanol	+	++	++	+	+
Ethanol	+	+	++	+	+

Azo Dyes	SQ1	SQ2	SQ3	SQ4	SQ5
CH_2Cl_2	+	++	++	+	++
$CHCl_3$	+	++	+	++	+
THF	++	++	++	++	++
Toluene	++	++	++	++	++
Ethyl Acetate	++	++	++	++	++
DMSO	++	++	++	++	++
DMF	++	++	++	++	++
H_2O	--	--	--	+-	+-
Benzene	+	--	--	+-	+-

Soluble at room temperature (++) Soluble upon heating(+)

Slightly Soluble upon heating (+-) Insoluble upon heating (--)

Table 3.4 Qualitative solubility data of azo esters

Azo Dyes	SQ1B	SQ3B	SQ4B	SQ5B	SQ1Fc	SQ3Fc	SQ4Fc
Pet Ether	--	--	--	--	--	--	--
Hexane	--	--	--	--	--	--	--
Methanol	+	+	+	+	+	--uu	--
Ethanol	+	+	+	+	++	+	+
DiethylEther	--	--	--	--	--	--	--
CH_2Cl_2	+	++	++	+	++	++	++
$CHCl_3$	+	++	+	++	+	++	++
THF	++	++	++	++	++	++	++
Toluene	++	++	++	++	++	++	++
DMSO	++	++	++	++	++	++	++
DMF	++	++	++	++	++	++	++
Benzene	+	--	--	+-	+-	--	--

3.2.3 FT-IR spectral characterization of the azo alcohols

The FT-IR spectral analysis provided strong agreement with the expected functional groups present in structure. Disappearance of two sharp (-NH_2) stretching peaks of primary amine (4,4 –nitrophenoxyanilne) in the range of 3400-3600 cm^{-1} and appearance of broad OH peak indicated the formation of product. Furthermore appearance of important (N=N) stretch at 1585-1590cm^{-1} confirmed the formation of azo linkage according to literature[46].

All alcohols except SQ2 showed broad peak for OH in the region of 3300-3400cm^{-1}. In contrast SQ2 showed a small peak at 3459.94cm^{-1} for N-H stretch and a sharp peak at 1738cm^{-1} for C=O . These peaks actually indicated the presence of hydrazo-keto form as dominant tatumeric form which was further confirmed by the single crystal analysis.

Aromatic moieties were recognized by their characteristic band in the region of 3000-3150 cm^{-1} and 1600-1615 $cm^{-1}$for aromatic C-H stretch and C=C stretch respectively in spectrum. The complete FT-IR data azo alcohols is represented in Table 3.3

Table 3.5 FT-IR spectroscopic data of azo alcohols

Compounds	NH Stretch cm^{-1}	-CH Stretch cm^{-1}	N=N Stretch cm^{-1}	-OH Stretch cm^{-1}	NO2 stretch cm^{-1}
SQ	3363 , 3442	3076 (w)		---------	1338 1585(s)
SQ1	-------	3115(w)	1597(w)	3402(b)	1341, 1570(s)
SQ2	3459.94	3055(w)	1581(w)		1337, 1569(s)
SQ3	------	3080(w)	1585(w)	3398(b)	1351,1590 (s)
SQ4	--------	3021(w)	1580(w)	3412(b)	1346, 1564(s)
SQ5	--------	3012(w)	1594(w)	3395(b)	1365, 1580(s)

b=Broad, s=sharp, w=weak

Similarly the FT-IR Spectra of all the synthesized esters illustrated the presence of expected functional groups in their respective regions. The synthesis of desired esters was

confirmed by the disappearance of broad peak of (-OH) in the region of 3300-3400cm^{-1}and appearance of a sharp peak of (C=O) in region of 1700-7140 cm^{-1}. The confirmation of (-C-O) linkage of ester was indicated by a strong peak at 1250-1280cm^{-1}. In the spectra of ferrocenyl esters Fe-Cp stretching vibration was indicated in the region of 470-490cm^{-1}.Further a band at 840-875cm^{-1}demonstrated para substitution on aromatic ring.

Table 3.6 FT-IR spectroscopic data of azo esters

Compounds	C=O stretch cm^{-1}	N=N Stretch cm^{-1}	C-O stretch cm^{-1}	NO2 stretch cm^{-1}
SQ1B	1738(s)	1583 (w)	1258 (s)	1341, 1595(s)
SQ3b	1735(s)	1597 (w)	1267 (s)	1348, 1560(s)
SQ4B	1732(s)	1581(w)	1274 (s)	1339, 1567(s)
SQ5B	1728(s)	1585(w)	1263(s)	1357 ,1599 (s)
SQ1Fc	1729(s)	1580(w)	1251(s)	1356, 1574(s)
SQ3Fc	1723(s)	1594(w)	1276 (s)	13658 1580(s)
SQ4Fc	1736(s)	1594(w)	1276 (s)	1375, 1581(s)

3.2.4 NMR spectral investigation of azo alcohols and esters:

3.2.4.1 ^{1}HNMR spectral data

For further structural investigation of azo alcohols and ester NMR spectroscopic techniques was also used. The NMR spectra were run in deuterated solvent like DMSO-d_6, chloroform-d_6 and acetone-d_6 solvents. All the NMR spectra were in accordance with the proposed chemical structure of the compound. In proton NMR of azo alcohols signal of deshielded –OH proton appeared in the region of 10-11 ppm. All the aromatic protons were present in between 7-8 ppm confirming the formation of azo alcohol. In case of azo esters the downfield signal of (OH) group was disappeared and only aromatic proton were present in their respective region of 7-8 ppm confirming the formation of ester linkage.Table3.7 and 3.8 are presenting ^{1}HNMR data of azo alcohols and azo ester. Proton NMR spectrum of representative azo alcohols is attached in **APPEDIX 11.**

Table 3.7 ^{1}H NMR data of azo alcohols

Compound	O-H proton signal (ppm)	Aromatic proton signal (ppm)
SQ1	10.3	6.93- 8.3
SQ2	15.2	6.9 - 8.6
SQ3	10.4	7.1 – 8.1
SQ4	11.2	6.99 – 8
SQ5	12.1,10.5	7.2-8.3

Table 3.8 ^{1}H NMR data of azo ester

Compound	O-H proton signal (ppm)	Aromatic proton signal (ppm)
SQ1B	----	7.11- 8.29
SQ3B	----	7.14-8.67
SQ4B	----	7.12-8.57
SQ5B	---	7.00-8.99

3.2.4.2 ^{13}CNMR spectra data

All the ^{13}C NMR spectra were recorded in above mentioned solvent used for recording ^{1}H NMR spectra. In organic ester deshielded carbonyl carbon was present at most downfield region (163-165 ppm).The rest of carbon were present in their respective region between 116-162 ppm. In case of ferrocene based ester the unsubstituted Cp ring appeared at 69 ppm and two substituted ring appeared at 66 and 68 ppm respectively.

Table 3.9 ^{13}C NMR azo esters

Compound	C=O (ppm)	Aromatic carbon signal (ppm)
SQ1B	164	116- 161
SQ3B	165	119 -163
SQ4B	164	118-161
SQ5B	164	117-161
SQ1Fc	166	116-161
SQ2Fc	165	114-161
SQ4Fc	167	115-61

3.2.5 Single crystal analysis of azo alcohols and esters:

Single crystals of azo alcohols and esters were obtained by slow evaporation of them in methanol solution at room temperature and subjected to Single crystal X-Ray analyses.

3.2.5.1 4-((4-(4-Nitrophenoxy)phenyl)diazenyl)phenol (SQ_1)

Single crystal of SQ_1 revealed the successful diazotization of aniline and coupling with phenol with following empirical formula $C_{18}\,H_{13}\,N_3$. It is evident from crystal structure that OH group is attached at para to azo group (N=N) and it further illustrate that azo-enol tautomeric form is predominant as there is no proton on N1 and N2. The crystal structure is shown in Figure 3.1. The determined unit cell dimensions of single crystal are; a = 9.8220(8) A◦. b = 5.6365(5) A◦, c = 27.593(2) A◦, α=90◦, β=90◦, γ =90◦. Cell coordinates confirmed the Orthorhombic crystalline form with P21/c space group as all the bond lengths are unequal and all the base angle are perpendicular to one another at 90◦. The cell volume was established to be 1527.6(2) $A^{0\ 3}$ and 4 number of molecules were found to be present per unit cell. The relevant data is presented in Table 3.10

The rings which are directly attached with azo chromophore are in plane and nitro group along with its ring is slightly twisted out of the plane.

Table 3.10 Some important bond lengths and bong angles in SQ1

Bond	Bond length	Bond angle	Degree
O(3)-N(3)	1.234(2)	C(2)-C(1)-C(6)	120.1(2)
O(4)-N(3)	1.226(2)	C(2)-C(1)-H(1)	119.9
N(1)-N(2)	1.247(2)	C(6)-C(1)-H(1)	119.9
N(1)-C(6)	1.430(2)	C(1)-C(2)-C(3)	119.6(2)
N(2)-C(7)	1.432(2)	C(1)-C(2)-H(2)	120.2
N(3)-C(16)	1.453(3)	C(3)-C(2)-H(2)	120.2
C(1)-C(2)	1.382(3)	O(1)-C(3)-C(4)	116.90(18)
C(7)-C(12)	1.402(3)	C(1)-C(6)-N(1)	124.78(18)
C(9)-H(9)	0.9500	C(8)-C(7)-N(2)	114.97(19)
C(10)-C(11)	1.382(3)	C(12)-C(7)-N(2)	124.87(18)
C(17)-C(18)	1.377(3)	C(11)-C(10)-C(9)	121.35(18)

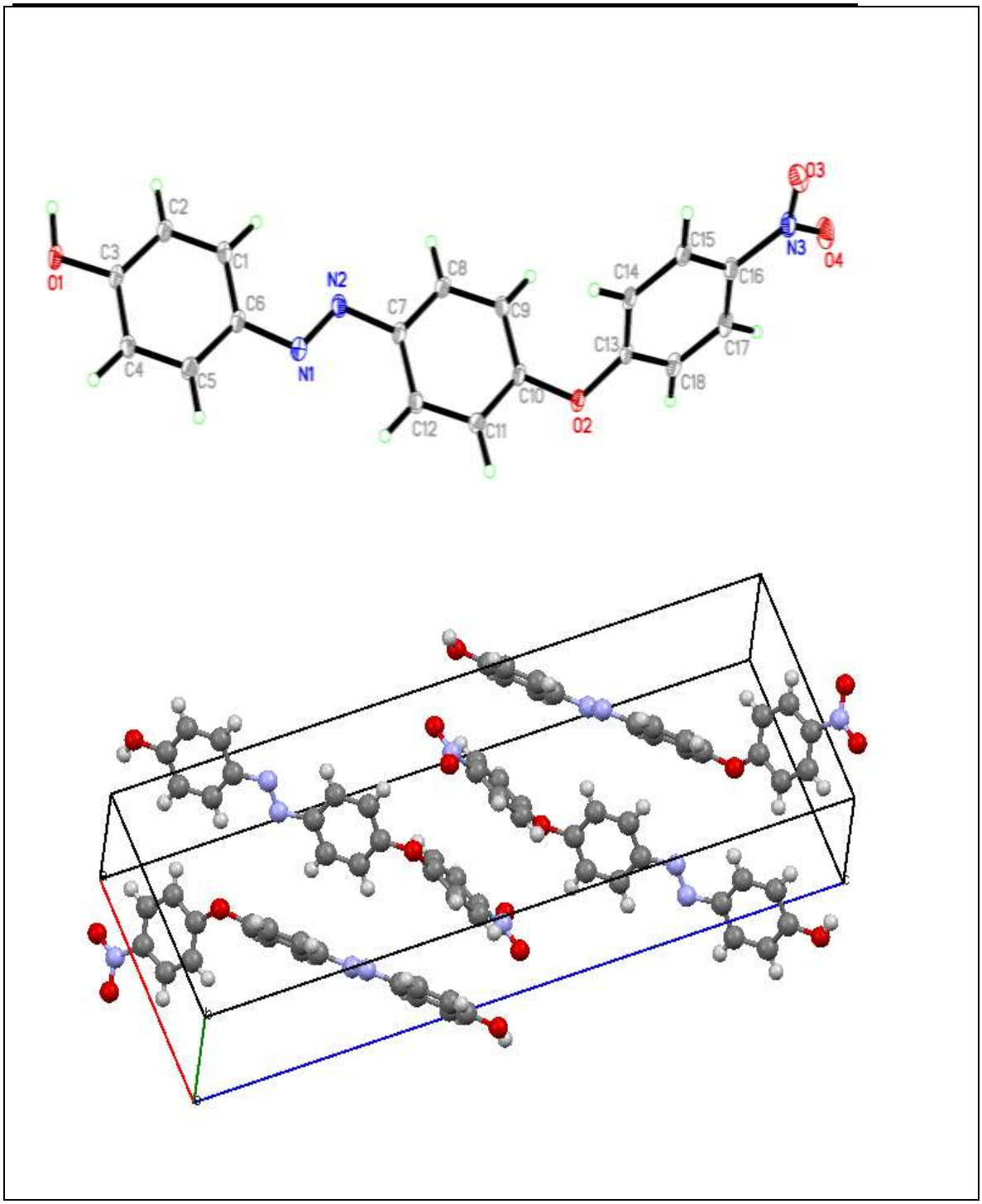

Fig 3.1 Crystal structure and packing diagram of SQ1

3.2.5.21-((4-(4-Nitrophenoxy)phenyl)diazenyl)naphthalen-2-ol (SQ_2)

The single crystal analysis of SQ_2 with following empirical formula C_{22} H_{15} N_3 O_4 revealed that compound crystallized in Monoclinic form as all the axial lengths were different a≠b≠c and α=λ=90◦≠β, having P21/n space group. Structural analysis further illustrated the fact that hydrazo –keto tautomeric form predominates in SQ_2 as one proton is present on N2 and there is no proton on O1 forming double with the carbon. The crystal structure is shown in Figure 3.2.

Inspection of the bond distances showed that interatomic bond distance between N1=N2 1.3029 Å is greater than typical (N=N) bond distance in Ar-N=N-Ar (1.225 Å) types of compounds, favoring Hydazo-Keto form Still it is not enough larger to be look upon as single bond (Nsp^2–N$sp^2$1.401 Å) bond and regard as exclusive hydrazo-keto form. Similarly C9–O1 1.2737(16) bond distance is shorter than average Csp^2–OH (1.362 Å) bond distance, indicating the pi bond character between carbon and oxygen.[47]

The conjugation of section O1–C9–C10–N1–N2 is also confirmed by comparing the interatomic bond distance value C11–N2 (1.4026 Å), typically use for pure σ Csp^2-N bond, with C11–N2 (1.3446(16)) Å), noticeably confirming double bond character in the latter one.[2] Thus by comparing bond lengths it is evident that SQ2 dominantly, but not exclusively present in hydraozone tautomeric form in solid state as shown below

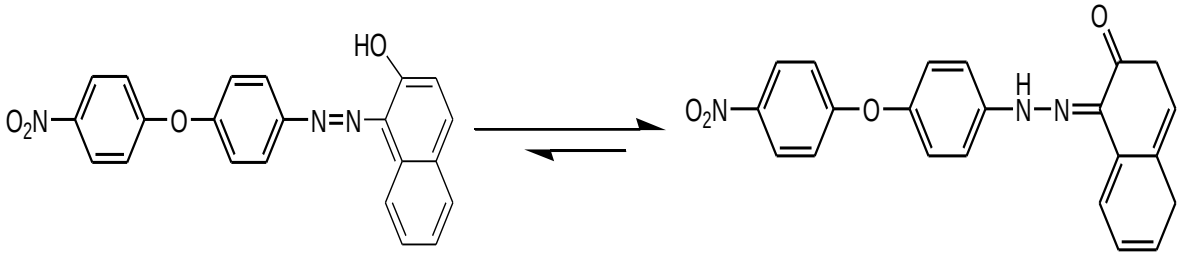

Azo Enol **Hydrazo-keto**

Cell volume was found to be 3592.19(16) $Å^3$ and number of molecules per unit cell were 4 as (Z=4).Unit cell dimensions and some important data regarding crystal is given in Table 3.11 and 3.12

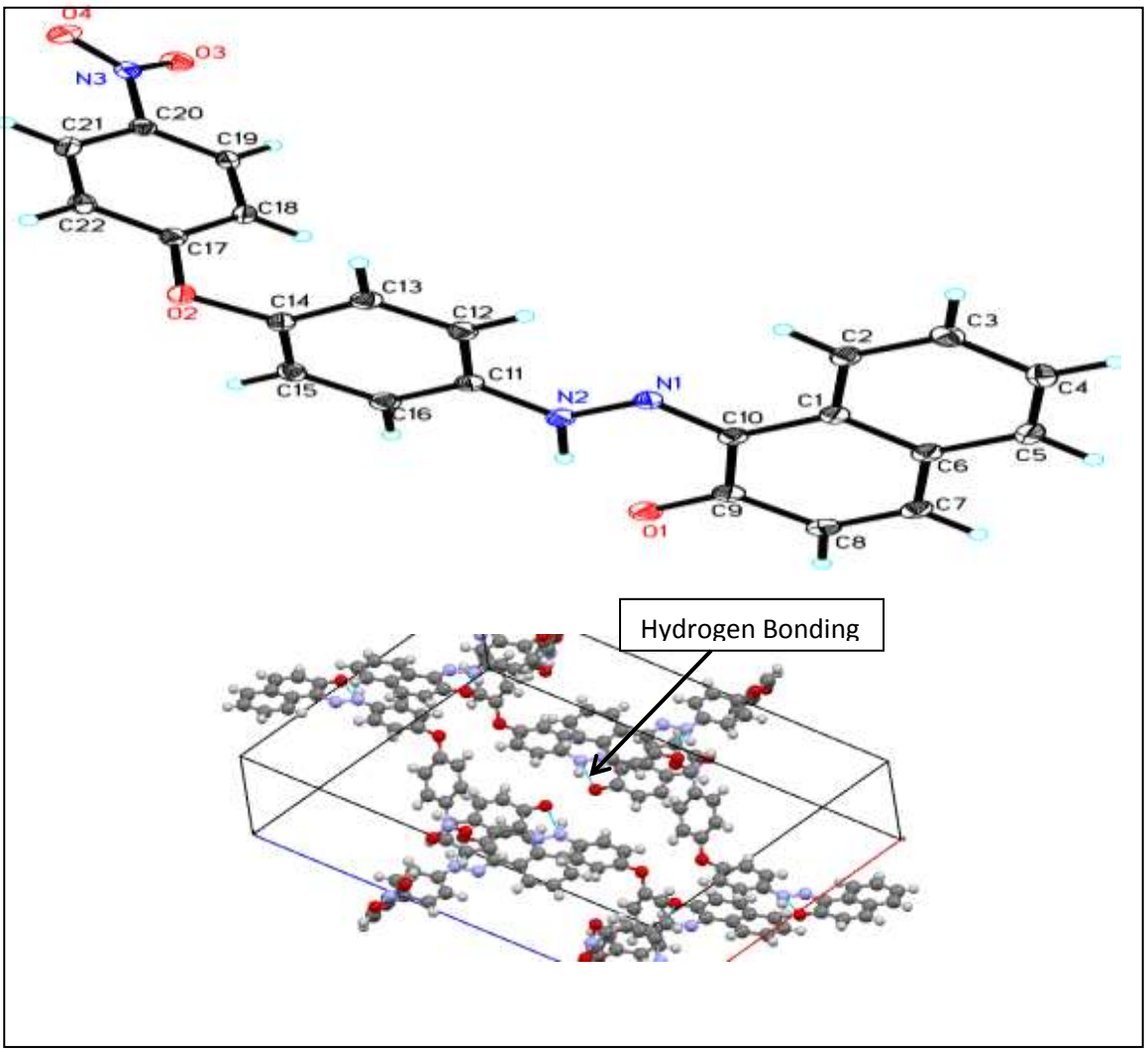

Fig 3.2 Crystal structure and packing diagram SQ2

Table 3.11 Unit cell dimensions of SQ_2

Crystal system	Monoclinic
Space group	$P2_1/n$
Unit cell dimensions	
a = 17.4821(4) Å	α=90°.
b = 7.9229(2) Å	β=104.
c = 26.7350(7) Å	γ = 90°.

Table 3.12 Some important bond lengths and bong angles in SQ2

Bond	Bond length	Bond angle	Degree
O(2)-C(14)	1.4009(15)	N(1)-N(2)-H(2AA)	115.0(11)
O(4)-N(3)	1.2294(14)	O(4)-N(3)-C(20)	118.50(11)
O(7)-N(6)	1.2273(13)	C(2)-C(1)-C(6)	118.58(12)
N(1)-N(2)	1.3029(14)	C(2)-C(3)-H(3)	119.7
N(1)-C(10)	1.3446(16)	C(5)-C(6)-C(1)	119.36(12)
N(2)-C(11)	1.4026(16)	O(1)-C(9)-C(8)	120.66(12)
N(4)-N(5)	1.3034(14)	N(1)-C(10)-C(1)	116.10(11)
N(5)-C(33)	1.4037(16)	C(16)-C(11)-N(2)	117.03(11)
C(2)-C(3)	1.3750(18)	C(13)-C(14)-O(2)	120.07(12)
C(20)-C(21)	1.3865(17)	C(15)-C(16)-H(16)	120.0
O(3)-N(3)	1.2307(14)	C(21)-C(20)-N(3)	119.08(11)
C(4)-C(5)	1.372(2)	C(5)-C(4)-H(4)	120.2

3.2.5.31-((4-(4-Nitrophenoxy)phenyl)diazenyl)biphenyl-4-ol (SQ_4)

Single crystal of SQ_4 was obtained by slow evaporation of its solution in DMF at room temperature. Analysis revealed the fact that SQ_4 with following empirical formula $C_{24}H_{17}N_3O_4$ crystallized out in triclinic geometry with P-1 space group. An interesting fact was revealed through analysis that biphenyl-4-ol was coupled at ortho position to azo group (N=N) not at para position probably due to strong intramolecular hydrogen bonding present in –OH and N=N group in ortho product which is not feasible in para product. Azo-enol tautomer predominates as compare to hydarzo-keto form as there is no proton on N1 and N2. The crystal structure is shown in Figure 3.3. Cell volume was found to be 981.28(4) Å3. Analyses showed that two only molecules can pack up in a unit cell as (Z=2). Some important data is provided in Table 3.13 and 3.14

It is valuable to describe that an intramolecular hydrogen bonding between hydrogen and nitrogen of azo group with a bond distance of H···N 2.532 (11) Å is present as shown in Fig 3.3.As a consequence five-membered C_2N_2H hydrogen-bonded cyclic ring is formed,

which is responsible to keep local planarity between the azo chromophore and two attached rings and second ring is completely out of plane.

Table 3.13 Unit cell dimensions of SQ4

Crystal system	Triclinic
Space group	P-1
Formula weight	411.4
Unit cell dimensions	
a = 7.3640(2) Å	α=100°.
b = 7.7256(2) Å	β=90.0°.
c = 17.8444(4) Å	γ = 100°.

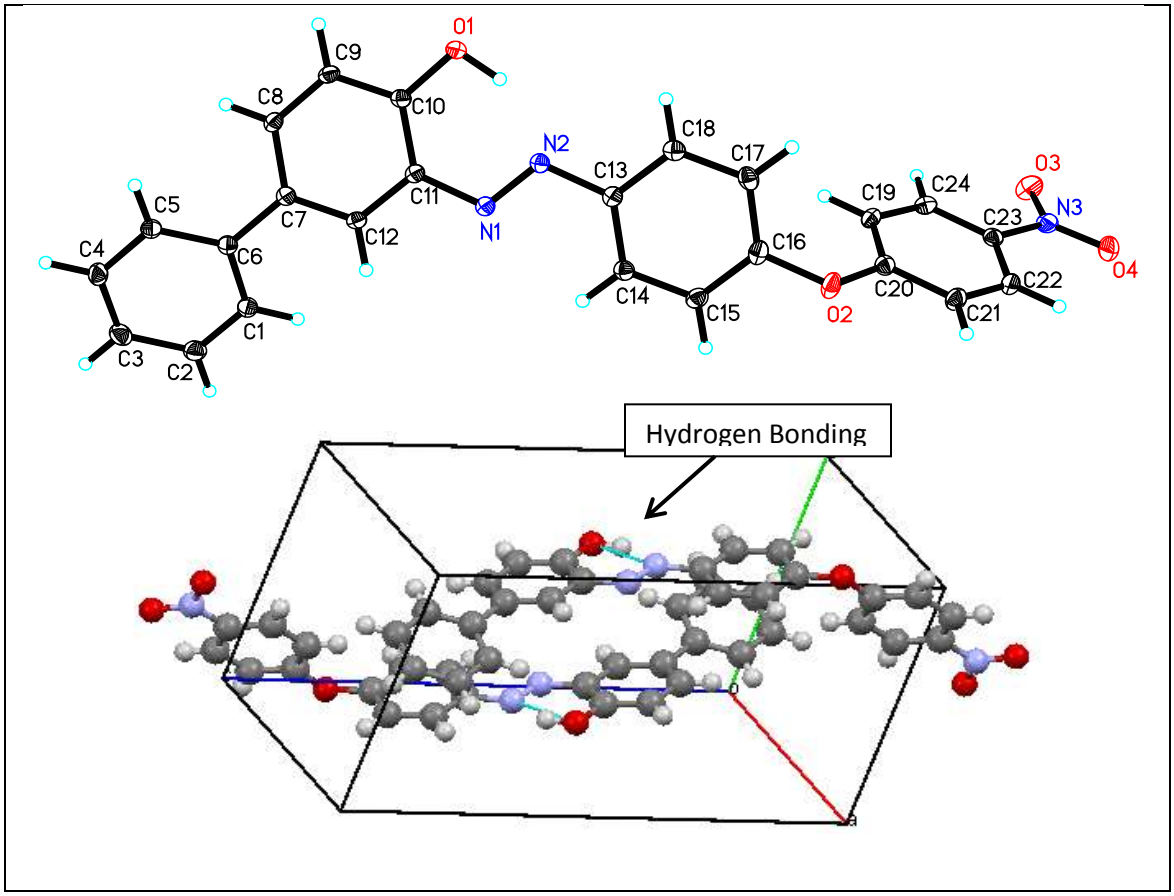

Fig 3.3 Crystal structure and packing diagram of (SQ4)

Table 3.14 Some important bond lengths and bong angles in SQ4

Bond	Bond length	Bond angle	Degree
O(2)-C(16)	1.3974(14)	N(2)-N(1)-C(11)	115.33(9)
O(3)-N(3)	1.2320(14)	O(4)-N(3)-O(3)	123.38(11)
N(1)-N(2)	1.2702(14)	C(20)-O(2)-C(16)	120.24(9)
N(2)-C(13)	1.4202(15)	C(2)-C(1)-H(1)	119.5
N(3)-C(23)	1.4577(16)	C(5)-C(6)-C(1)	119.36(12)
C(6)-C(7)	1.4857(16)	C(1)-C(2)-H(2)	119.8
C(8)-C(9)	1.3794(17)	C(4)-C(3)-H(3)	120.3
C(11)-C(12)	1.3999(16)	C(3)-C(4)-H(4)	119.8
C(14)-C(15)	1.3811(17)	C(5)-C(6)-C(1)	118.12(11)
C(21)-C(22)	1.3757(18)	O(1)-C(10)-C(9)	119.36(10)
C(23)-C(24)	1.3844(17)	N(1)-C(11)-C(10)	125.27(11)
C(19)-C(24)	1.3828(17)	C(11)-C(12)-H(12)	119.0

3.2.6.4 4-((4-(4-Nitrophenoxy)phenyl)diazenyl)benzene-1,3-diol (SQ5)

Single crystal of resorcinol coupled dye was obtained by slow evaporation of methanol solution of pure product at room temperature. Analysis demonstrated that dye with following empirical formula C_{18} H_{13} N_3 O_5 crystallized out in Monoclinic geometry as $a \neq b \neq c$ and $\alpha=\lambda=90^{\circ}\neq\beta$, having $P2_1/c$ space group. The crystal structure is depicted in Figure 3.4.

The azo enol tautomeric form is predominates as there is no proton on N1 and N2. Cell volume was found to be 1562.00(10) $Å^3$. Analyses showed that unit cell consists of 4 molecules per unit cell as (Z=4). Some significant data regarding crystal is shown in Table 3.15 and 3.16

Intramolecular hydrogen bonging between N(2) and H of oxygen(1) forms five membered cyclic ring which keeps phenyl rings, directly attached with azo group in plane, and other ring attach to nitro group is slightly out of plane.

Table 3.15 Unit cell dimensions of SQ5

Crystal system	Monoclinic
Space group	$P2_1/c$
Formula weight	351.31
Unit cell dimensions	
a = 10.1351(4) Å	α=90°.
b = 5.6345(2) Å	β= 92.605(2)°..
c = 27.3808(10) Å	γ = 90°.

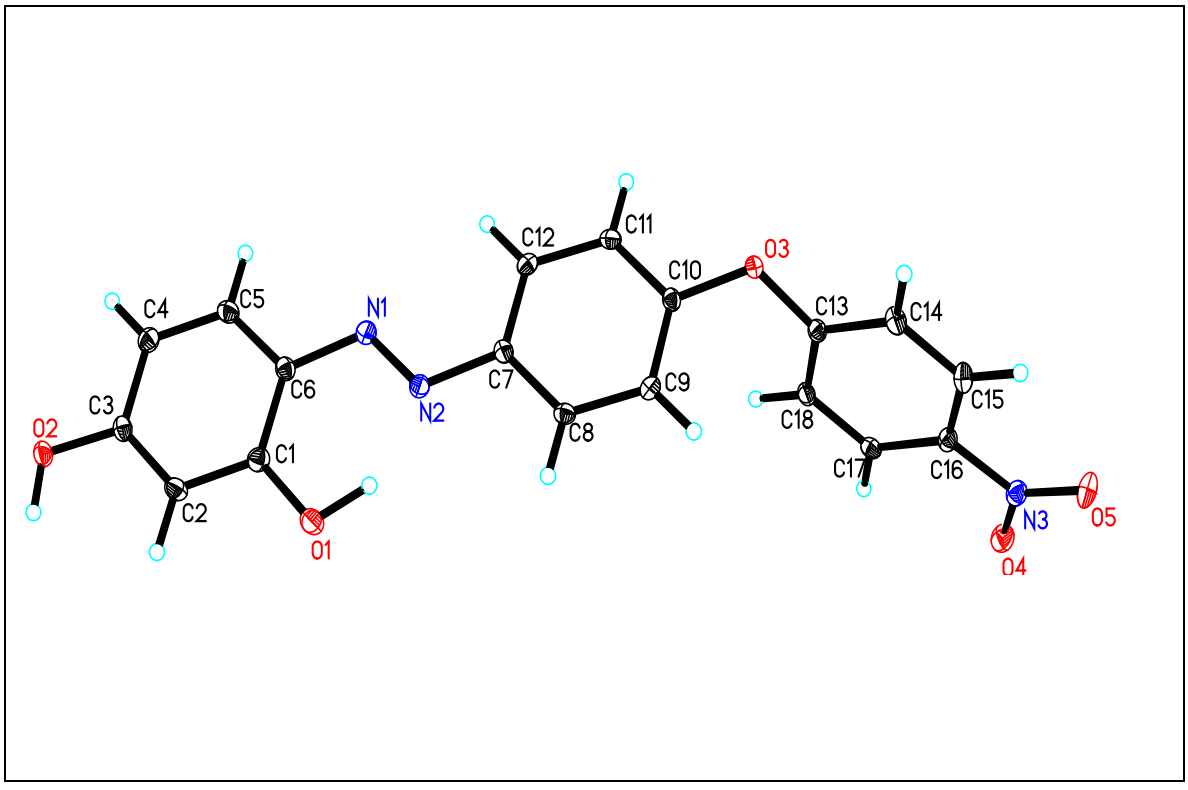

Fig 3.4 Crystal structure4-((4-(4-nitrophenoxy)phenyl)diazenyl)benzene-1,3-diol (SQ5)

Table 3.16 Some important bond lengths and bong angles in SQ5

Bond	Bond length	Bond angle	Degree
O(1)-C(1)	1.3438(18)	C(1)-O(1)-H(1AA)	105.2(15)
O(3)-C(13)	1.3829(18)	N(2)-N(1)-C(6)	115.11(12)
O(4)-N(3)	1.2375(17)	O(5)-N(3)-O(4)	122.71(13)
N(1)-N(2)	1.2755(17)	O(4)-N(3)-C(16)	118.30(12)
N(3)-C(23)	1.4577(16)	O(1)-C(1)-C(6)	121.67(13)
N(3)-C(16)	1.4577(19)	C(3)-C(2)-C(1)	119.63(14)
C(2)-C(3)	1.383(2)	O(2)-C(3)-C(2)	122.00(13)
C(15)-C(16)	1.382(2)	C(2)-C(3)-C(4)	121.35(13)
C(16)-C(17)	1.387(2)	N(1)-C(6)-C(5)	116.26(13)
C(18)-H(18)	0.9500	C(8)-C(7)-N(2)	115.27(13)
O(2)-H(2A)	0.87(3)	C(7)-C(12)-H(12)	120.3

The single crystal analysis of synthesized azo based alcohols provided most important information regarding the predominant taumeric form of alcohol which is summarized below.

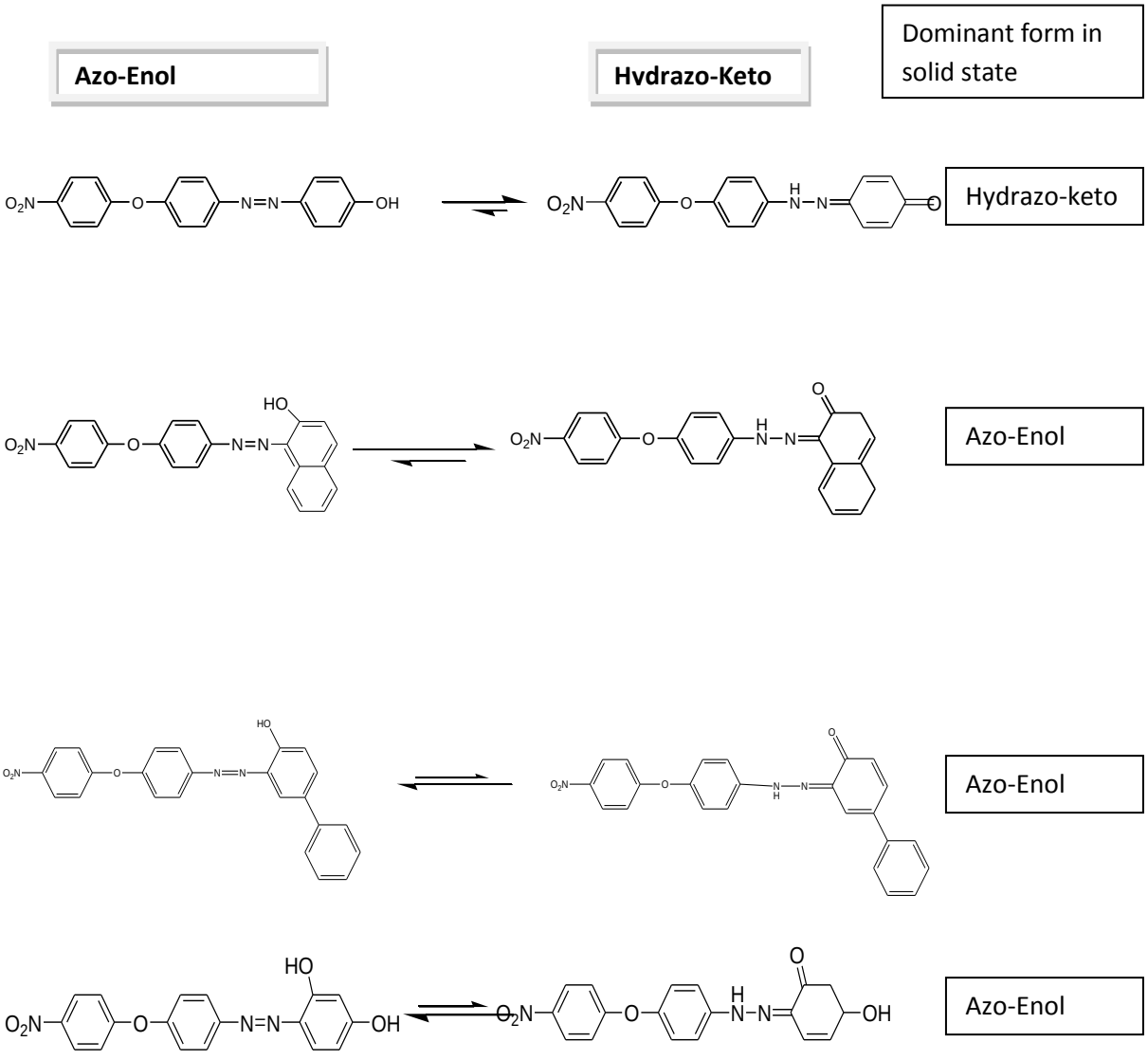

3.2.5.5 Single crystal analysis of 1-((4-(4-nitrophenoxy)phenyl)diazenyl)biphenyl benzoate(SQ_4B)

The single crystal analysis of 1-(nitrophenoxy)phenyl)diazenyl)biphenyl benzoate(SQ_4B) with following empirical formula $C_{31}H_{21}N_3O_5$ demonstrated that compounds crystallized out in Triclinic form as $a \neq b \neq c$ and $\alpha \neq \beta \neq \lambda \neq 90^{o}$.The crystal structure and packing diagram

is presented in Figure 3.5. Space group for the system is P−1. Unit cell volume was found to be 1212.36(6) $Å^3$, and only two molecules present per unit as Z=2. Unit cell dimensions and some important bond lengths and bond angles are shown in Table 3.17 and 3.18 respectively. No intermolecular hydrogen bonding is present between the molecules.

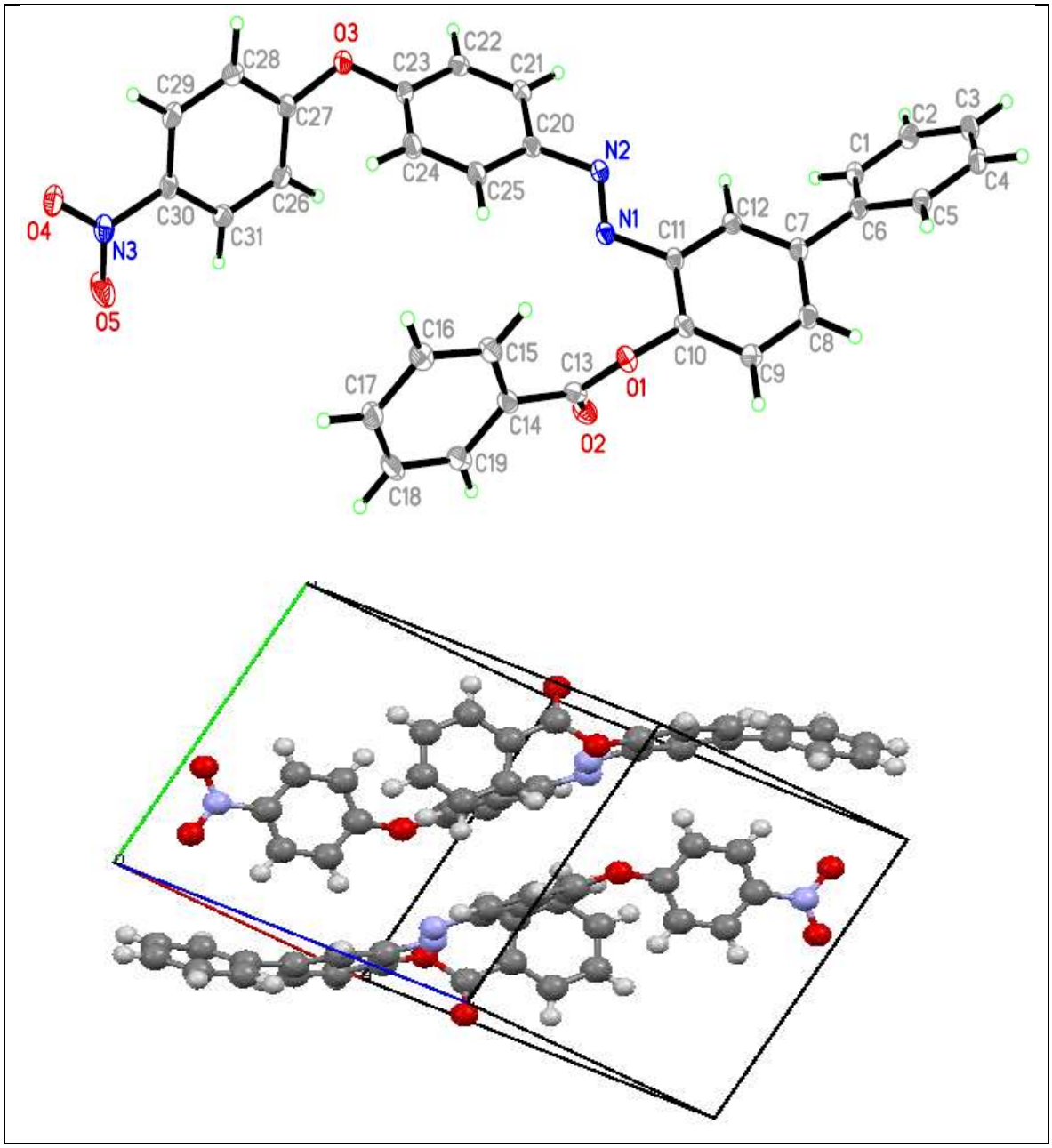

Fig 3.5 Single crystal and packing diagram of (SQ$_4$B)

Table 3.17 Unit cell dimensions of SQ4B

Crystal system	Triclinic
Space group	P-1
Temperature	100(2) K
Unit cell dimensions	
a = 9.9428(3) Å	α=89.74°.
b = 10.2554(3) A	β=74.70°.
c = 12.3673(4) A	γ = 85.43°.

Table 3.18 Some important bond lengths and bong angles in SQ4B

Bond	Bond Length	Bond angle	Degree
O(1)-C(13)	1.3639(16)	N(2)-N(1)-C(11)	114.44(10)
O(2)-C(13)	1.2011(17)	N(1)-N(2)-C(20)	113.36(10)
O(4)-N(3)	1.2239(16)	O(5)-N(3)-O(4)	123.43(13)
N(1)-N(2)	1.2559(16)	O(5)-N(3)-C(30)	118.19(12)
N(1)-C(11)	1.4241(16)	C(3)-C(2)-H(2)	119.8
C(1)-C(2)	1.3885(19)	C(4)-C(3)-C(2)	119.71(13)
C(5)-C(6)	1.4001(19)	C(4)-C(3)-H(3)	120.1
N(3)-C(30)	1.4716(18	C(2)-C(3)-H(3)	120.1
C(6)-C(7)	1.4890(17)	C(10)-C(11)-N(1)	115.19(11)
C(7)-C(12)	1.3957(18)	C(12)-C(11)-N(1)	125.45(12)

3.2.5.6 Single crystal analysis of 4-((4-(4-nitrophenoxy)phenyl)diazenyl)benzene-1,3-benzoate (SQ_5B)

Ester with following empirical formula C_{32} H_{21} N_3 O_7 crystallized out in monoclinic geometrical form with $P2_1/n$ space group. Crystal structure is presented in Fig 3.6**.** Unit

cell dimensions and some important bond lengths and are angles are shown in Table 3.19 and 3.20 respectively. Cell volume was found to be 2646.94(17) Å3 and Z=4 which reveals the presence of molecule in unit cell.

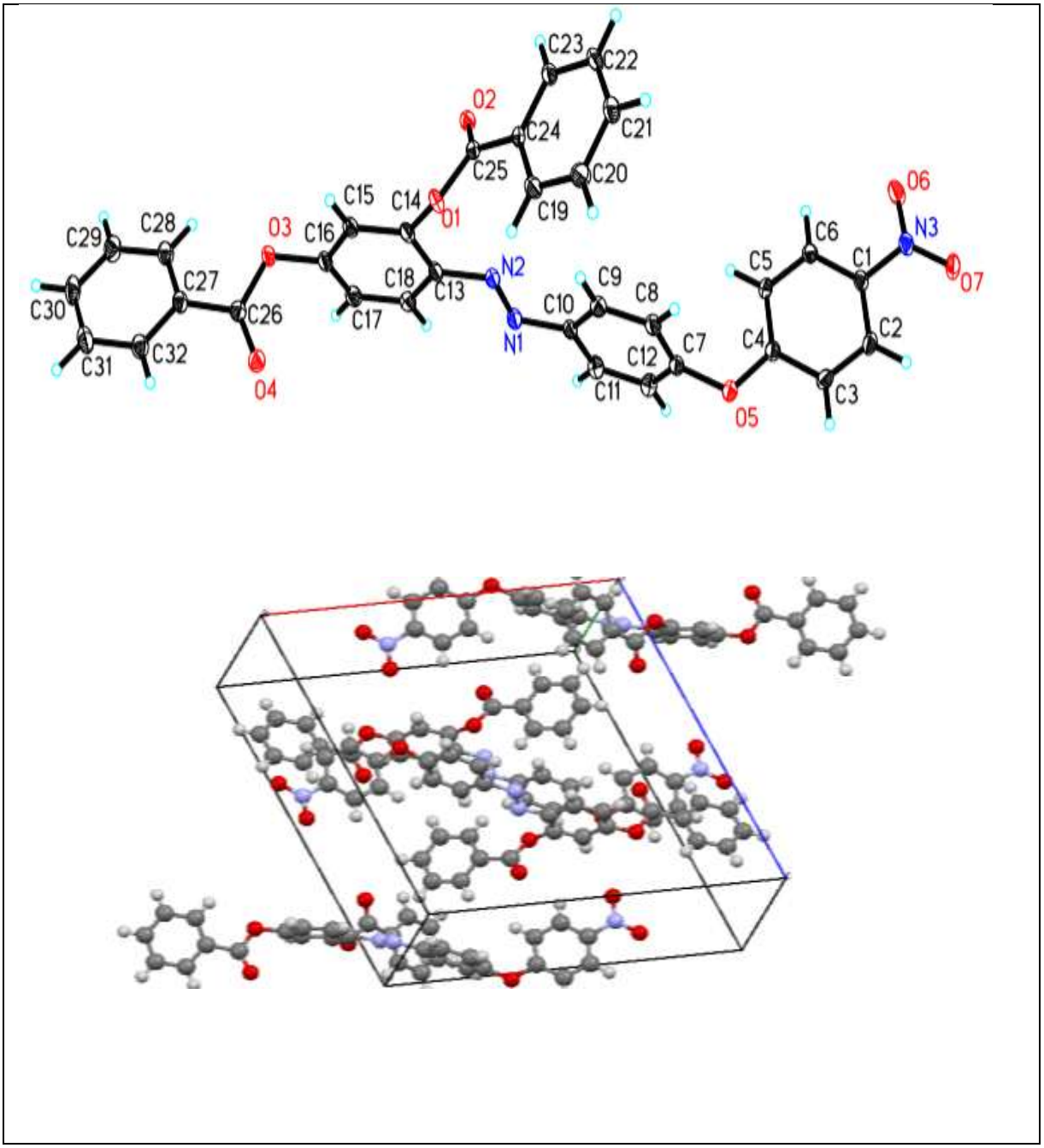

Fig 3.6 Single crystal and packing diagram of (SQ_5B)

Table 3.19 Unit cell dimensions of SQ5B

Crystal system	Monoclinic
Space group	$P2_1/n$
Unit cell dimensions	
a = 16.4444(6) Å	α=90°.
b = 9.9892(4) Å	β=10°6.01
c = 16.7716(6) Å	γ = 90°.

Table 3.20 Some important bond lengths and bong angles in SQ5B

Bond	Bond Length	Bond angle	Degree
O(1)-C(14)	1.396(2)	C(26)-O(3)-C(16)	116.57(13)
O(2)-C(25)	1.198(2)	C(4)-O(5)-C(7)	118.64(13)
O(3)-C(26)	1.368(2)	N(1)-N(2)-C(13)	114.13(14)
O(3)-C(16)	1.407(2	O(7)-N(3)-O(6)	122.98(15)
N(1)-N(2)	1.258(2)	O(7)-N(3)-C(1)	118.94(15)
N(1)-C(10)	1.431(2)	O(6)-N(3)-C(1)	118.08(14)
O(5)-C(4)	1.376(2)	C(6)-C(1)-C(2)	122.22(16)
O(5)-C(7)	1.402(2)	C(6)-C(1)-N(3)	118.24(15)
O(6)-N(3)	1.2327(19)	C(2)-C(1)-N(3)	119.50(15)
O(7)-N(3)	1.2289(18)	C(3)-C(2)-C(1)	118.32(15)

3.3 Applications

3.3.1 Non biological applications:

3.3.1 pH-sensitive colorimetric sensor:

The significance of pH cannot be denied in any field of life whether it is agriculture , pharmaceutical or cosmetic industry, and the most important role in human body cannot be neglected[19, 48]. A slight fluctuation in pH can result in large scale physiological and pathological consequence in the whole system. [49, 50] As a result from many years, designing of new investigation tools for determination of hydrogen ion concentration has captured the attention of researchers. These studies have leads to development of more innovative, more sensitive but less expensive pH sensors**.**

However many fluorescent probe detection methods[51] have been reported for accurate determination of hydrogen ion concentration, but visible colorimetric chemosensors are always broadly welcome, because experimental changes in analyte can be determined with naked eyes.[52, 53]

Dyes having D–π–A azo chromosphere have wider chances of acting as pH-sensitive chemosensors, where D is electron donating group and A is an acceptor group; bridged with π bond of azo group. Often D–π–A types of chromosphere show extended conjugation because of the delocalization of electron on donating and withdrawing group.[54] This electron push pull effect the molecule results in high color fastness and also induces halochromic (change in color upon change in pH) properties in the molecule).

A visible colorimetric pH sensor has been designed based on D–π–A system azo chromospheres. Here in the chemical structure, biphenyl moiety of the coupling component H-acid was acting as donor group and NO_2 was incorporated as electron withdrawing unit. The ideal structure representing a pH-sensitive colorimetric system (SQ_4) having a D–π–A system is shown **Fig 3.7**

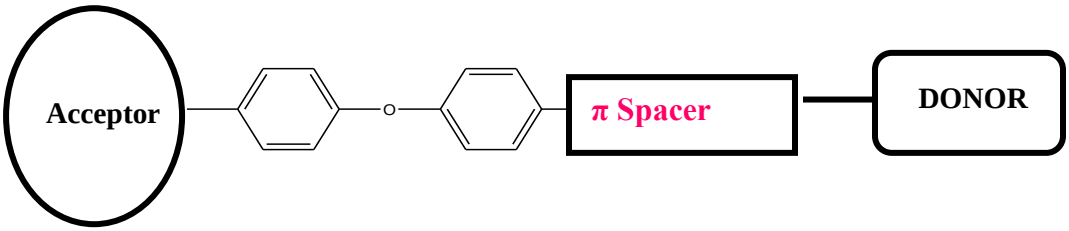

D–π–A Molecular Structure

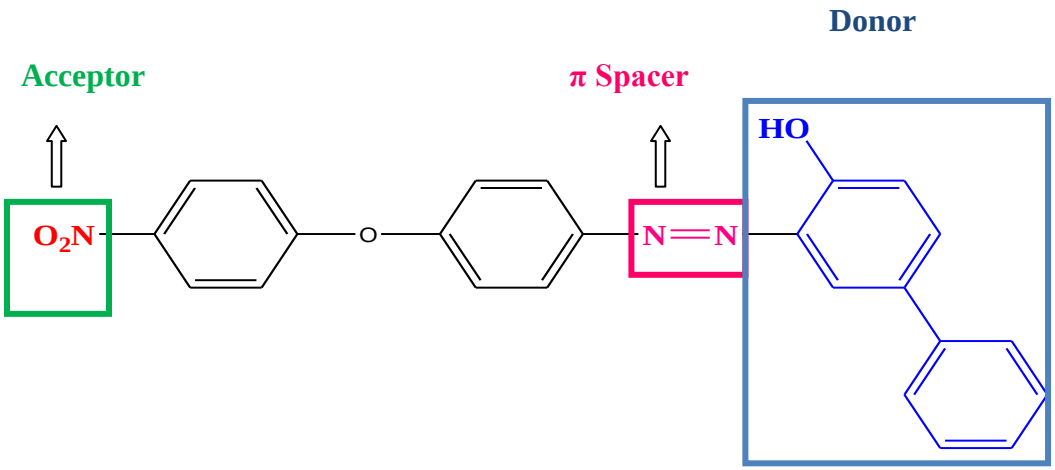

Fig 3.7 Designed molecular structure for SQ4

Spectral investigation and pH-sensitivity of dyes with a D–π–A chemosphere:

A solution (DMSO–water 9:1v/v) of SQ4 was used to explore the pH responsive properties. The effect of pH towards the dye was investigated by observing a reversible and rapid color change from yellow to red at pH 8 and 11**.** Fig 3.8 is representing the vivid change in color of the solution at different pH. A bathochromic of shift 122nm was observed in UV-VIS spectrum the compounds.

For further mechanistic investigation and to study the influence of acid and base on absorption spectrum of the chemosensor, a UV/Vis titration of chemosensor was done with triethylamine (TEA), using (5×10^{-5}mol/L) concentration of chemosensor in 9:1DMSO-H2O system. The dye underwent vivid color change from yellow (399nm) to red (521nm), representing an obvious bathochromic shift of 122 nm. . With increasing pH, a decrease in absorption intensity at 399nm and increase at 521 nm observed as shown in Fig 3.9. Equilibrium between the two species was indicated by the isosbestic point observed at 460nm.

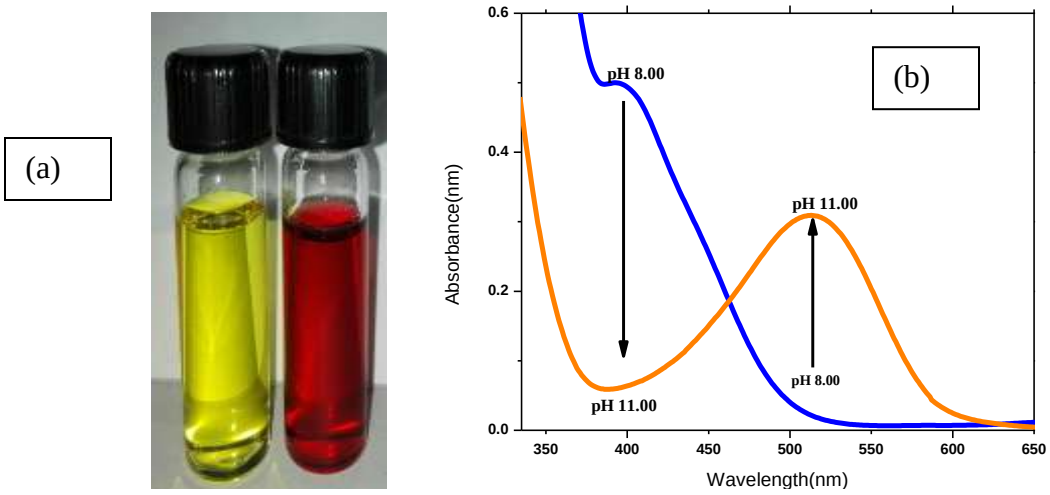

Fig 3.8 (a) Photograph of colorimetric compound (SQ4) at different pH (b) and UV/ Vis spectra (3× 10^{-5}mol/L) in DMSO at two different pH

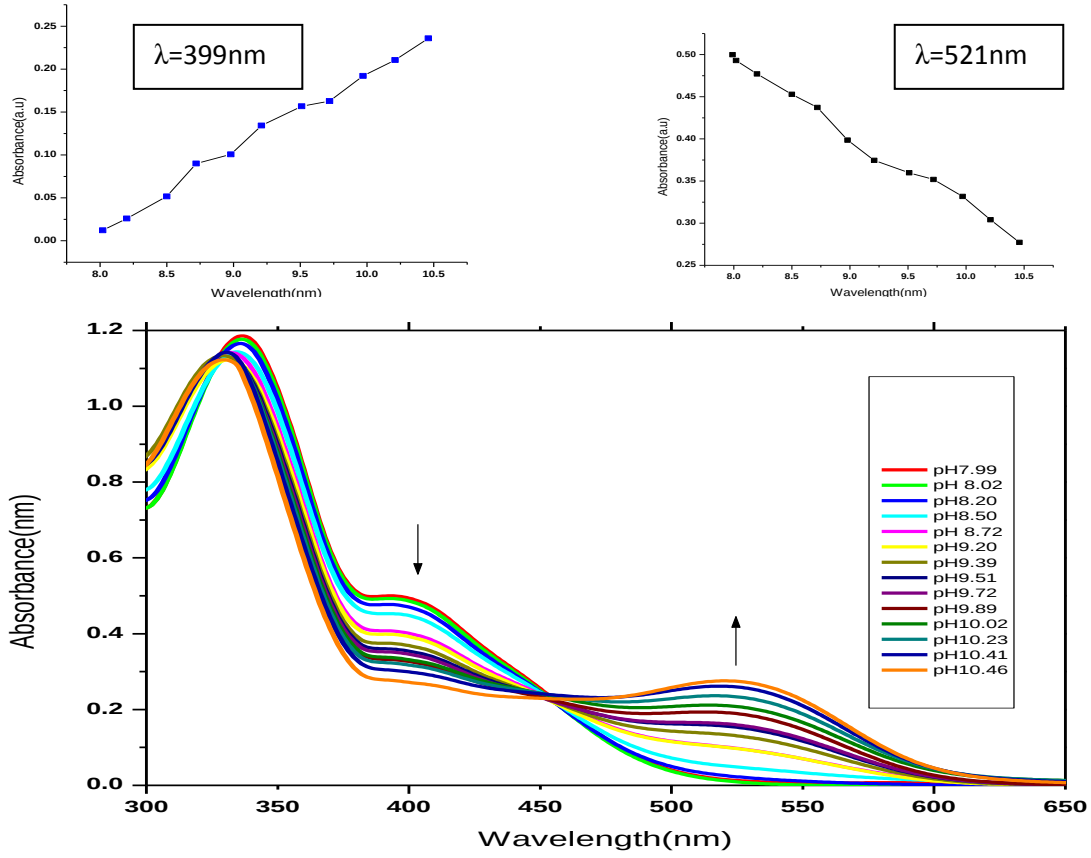

Fig. 3.9 (a) pH-dependent value of absorbance at (399 nm); (b) pH-dependent value of absorbance at 521 nm; (c) UV/Vis absorption spectra of dye (5× 10^{-5}mol/L) at varying pH in DMSO solution containing 10% water.

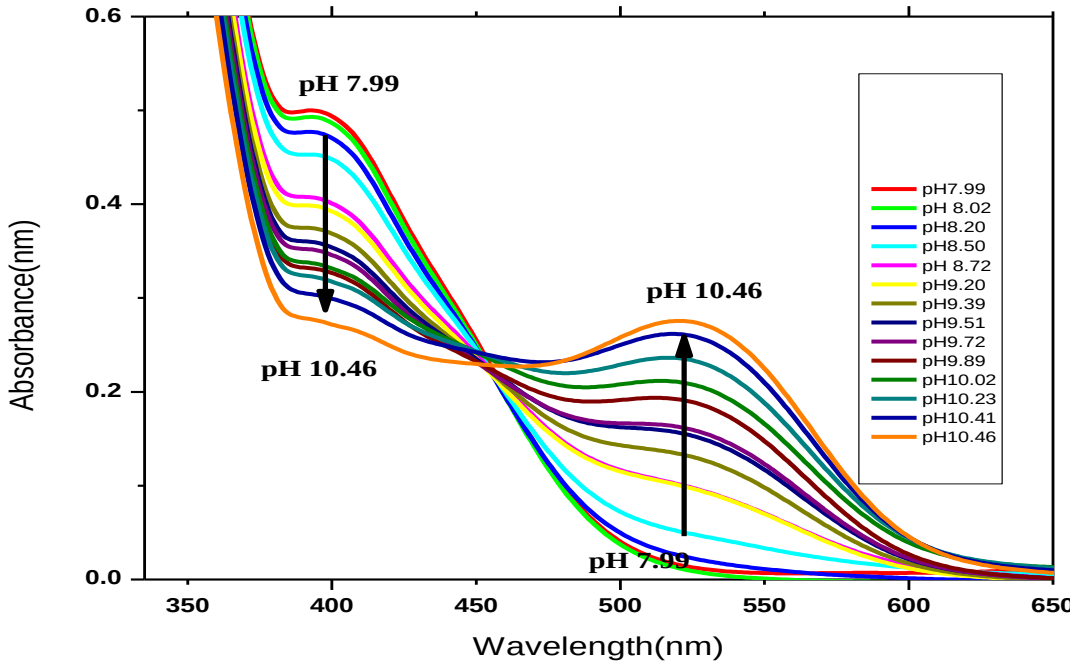

Fig 4.3 A clear view of bathochromic shift

Proposed pH-sensitivity mechanism for the chemosensor dye:

Mechanism for this bathochromic shift in chemosensor can be explained on the basis of its structural features. Since chemosensor has biphenyl 4-ol moiety in its chemical structure, having that aptitude to interchange between phenol and phenolate form in acidic and basic media respectively; leading to significant change in optical and physiological properties of the compound. Upon increasing pH, deprotonation of biphenyl -4 ol occur converting in to active phenoxide, this deprotonation affect the electronic properties of chromospheres because of increased conjugation and induced some new charge transfer intramolecular interaction leading to visible color change and shifting λ_{max} in UV/Vis spectrum.

Further the shift can be explained on the basis of increased stabilization of the excited state comparative to the ground state because of increased polarity of the solution system, which minimizes the energy gap between excited and ground state leading to positive slovatochomism (bathochromic shift).Thus intramolecular charge transfer, rearrangement versus isomerization can be the reasons of this spectral changes Fig 3.10.

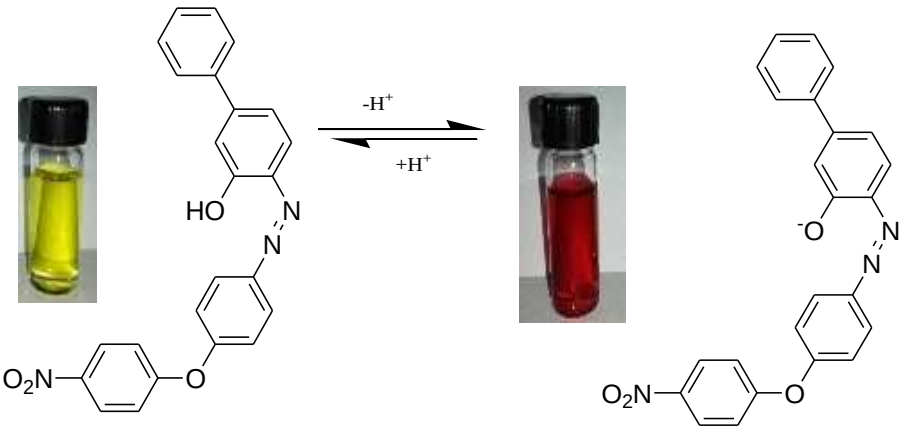

Fig 3.10 Equillibrium between azo –enol and azo-enolate

Reversibility Test:

Investigation about the reversibility of the chemosensor was done by changing the pH between 8 to 11 and then reverses to the 8 for over 4 rounds, using saturated sodium hydroxide and Hydrochloric acid as shown in Fig 3.11 Accordingly expectation different colors of medium reappeared at repetition of cycle and response time was less than 1 second. This study indicate that the change in color of chemosensor was fast responsive and fully reversible over a narrow PH range

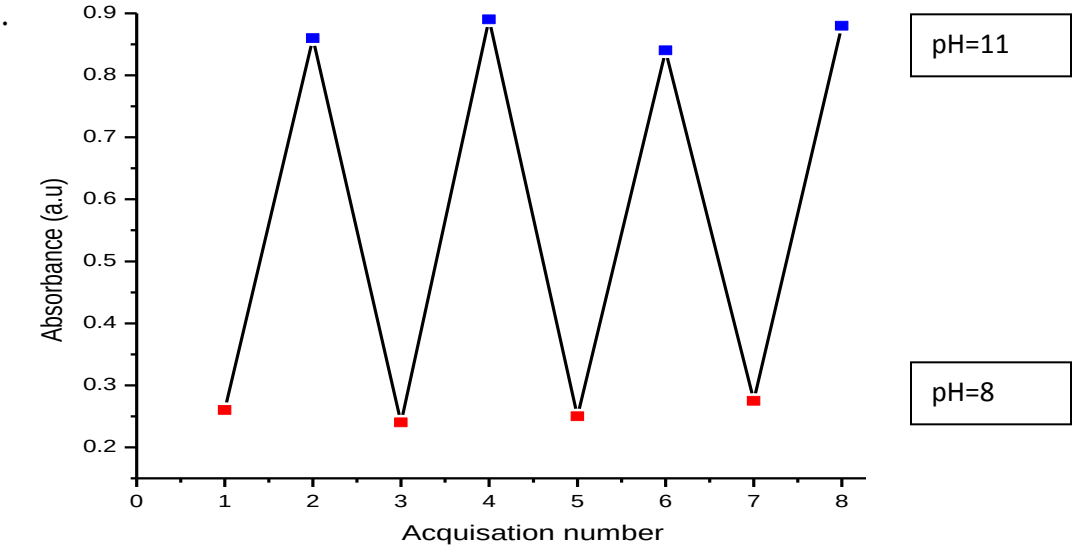

Fig 3.11 Reversibility of color change (measured at 521nm)

3.3.2. Photoisomerization investigation:

On the basis of azo moiety, photoisomerization phenomenon was investigated in all the synthesized compounds, and positive results were obtained. Trans configuration of azo containing compounds showed high intensity of absorption in UV region due to π to π* transition and a weaker band in visible region due to n- π* transition. In actual n- π* transition is forbidden in trans configuration according to the symmetry rules, but allowed in less stable cis configuration. [55]

After irradiating the compounds solution with 350 nm UV light for controlled varying time scale, a decrease in intensity of absorption in 300-400 nm region, and increase in absorption in visible region was observed, which confirmed the conversion of trans configuration to cis one. Spectra of some representative dyes and ester are show in Fig (3.12), (3.13) and (3.14).

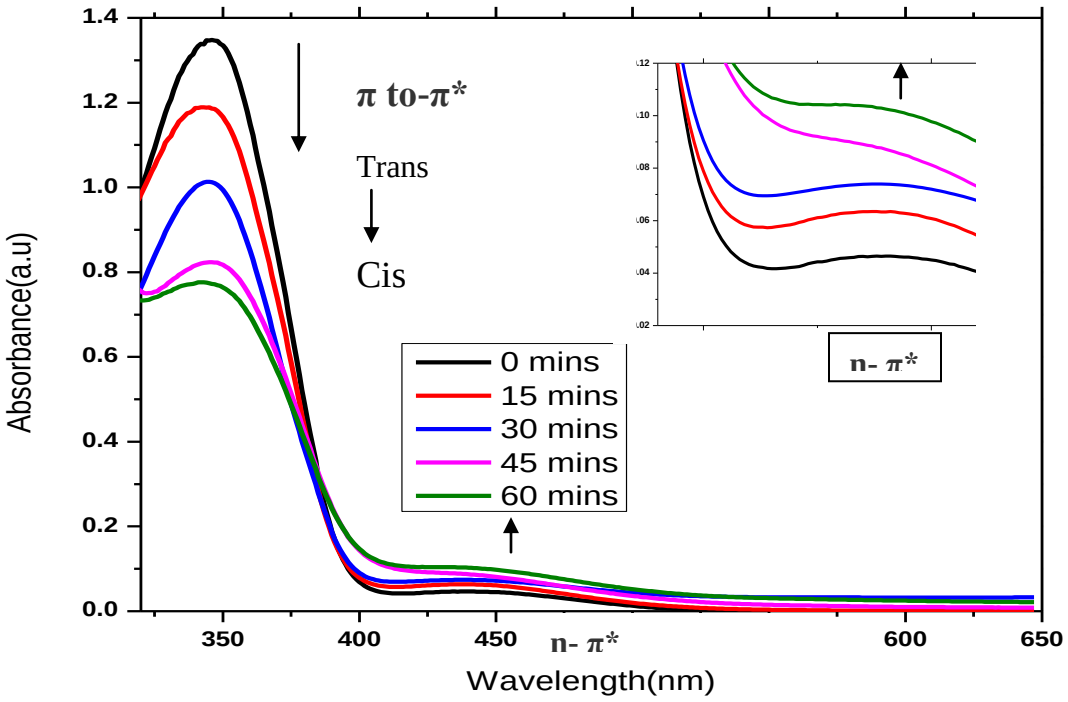

Fig 3.12 Photo-induced isomerization in SQ5 recorded as a time sequence
The arrows in spectra indicate the direction of the peak movement during the reaction.

In SQ5 ester decrease in absorption intensity at 350 cm^{-1} (π to π*) and increase a peak at 450cm^{-1} (n to π*) confirms the trans to cis isomerization. Similar effect was also

observed in the spectra of SQ1B ester and SQ4 azo alcohol. Photoisomerization in these compounds is reversible and it was confirmed by placing these solutions in dark and recording spectra, which revealed the back conversion of cis form to trans form. According to the literature both out of plane rotation of N=N and in plane inversion mechanistic pathway is possible for photoisomerization[56]

Relying on these results it can be concluded that these compounds are photoactive and this property can lead them to be use in molecular switches, photosensitive devices such as intelligent enzymes, as smart polymers or liquid crystals.

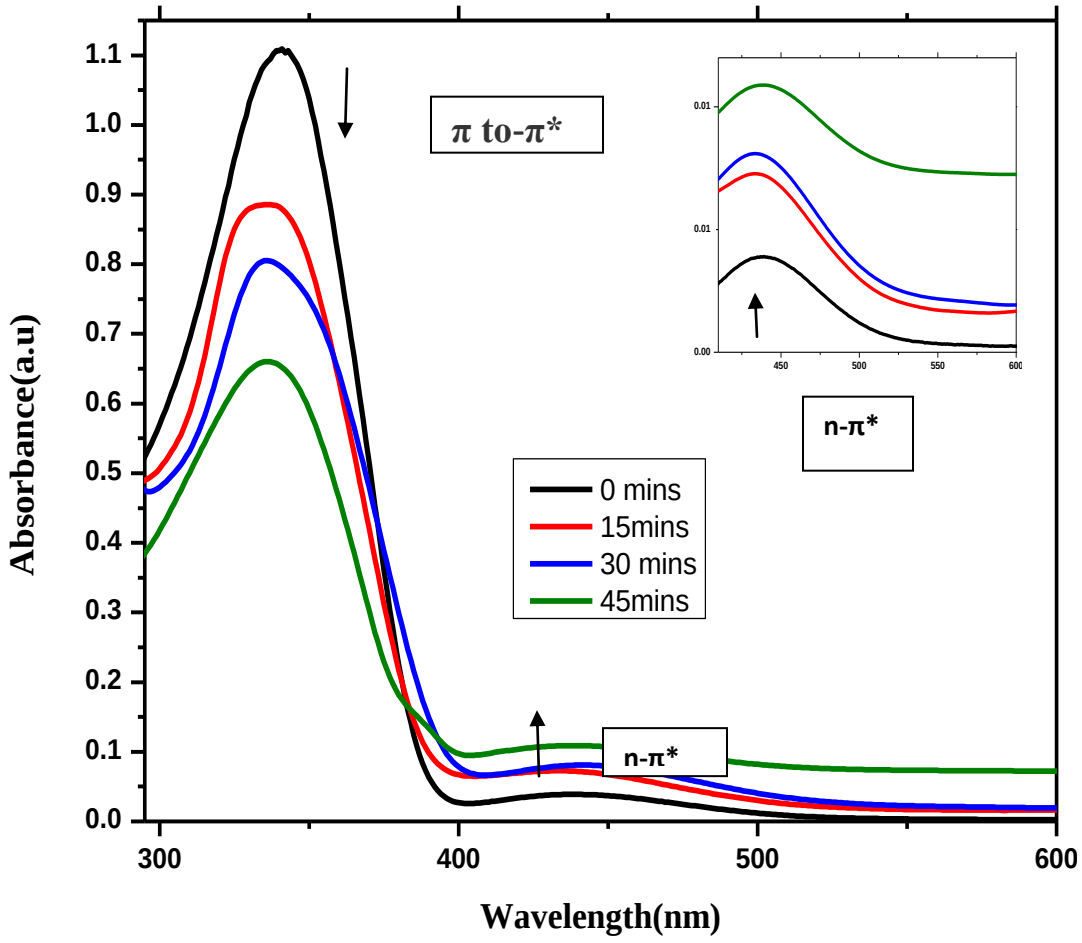

Fig 3.13 Photo-induced isomerization in SQ1B ester recorded as a time sequence. The arrows in spectra indicate the direction of the peak movement during the reaction.

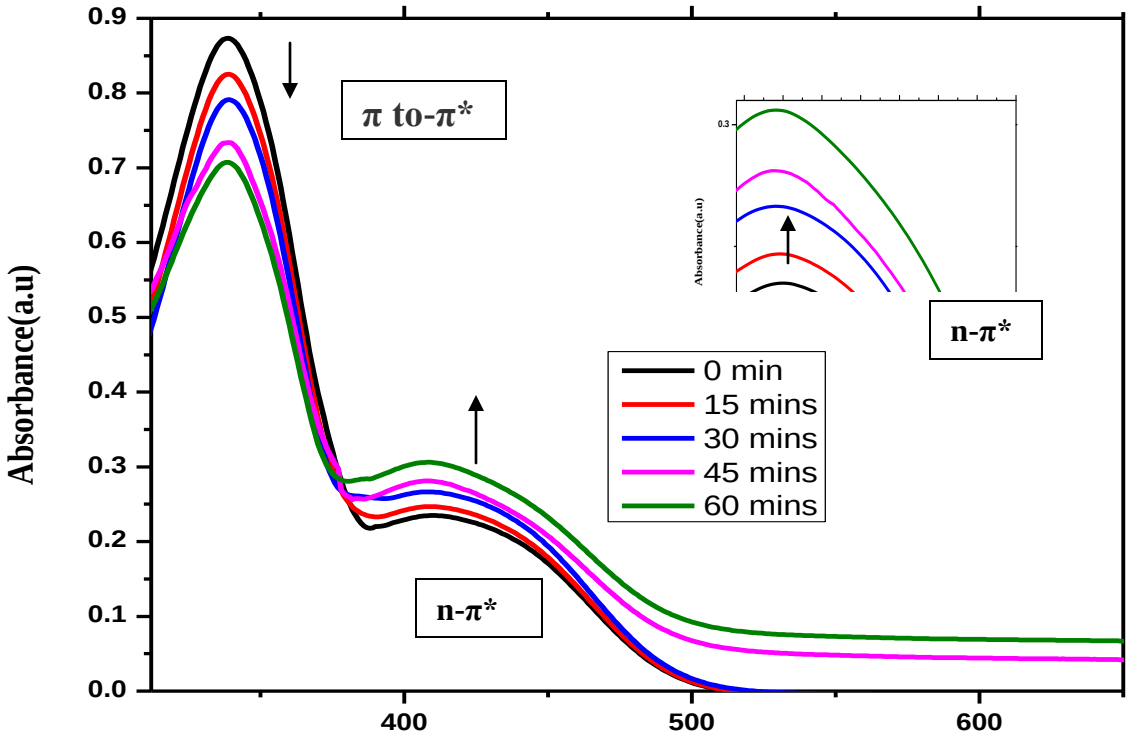

Fig 3.14 Photo-induced isomerization in SQ4 azo-alcohol recorded as a time sequence.

Biological applications

3.3.3 DNA-binding investigation using UV-Vis spectroscopic technique:

The relative DNA binding of dye and their ester was studied using electronic absorption spectroscopic technique employing 5 mmol tris-HCl /50 mmol NaCl buffer (pH7.2).The Calf thymus DNA solution gave ratio of absorbance 1/1.8 at 260 and 280 nm which gave indication that DNA solution is sufficiently free from protein[57]. The concentration of DNA was investigated by its absorption peak at 260 nm using $6600M^{-1}cm^{-1}$ molar extension coefficient

The absorption titration was performed by using constant concentration of dyes and ester and varying concentration of CT-DNA from 0-200 ul. The samples were allowed to incubate for 5 mins before taking each spectrum.

Relying on variation in absorbance intrinsic binding constants of the compounds were calculated following **Benesi-Hinderbrand Equation [55]**

$$\frac{[DNA]}{\varepsilon a - \varepsilon f} = \frac{[DNA]}{\varepsilon b - \varepsilon f} + 1/Kb(\varepsilon b - \varepsilon f)$$

Where [DNA] = concentration of DNA

Kb =Binding constant (Product of slope and intercept)

εa =is calculated by taking ratio of A_{obsd}/Compound

εf=Extintion cofficeint of non-bonded/ free compound

εb= Extintion coefficient of fully bounded form

A hyprochromic shift in absorbance was observed for all the dyes and ester. Theses investigation revealed the fact that, upon varying the concentration of DNA all the azo alcohols and esters undergo hypochromism (decrease in intensity of absorption) with red shift of 2 to5(nm).These effect on UV/VIS spectra suggests intercalating binding mode [58].

The spectrum of SQ2 is shown in Fig (3.15). In the visible region two peaks were observed indicating equilibrium established between the azo-enol and hydrazo-keto form in solution. The λ_{max} observed at 476nm with 0.66 absorption intensity was due to n-π* transition of azo group. After titrating with a DNA, absorption intensity was decreased up to 0.53 with a bathochromic shift of 5nm.

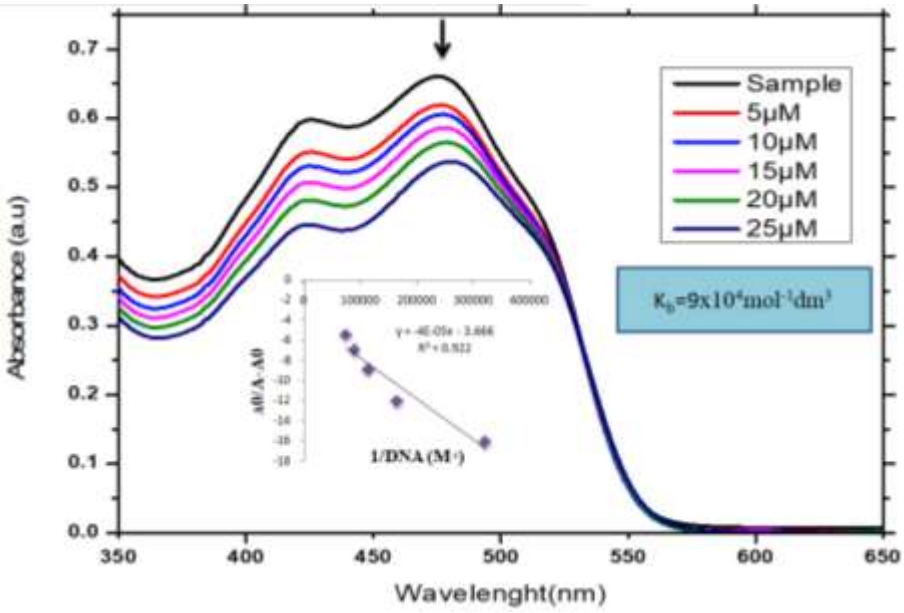

Fig 3.15 DNA binding spectra of SQ_2 (1×10^{-5} mol/dm^3) without and with DNA

The value of binding constant **9 x10^4 (M^{-1})** which also suggest the intercalating binding mode. Similar spectra for SQ4 is shown in Fig (3.16). Two peaks are observed, one intense peak at 337 nm is due to π-π* and shoulder is assigned to n- π*. Upon adding DNA, due to hypochromism intensity of absorption decrease from 0.7021 to 0.5869 with a bathochormic shift of 2nm, again suggesting intercalating mode of DNA binding. The calculated binding constant of **5.8 ×10^4 (M^{-1})** also suggest intercalating mode.

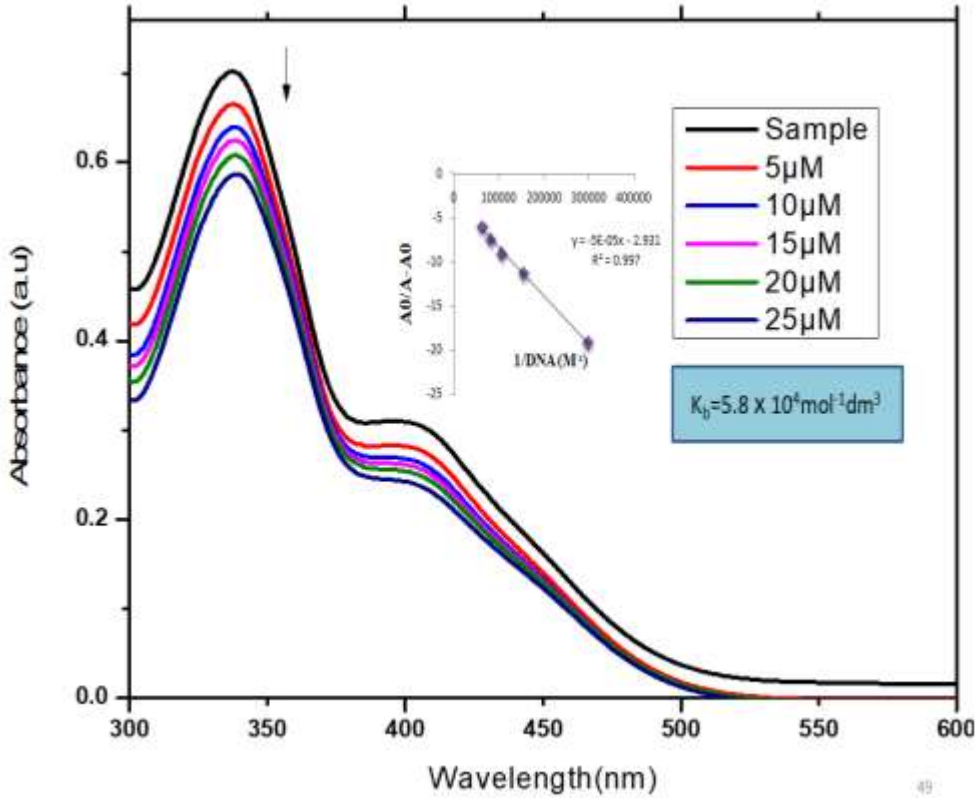

Fig 3.16 DNA binding spectra for SQ4 (1× 10^{-5} mol/dm^3) without and with DNA

Similarly absorption spectrum for SQ5 with varying concentration of CT-DNA represented in Fig (3.17). Upon increasing DNA concentration absorption intensity at 341 nm was decreased from 1.5748 to 1.2432 with a bathochromic shift of 2 nm, indicating a intercalative DNA binding mode. Greater value of K_b also suggests **6.0×10^4 (M$^{-1)}$** intercalating binding mode.

Such intercalating binding mode of azo alcohols can be interpreted on the basis of their chemical structure, having potential of strong hydrogen bonding between nitrogenous bases. Strong hydrogen bonding between the lone pair of azo group and DNA, depress in n- π^* transition leading to hypochromism. This hydrogen bonding leads to hindering the rotation of azo group and increases the probability of planarity within the molecule.

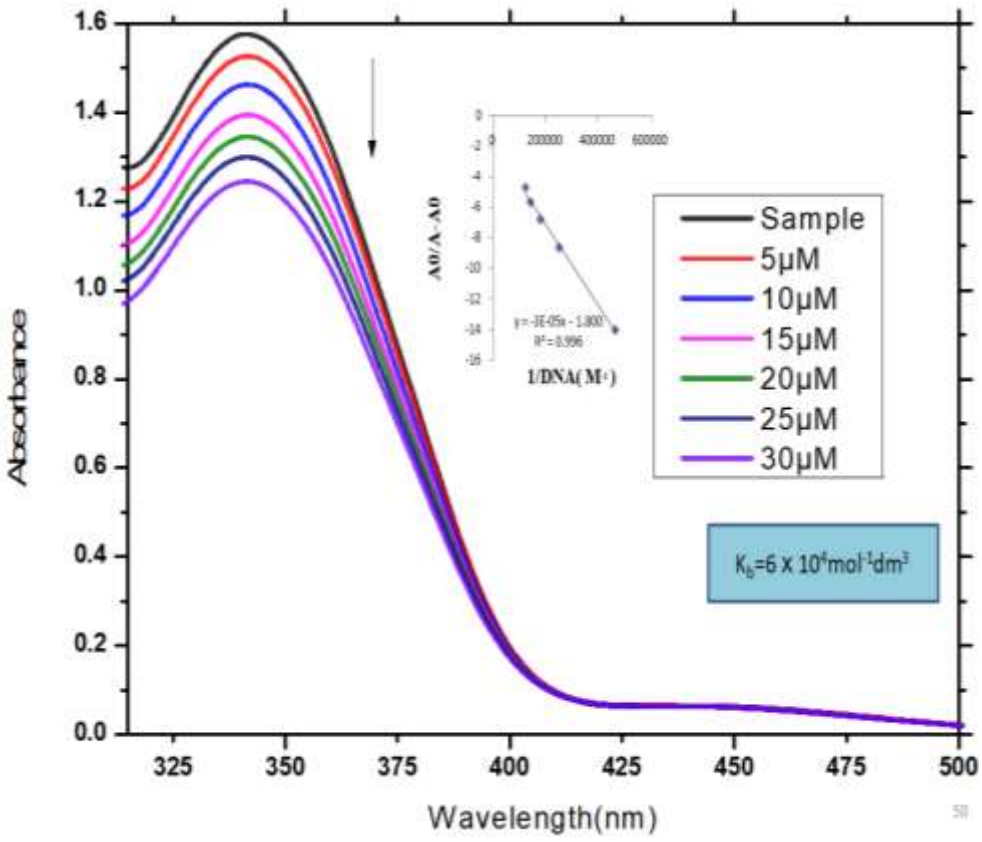

Fig 3.17 DNA binding spectra for SQ5 (1×10^{-5} mol/dm^3) without and with DNA

As planarity is the key feature for intercalating bind mode.[59] Planarity in the molecule increases the chances of penetration of azo alcohol in DNA strain causing stretching of DNA double helical structure. Expansion of DNA also explains the hypochromism effect[60, 61].However on the basis of mixed structural features (planarity ,nonplanairty) azo alcohols and the presence of phenolic (-OH) group which have strong affinity hydrogen bonding with backbone of DNA we suggest mixed binding mode for these azo alcohols with dominant intercalating mode[62]

In comparison to azo alcohols; azo esters showed a slight hypsochromic effect (blue shift) along with hypochromism, suggesting major or minor groove binding or surface binding to the DNA. The spectrum of SQ5B is shown in Fig (3.18) .The λmax was observed at 390nm with absorption intensity 0.7493. DNA titration resulted in decrease of absorption intensity; to 0.5848 with a blue shift of 4 nm indicating groove binding. The value of binding constant $\mathbf{K_b}$ $\mathbf{1.2\times10^4(M^{-1})}$ also suggest groove or surface binding.[63]

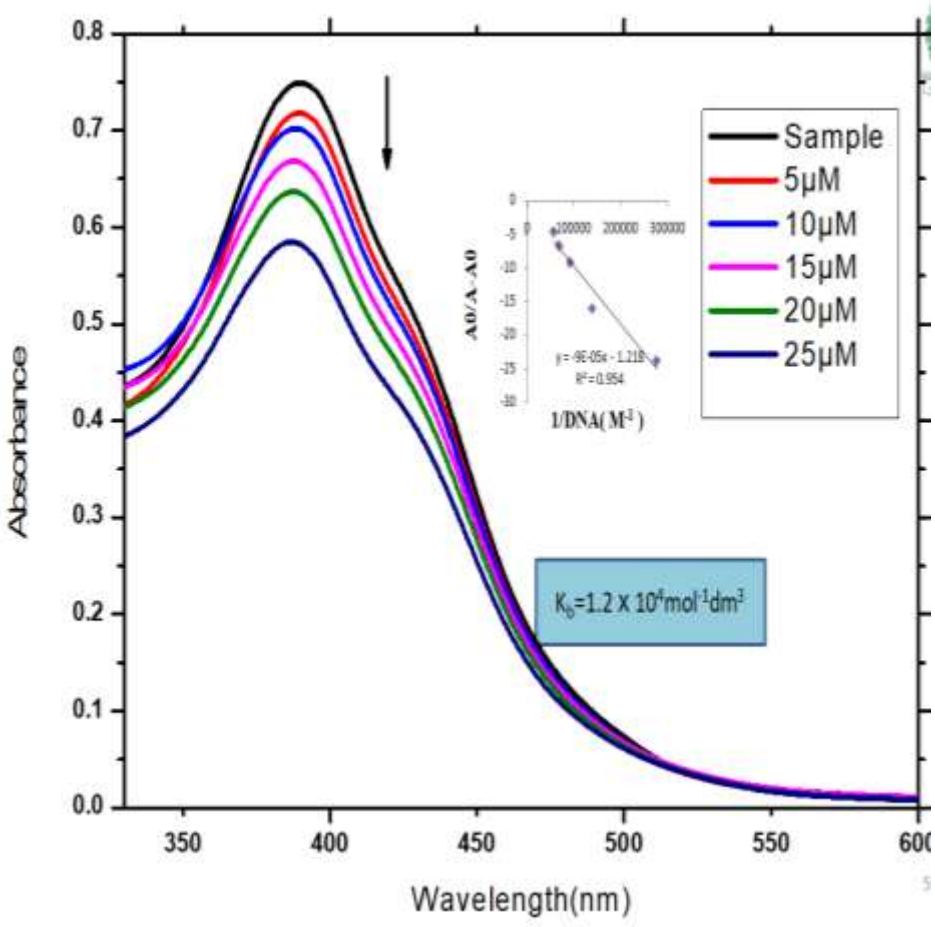

Fig 3.18 DNA binding spectra for SQ1B (1×10^{-5} mol/dm^3) without and with DNA

3.3.4 DPPH free radical scavenging activity:

2,2-Diphenyl-1-Picrylhydrazyl is actually a free radical that can take up an electron from that antioxidants leading diamagnetic compound which show different physical property

from the previous one. Its stable free radical form show λ_{max} at517nm, having intense violet color because of extended delocalization of the free electrons. But when DPPH is reduced during the assay by accepting electron from antioxidant its color changes from violet to yellow. The color change leads to decrease in absorption at 517 nm which is indirect measure of free radical-scavenging aptitude of the compounds or simply it measures the antioxidant potential of the compounds.[64]

The antioxidant activity has been broadly used to analyze the compound to be active as free-radical scavengers or proton donors. According to the Pub Med database this assay has been employed in more than 850 studies from the previous 50 years.[65]

Synthesized azo dyes and esters were examined to assess antioxidant capability following the reported method. The scavenging effect is expressed as inhibition percentage and following equation was used to calculate the scavenging effect.

$$\% \text{ Scavenging effect} = \frac{Acontrol - Asample}{Acontrol} * 100$$

Here Acontrol is absorbance of the reagent solution without test compound

The result acquired from the DPPH assay is presented in Fig 3.19 and 3.20**.** Significant variation was observed between the results of dyes and esters. The dyes have been observed to have significantly high free radical scavenging activity as compare to esters. The noticeably high antioxidant activity of the Azo alcohols (**up to 75%**) can be interpreted on the basis of their chemical structure. Since all the dyes have phenolic moiety, having (-OH) group in the structural pattern which can easily donate its H atom to DPPH radical to convert it into its diamagnetic form[66]. Further presence of aromatic moiety with oxygen atom would lead to stabilization of phenoxide radical of the dye formed, and thus, improves antioxidant activity of the dyes. Furthermore presence of NO_2 group in the chemical structure also enhances antioxidant potential of the dye regarding its electron withdrawing effect on the OH group. Highest activity observed for **SQ5** can be related to presence of 2 OH groups in the structural pattern.

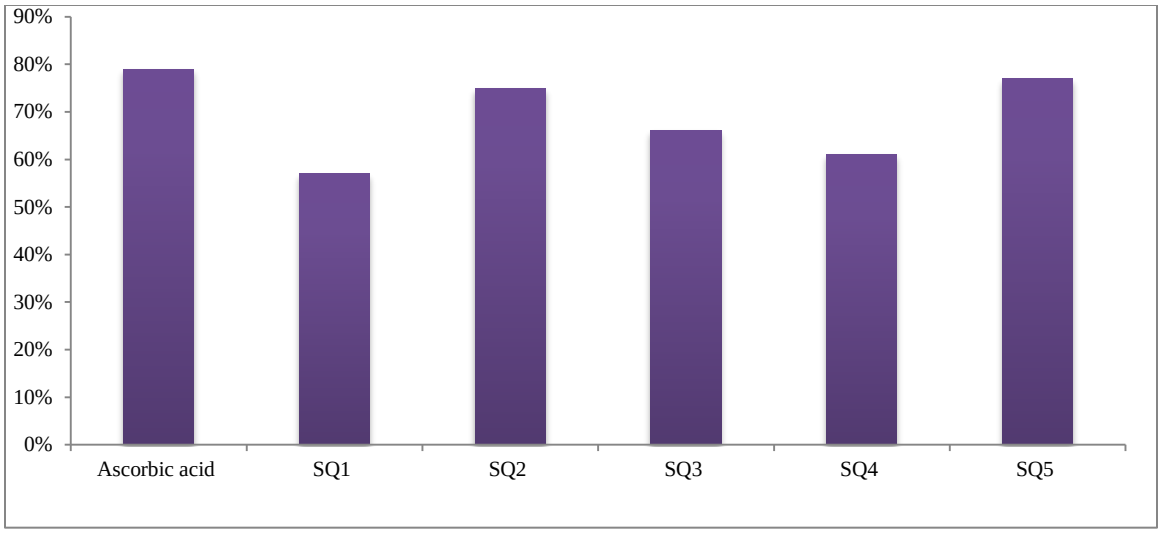

Fig 3.19: Graphical representation of DPPH free radical scavenging activity of azo alcohols

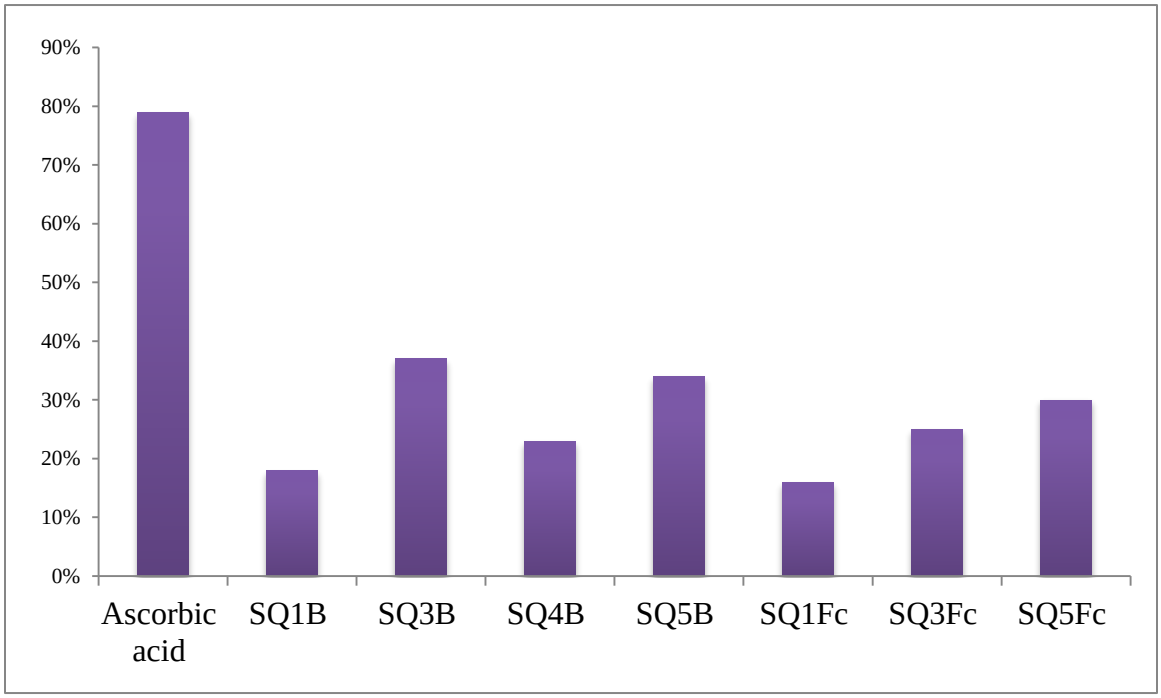

Fig 3.20 : Graphical representation of DPPH free radical scavenging activity of azo esters

In comparison to azo alcohols, Azo Esters showed very poor antioxidant activity (up to 39%),as there was no labile H atom was further present in ester. Ferrocenyl based ester SQ1Fc, SQ3Fc, SQ4Fc displayed minimum activity because of further decrease in

lability of H atom due to electron donating behavior of Ferrocenyl moiety.

3.3.5 Hydrogen peroxide scavenging activity:

Hydrogen peroxide scavenging activity relies on the formation of water and oxygen by a reduction reaction between H_2O_2 and antioxidant specie. This activity was investigated in both azo alcohols and esters and according expectations azo alcohols were observed to show very high antioxidant activity because of labile hydrogen atom in their chemical pattern. Gallic acid was used as standard Fig 3.21. SQ_5 revealed the highest activity because it has hydroxyl group in chemical structure at ortho and para position to the azo group[67].

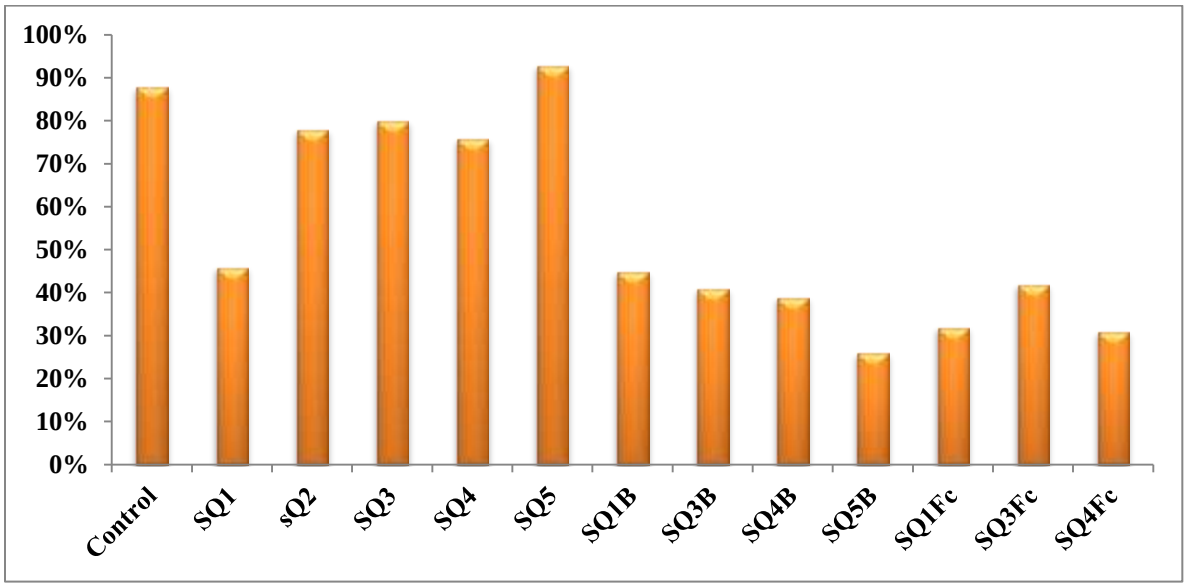

Fig 3.21: Graphical representation of H_2O_2 free radical scavenging activity of azo alcohols

CONCLUSIONS:

A new class of azo alcohols was successfully synthesized by diazotization of 4,4-nitrophenoxyaniline. Further two, new series of esters were formed by the condensation of azo alcohols. Compounds were characterized by physical techniques, IR, NMR and single crystal analysis. In IR study, appearance of OH peak at 3300-3400 cm^{-1} and (C=O) stretch at (1730-1735 cm^{-1}) confirmed the formation of azo alcohols and esters respectively. Similarly in ^{1}HNMR appearance of signal at 10 ppm corresponding to -OH confirmed the formation of alcohol. In ^{13}CNMR appearance of signal at 164-165 ppm corresponding to carbonyl carbon confirms the formation of ester. All the azo–alcohols and esters were completely soluble in DMSO and DMF while showed less solubility towards organic solvent like n-hexane, pet ether and diethyl ether. SQ4 showed reversible chemosensing property in a specific pH range of 7.99-10.46 with a naked eye color change from yellow to red. Cis–Trans conformational changes were observed in all azo compounds and they can be used as photoswitchers with further mechanistic investigation.

DNA binding studies were also performed for all these compounds. Studies suggested both intercalative and groove binding mode for azo alcohol and only groove binding for azo esters. Antioxidant aptitude to the compounds was assessed by DPPH free radical and H_2O_2 scavenging method. High activity observed for azo alcohols might be attributed of presence of (-OH) group in chemical structure, studies showed that these compounds can used to design new antioxidant tools.

REFERENCES:

1. Mohammadi, A., Ghafoori, H., Ghalami, B., Rohinejad, R. *Synthesis, solvatochromic properties and biological evaluation of some novel azo-hydrazone tautomeric dyes*. Journal of Molecular Liquids. **2014**;198:44-50.
2. Racane, L., Mihalic, Z., Cernc, H., Popovic, J., Tralic, V. *Synthesis, structure and tautomerism of two benzothiazolyl azo derivatives of 2-naphthol: A crystallographic, NMR and computational study*. Dyes and Pigments. **2013** ;96(3):672-8.
3. Qiu, J., Tang, B., Zhang, S. *Stable diazonium salts of weakly basic amines—Convenient reagents for synthesis of disperse azo dyes.* Dyes and Pigments. **2017**;136:63-9.
4. Khera, R.A., Iqbal, M., Tahir, M.A., Hanif, M.A., Langer, P. *One Pot Synthesis and Characterization of Mono and Di-Substituted Azo-Containing Amides*. Asian Journal of Chemistry. **2015**;27(6):2001-4.
5. Menek, N., Basaran, S., Turgut, G., Odabasoglu, M. *Polarographic and voltammetric investigation of 3-allyl-4-hydroxyazobenzene.* Dyes and Pigments. **2004**;61(1):85-91.
6. Refat, M.S., El-Deen, I.M., Anwer, Z.M., El-Ghol, S. *Spectroscopic studies and biological evaluation of some transition metal complexes of Schiff-base ligands derived from 5-arylazo-salicylaldehyde and thiosemicarbazide*. Journal of Coordination Chemistry. **2009**;62(10):1709-18.
7. Gong, C., Yang, Y., Yang, Y., Zheng, A,, Liu, S., Tang, Q. *Photoresponsive hollow molecularly imprinted polymer for the determination of trace bisphenol A in water. Journal of Colloid and Interface Science*. **2016**;481:236-44.
8. Sava, I., Sacarescu, L., Stoica, I., Apostol, I., Damian, V., Hurduc, N. *Photochromic properties of polyimide and polysiloxane azopolymers.* Polymer International. **2009**;58(2):163-70.
9. Ciminelli, C., Granucci, G., Persico, M. *The Photoisomerization Mechanism of Azobenzene: A Semiclassical Simulation of Nonadiabatic Dynamics.* Chemistry – A European Journal. **2004**;10(9):2327-41.

10. Biswas, M., Burghardt, I. *Azobenzene Photoisomerization-Induced Destabilization of B-DNA*. Biophysical Journal. **2014**;107(4):932-40.
11. Mallakpour, S., Rafiemanzelat, F., Faghihi, K. *Synthesis and characterization of new self-colored thermally stable poly(amide-ether-urethane)s based on an azo dye and different diisocyanates*. Dyes and Pigments. **2007**;74(3):713-22.
12. Carlescu, I., Scutaru, A.M., Apreutesei, D., Alupei, V., Scutaru, D. *The liquid crystalline behaviour of ferrocene derivatives containing azo and imine linking groups.* Liquid Crystals. **2007**;34(7):775-85.
13. Yin, J., Guan, J., Mei, F., Liu, S.H. *Synthesis and properties of conjugated bimetallic ruthenium complexes with σ,σ-bridging azobenzene chains.* Journal of Organometallic Chemistry. **2005**;690(19):4265-71.
14. Antonov, L. *Tautomerism: Methods and Theories*: John Wiley & Sons; 2013.
15. Kelemen, J., Moss, S., Glitsch, S. *Azo-hydrazone tautomerism in azo dyes. IV. Colour and tautomeric structure of adsorbed 1-phenylazo-2-naphthylamine and 1-phenylazo-2-naphthol dyes.* Dyes and Pigments. **1984** ;5(2):83-108.
16. Rauf, M., Hisaindee, S., Saleh, Ni. *ChemInform Abstract: Spectroscopic Studies of Keto—Enol Tautomeric Equilibrium of Azo Dyes* **2015** ;107(4):932-40.
17. Ball, P., Nicholls, C.H. *Azo-hydrazone tautomerism of hydroxyazo compounds—a review*. Dyes and Pigments. **1982**;3(1):5-26.
18. Hamidian, K., Irandoust, M., Rafiee, E., Joshaghani, M. *Synthesis, Characterization, and Tautomeric Properties of Some Azo-azomethine Compounds* Dyes and Pigments **2012;**34(7):775-85.
19. Wang, Y., Tang, B., Zhang, S. *A visible colorimetric pH sensitive chemosensor based on azo dye of benzophenone*. Dyes and Pigments. **2011**;91(3):294-7.
20. Zhang, X., Gooch, J., Sun, W., Wang, H., Wang, K. *Photo- and pH-sensitive azo-containing cationic waterborne polyurethane.* Polymer Bulletin.**2015**;72(4):881-95.
21. Park, J., Kim, S.H., Bae, J.S. *Quinaldine and Indole based pH sensitive Textile chemosensors.* Dyes and Pigments **2011**. 696-9 p.

22. Peng, Q., Li, M., Gao, K., Cheng, L. *Hydrazone-azo tautomerism of pyridone azo dyes: Part III—effect of dye structure and solvents on the dissociation of pyridone azo dyes*. Dyes and Pigments. **1992** ;18(4):271-86.

23. Feigl, V.A. *Spot Tests in Inorganic Analysis,* John and Willey **1980** :83-108.

24. Gür, M., Kocaokutgen, H., Tas, M. *Synthesis, spectral, and thermal characterisations of some azo-ester derivatives containing a 4-acryloyloxy group.* Dyes and Pigments. **2007** ;72(1):101-8.

25. Al-Hamdani, U.J., Gassim, T.E, Radhy, H.H. *Synthesis and Characterization of Azo Compounds and Study of the Effect of Substituents on Their Liquid Crystalline Behavior. Molecules.* **2010**;15(8):5620.

26. Moanta, A., Ionescu, C., Dragoi, M., Tutunaru, B., Rotaru, P. *A new azo-ester: 4-(phenyldiazenyl)phenyl benzene sulfonate - Spectral, thermal, and electrochemical behavior and its antimicrobial activity* **2015**;1151(2)-61 p.

27. Jain, B.B., Sharma, V.S., Chauhan, H.N., Patel, R.B. *Mesomorphism of azo-esters and chalcone-esters.* Molecular Crystals and Liquid Crystals. 2016;630(1):102-11.

28. Kauffman, G.B. *The discovery of ferrocene, the first sandwich compound*. Journal of Chemical Education. **1983;**60(3):185.

29. Apreutesei, D., Mehl, G.H., Scutaru, D. *Ferrocene- containing liquid crystals bearing a cholesteryl unit*. Liquid Crystals **2007** ;34(7):819-31.

30. Hagadorn, J.R., Arnold, J. *Synthesis, reactivity, and crystal structures of ferrocene-substituted amidinate derivatives.* Journal of Organometallic Chemistry. **2001**;637-639:521-30.

31. Quirante, J., Dubar, F., Gonzalez, A., Lopez, C.Cascante, M., Cortes,R.*Ferrocene-Indole Hybrids for Cancer and Malaria Therapy*.**2011**. 1011-7 p.

32. Astruc, D., Ornelas, C., Ruiz, J. *Metallocenyl Dendrimers and Their Applications in Molecular Electronics, Sensing, and Catalysis*. Accounts of Chemical Research. **2008**;41(7):841-56.

33. Epton, R.M., Rogers, G. K. *The ferrocene analogues of salicylic acid and aspirin. Journal of Organometallic Chemistry*. **1976**;110(2.

34. Rahman, S.A, Gohary, N.S., Bendary, E.R., Ashry, S.M., Shaaban, M.I. *Synthesis, antimicrobial, antiquorum-sensing, antitumor and cytotoxic activities of new series of cyclopenta(hepta)[b]thiophene and fused cyclohepta[b]thiophene analogs*. European Journal of Medicinal Chemistry. **2017**;140:200-11.

35. Zhai, Y. Wang, L., Deng, Z., Abdin, Z., Chen, Y. *Synthesis of ferrocene- and azobenzene-based compounds for anion recognition*. Journal of Zhejiang University-science A. **2016;**17(2):144-54.

36. Bellisola, G., Sorio, C. *Infrared spectroscopy and microscopy in cancer research and diagnosis*. American journal of cancer research. **2012**:2(1).

37. Gandhimathi, R., Vijayaraj, S., Jyothirmaie, M. P. *Analytical Process of Drugs by Ultraviolet (UV) Spectroscopy–A Review*. International Journal of Pharmaceutical Research and Analysis. **2012**:2(1), 72-8.

38. Fernandes, C.D., Johnson, D., Bridges, J. C.,Grady, M. *UV-Vis spectroscopy of stardust*. International Journal of Astrobiology. **2006**:, 5(4), 287-93.).

39. Miao, J., Charalambous, P., Kirz, J., Sayre, D. *Extending the methodology of X-ray crystallography to allow imaging of micrometre-sized non-crystalline specimens*. Nature. **1999**: 342-4.

40. Mlynarik, V. *Introduction to nuclear magnetic resonance.* Analytical Biochemistry. **2017**;529(1):4-9.

41. Gabra, N.M., Bakheit, K., Yata, P. *Synthesis, Characterization, DNA Binding Studies, Photocleavage, Cytotoxicity and Docking Studies of Ruthenium(II) Light Switch Complexes*. Journal of Fluorescence. **2014**;24(1):169-81.

42. Pradeepa, S., Vinay ,K.B., Indira, P. K., Barik, C. *DNA binding, photoactivated DNA cleavage and cytotoxic activity of Cu(II) and Co(II) based Schiff-base azo photosensitizers.* Spectrochimica Acta Part A: Molecular and Biomolecular Spectroscopy. **2015** ;141:34-42.

43. Eshkourfu, C. R., Vujcic,B., Turel,M., Pevec, I., Sepcic,A., Zec,K., Radulovic, M., . *Synthesis, characterization, cytotoxic activity and DNA binding properties of the novel dinuclear cobalt(III) complex with the condensation product of 2-acetylpyridine and malonic acid dihydrazide.* Journal of Inorganic Biochemistry. **2011** ;105(9):1196-203.

44. Zhao, K.Q., Xuh B. 4-Ferrocenylbenzoic acid. Molecules. **2001**;6(12):M246.
45. Nigar, A., Akhte,r Z., Bolte, M., Siddiqi, H.M., Hussain, R. *N-[4-(4-Nitrophenoxy)phenyl]propionamide. Acta Crystallographica Section E.* Journal of Inorganic Biochemistry. **2008**;64(11):2186.
46. Fatiadi, A.J. *Infrared Absorption Spectra of 2-0xo-l,3-bis(phenylhydrazono) Derivatives and Related Bis- and Tris-phenylhydrazones* JOURNAL OF RESEARCH of the National Bureau of Standards - A. Physics and Chemistry; **1967**;51(11):86 .
47. Schmidt, M., Brüning, J., Wirth, D., Bolte, M. *Two azo pigments based on B-naphtho ol* Dyes and Pigments.**2008**; 474-7 p.
48. Seger, B., Vinodgopal, K., Kamat, P.V. *Proton activity in Nafion films: probing exchangeable protons with methylene blue*. Langmuir. **2007**;23(10):5471-6.
49. Zhang, M., Zhao, Q., Zhang, D., Zhang, J.*Novel Y-type two-photon active fluorophore: synthesis and application in fluorescent sensor for cysteine and homocysteine. Tetrahedron letters*. **2007**;48(13):2329-33.
50. Hill, G.A. *Measurement of overall volumetric mass transfer coefficients for carbon dioxide in a well-mixed reactor using a pH probe.* Industrial & engineering chemistry research. **2006**;45(16):5796-800.
51. Galande, A.K., Weissleder, R., Tung,C. *Fluorescence probe with a pH-sensitive trigger. Bioconjugate chemistry*. **2006**;17(2):255-7.
52. Yao, S., Hales, K.J., Belfield, K.D. *A new water-soluble near-neutral ratiometric fluorescent pH indicator*. Organic letters. **2007**;9(26):5645-8.
53. Fang,W., Wang, Z,, Zong, S., Chen, H., Zhong, Y.*pH-controllable drug carrier with SERS activity for targeting cancer cells.* Biosensors and Bioelectronics. **2014**;57:10-5.
54. Xie, K. Gao, M. *Highly water-soluble and pH-sensitive colorimetric sensors based on a D–π–A heterocyclic azo chromosphere.* Sensors and Actuators B: Chemical. **2014** ;204:167-74.
55. ElDeen, I.M., Shoair, A.F., Bindary, M.A. *Synthesis, structural characterization, molecular docking and DNA binding studies of copper complexes*. Journal of Molecular Liquids. **2018**;249:533-45.

56. Merino, E., Ribagorda, M. *Control over molecular motion using the cis–trans photoisomerization of the azo group*. Beilstein Journal of Organic Chemistry. **2012**;8:1071-90.

57. Zhang, N., Yang, Z., Tao, Z. *Redox active and inactive binuclear cobalt(II) and zinc(II) complexes with N_6O/N_3O coordinating ligands: synthesis, biological activities and cytotoxicity*. Applied Organometallic Chemistry. **2017**;31(1):3548.

58. Zhang, S., Sun, Y., Jiang, X. *Interaction of DNA with Bis(diiminosuccinonitrilo)platinum(II).* Chinese Journal of Chemistry. **2008**;26(3):463-6.

59. Janjua, N.K., Shaheen, A., Yaqub, A., Perveen, F., Sabahat, S., Mumtaz, M. *Flavonoid–DNA binding studies and thermodynamic parameters*. Spectrochimica Acta Part A: Molecular and Biomolecular Spectroscopy. **2011;**79(5):1600-4.

60. Jamil, M., Altaf, A.A, Badshah, A., Ahmad, I., Zubair, M.. *Naked Eye DNA detection: Synthesis, characterization and DNA binding studies of a novel azo-guanidine.* Spectrochimica Acta Part A: Molecular and Biomolecular Spectroscopy. **2013**;105:165-70.

61. Nafisi, S. Saboury, A.A., Keramat, N., Neault, F., Riahi, A. *Stability and structural features of DNA intercalation with ethidium bromide, acridine orange and methylene blue. Journal of Molecular Structure.* **2007**;827(1):35-43.

62. Bindary, A.A., Hassan, N., Afify, M.A. *Synthesis and structural characterization of some divalent metal complexes: DNA binding and antitumor activity*. Journal of Molecular Liquids. **2017**;242:213-28.

63. Iyer, P., Srinivasan, A., Singh, S.K., Mascara, G.P, Zayitova, S., Sidone, B. Synthesis and *Characterization of DNA Minor Groove Binding Alkylating Agents.* . 2013;26(1):156-68.

64. Rayzah, T., Diego, V., Ricardo S.. *Phytochemical Screening and comparison of DPPH radical scavenging from different samples of coffee and Yerba Mate beverages*. International Journal of Scientific and Research Publication. **2014**; ;64(11):2186.

65. Bartosz, G. *Determination of antiradical and antioxidant activity: basic principles and new insights*. Beilstein Journal of Organic Chemistry **2010**;139-42.

66. Mohammadi, A., Ghafoori, H., Rassa, M., Safarnejad, M. *Aryl azo 5-arylidene-2,4-thiazolidinone dyes as novel antioxidant and antibacterial compounds* Chemical Research in Toxicology **2015**;52(10):2156.

67. Sroka, Z., Cisowski, W. *Hydrogen peroxide scavenging, antioxidant and anti-radical activity of some phenolic acids.* Food and Chemical Toxicology. **2003**;41(6):753-8.

APPENDIX I

FT-IR spectrum of a representative Azo Alcohol

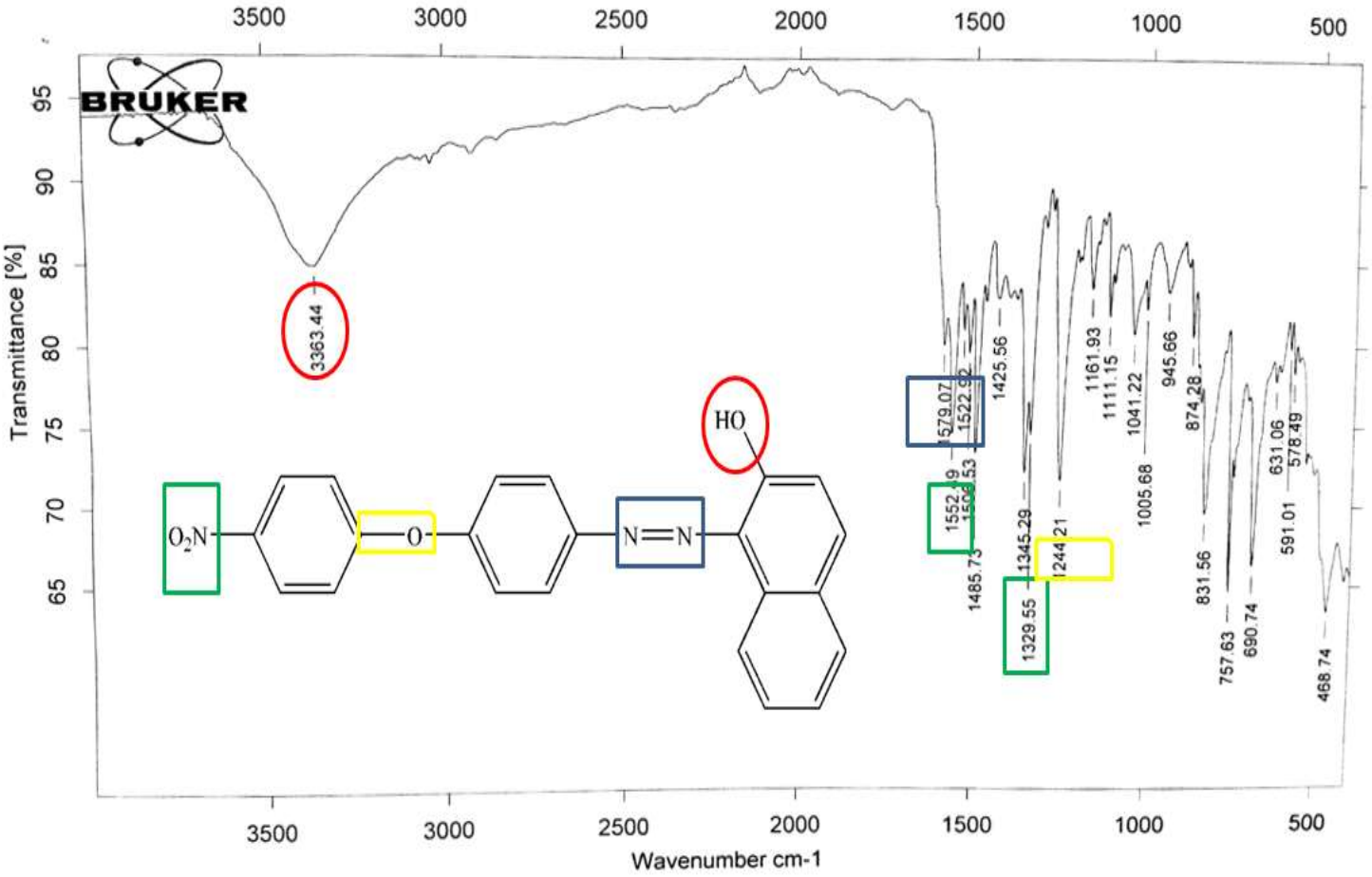

APPENDIX II

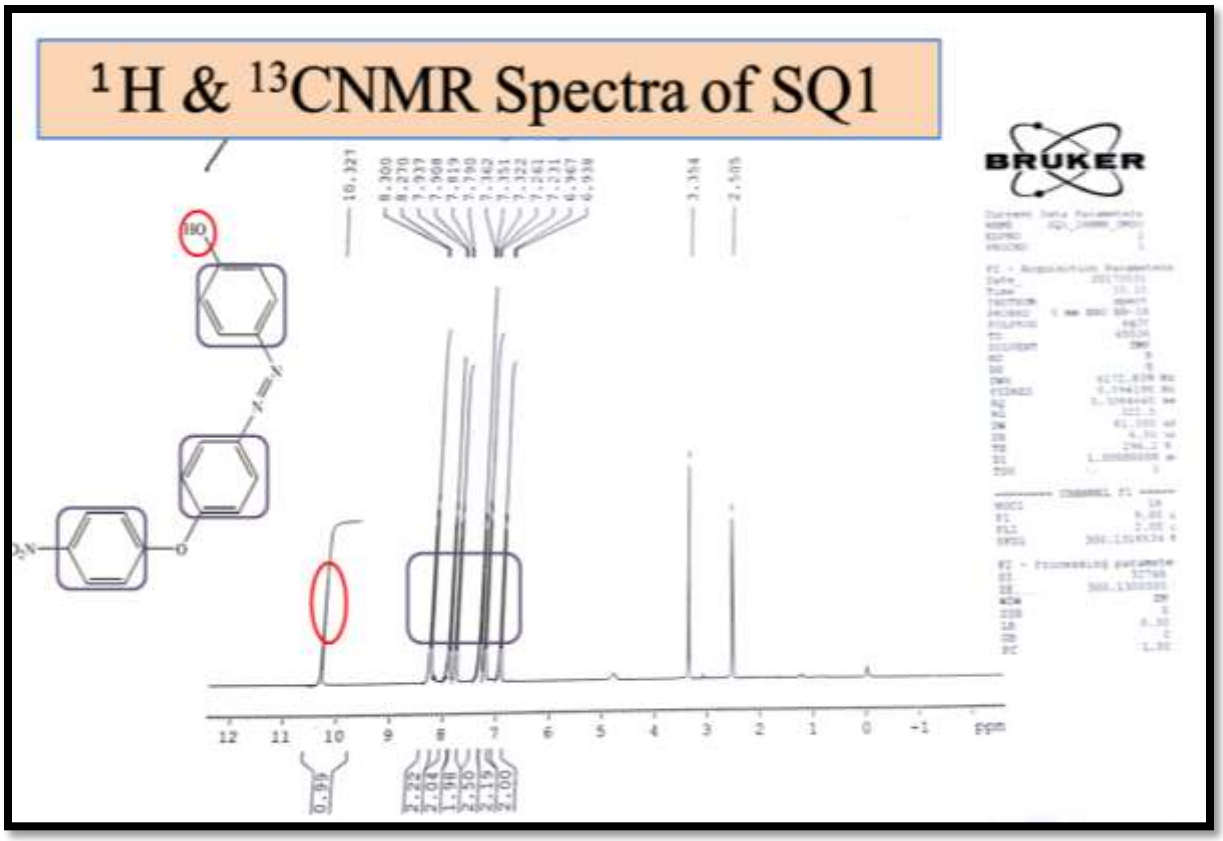
1H & 13CNMR Spectra of SQ1
BRUKER

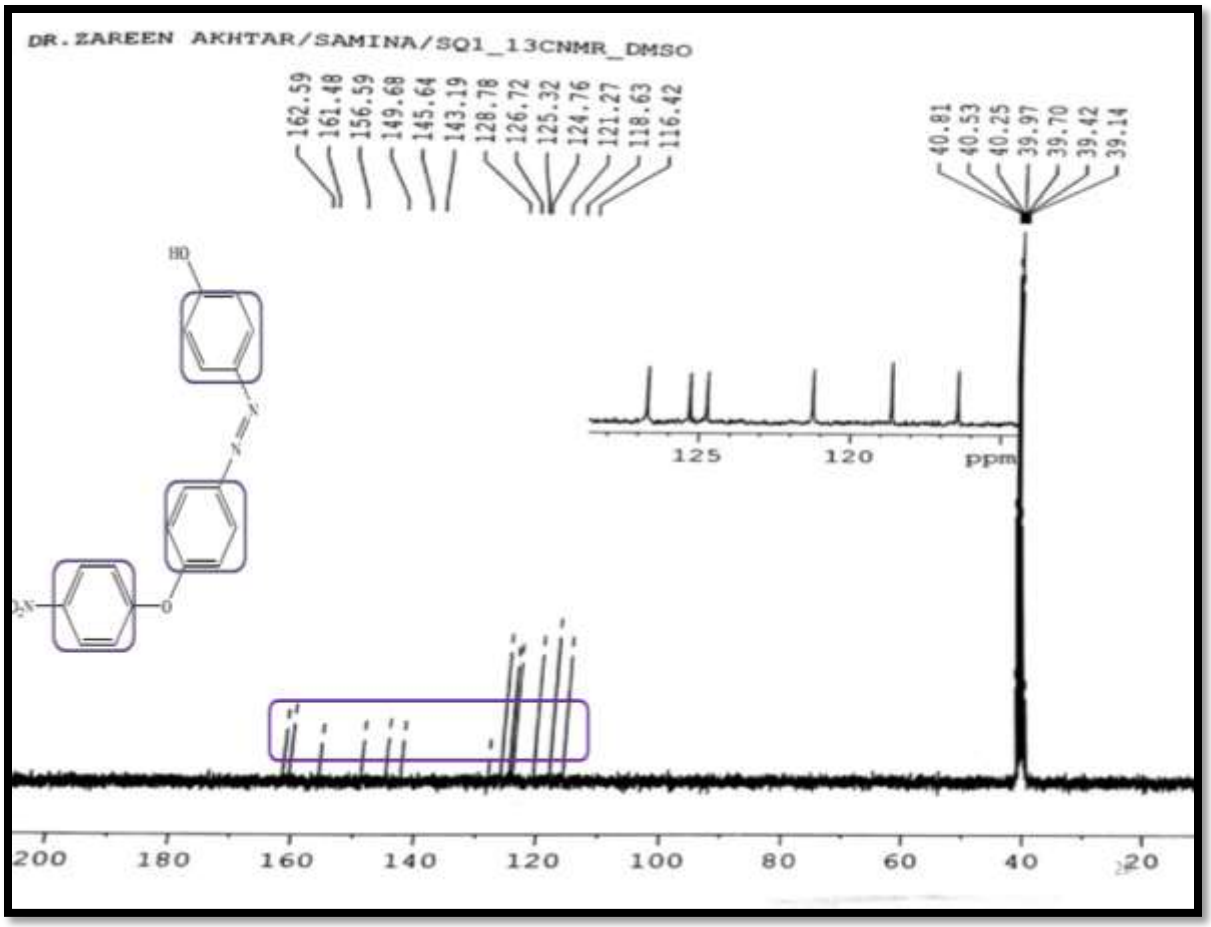
DR.ZAREEN AKHTAR/SAMINA/SQ1_13CNMR_DMSO
162.59
161.48
156.59
149.68
145.64
143.19
128.78
126.72
125.32
124.76
121.27
118.63
116.42
40.81
40.53
40.25
39.97
39.70
39.42
39.14
125
120
ppm

^{1}H & ^{13}C NMR Spectra of SQ5

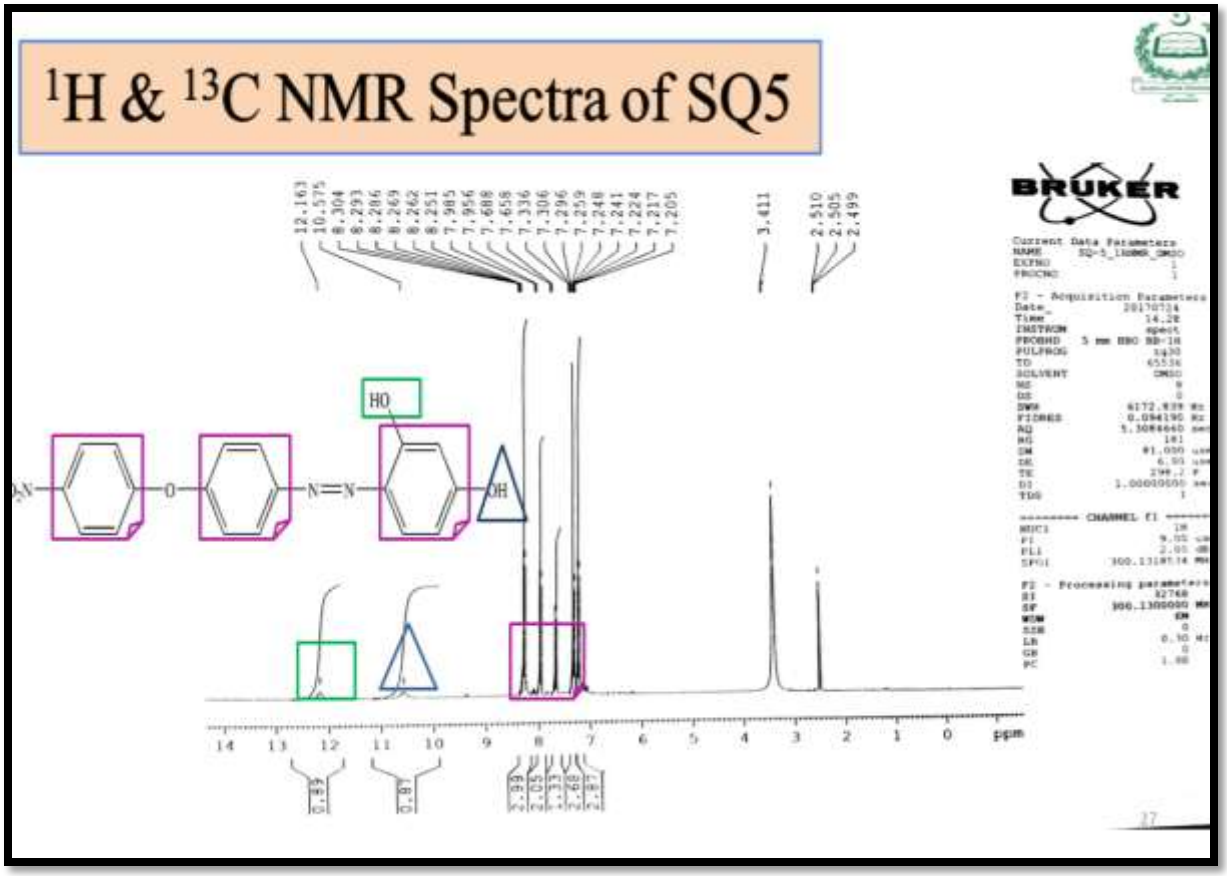

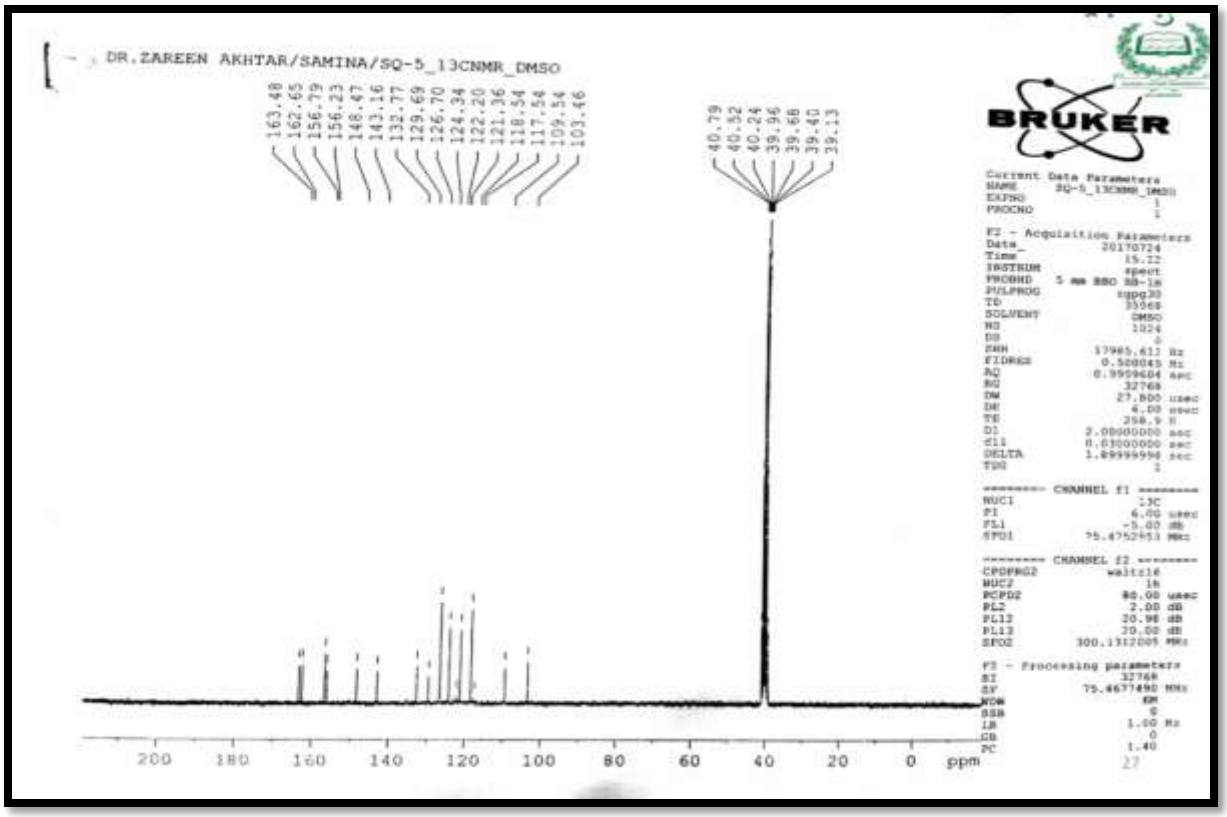

^{1}H & ^{13}C-NMR Spectrum of SQ1B

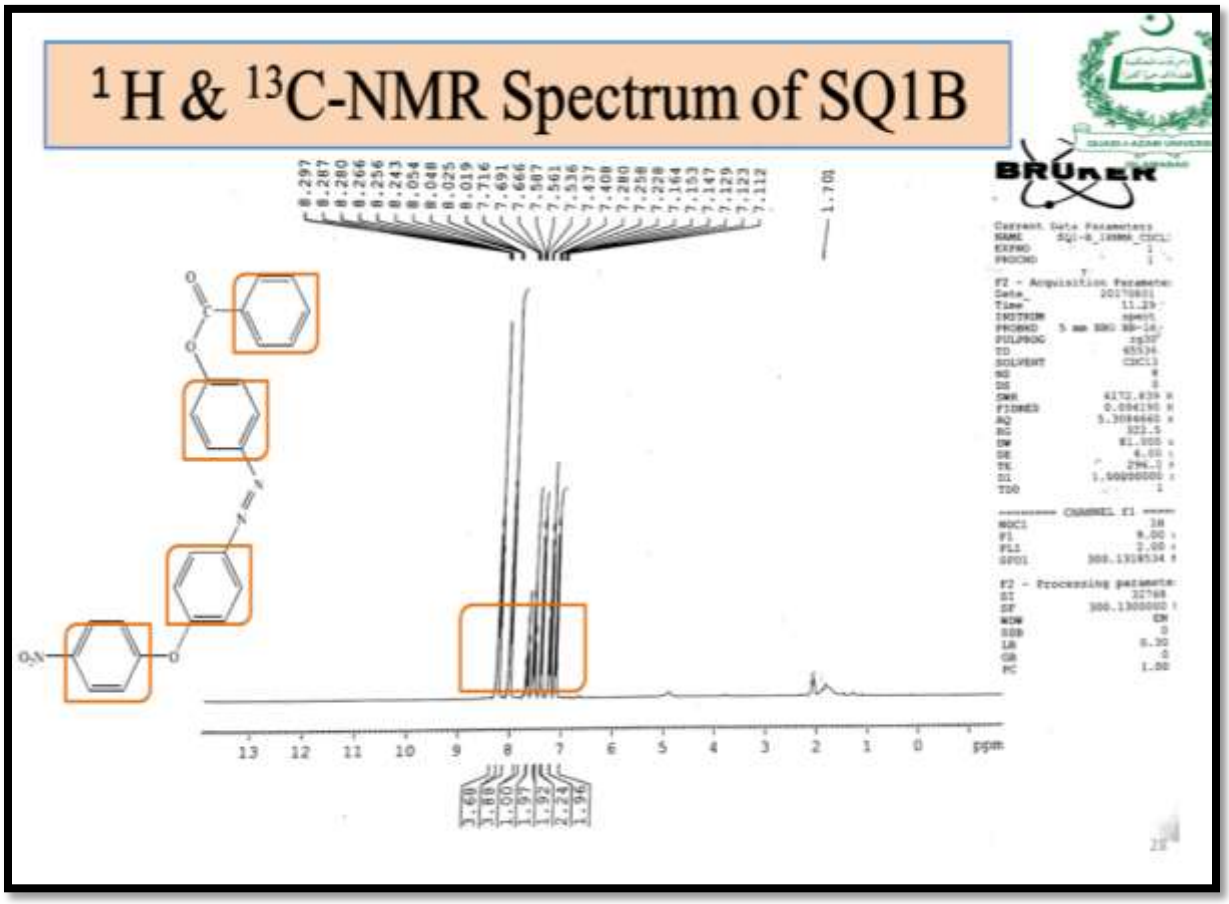

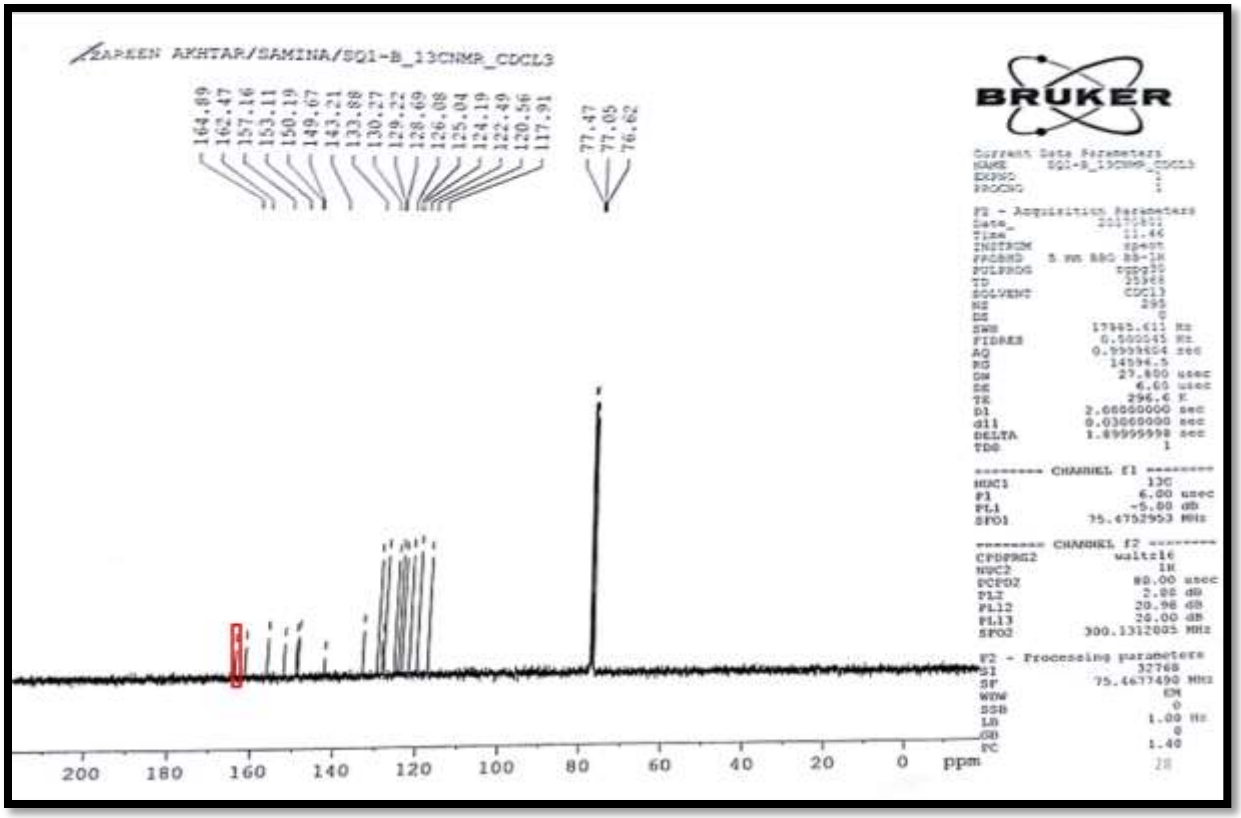

^{1}H & ^{13}C NMR Spectrum of SQ4B

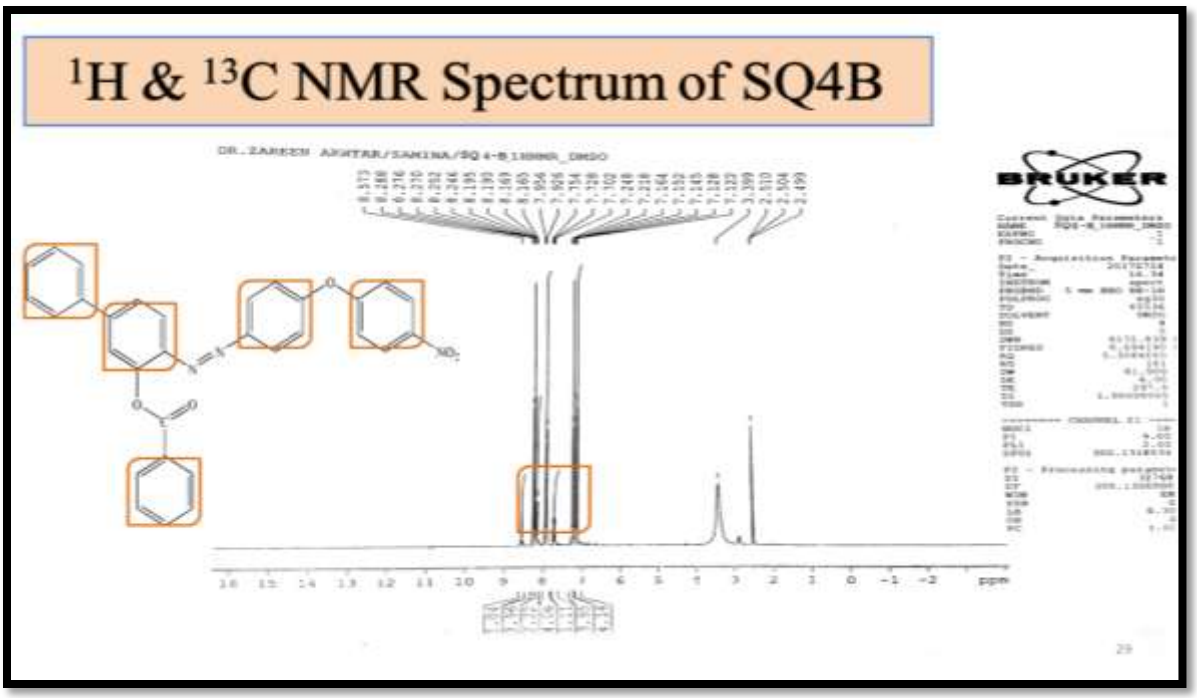

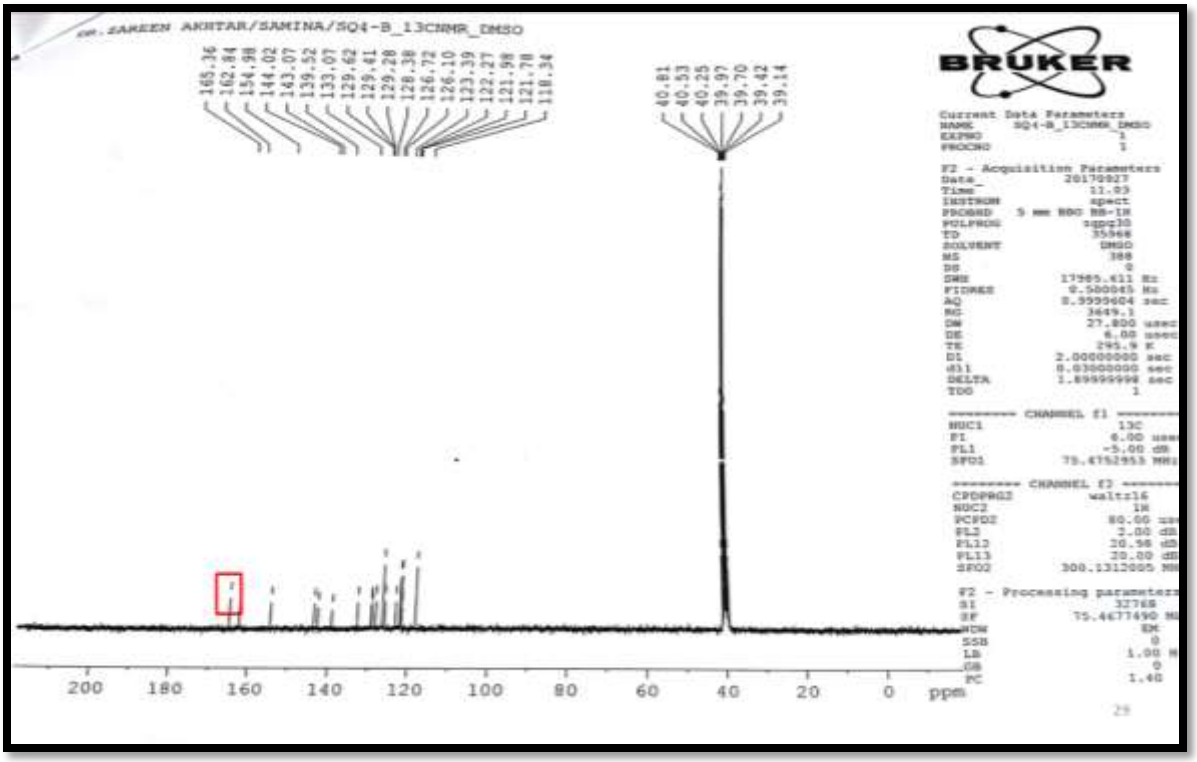

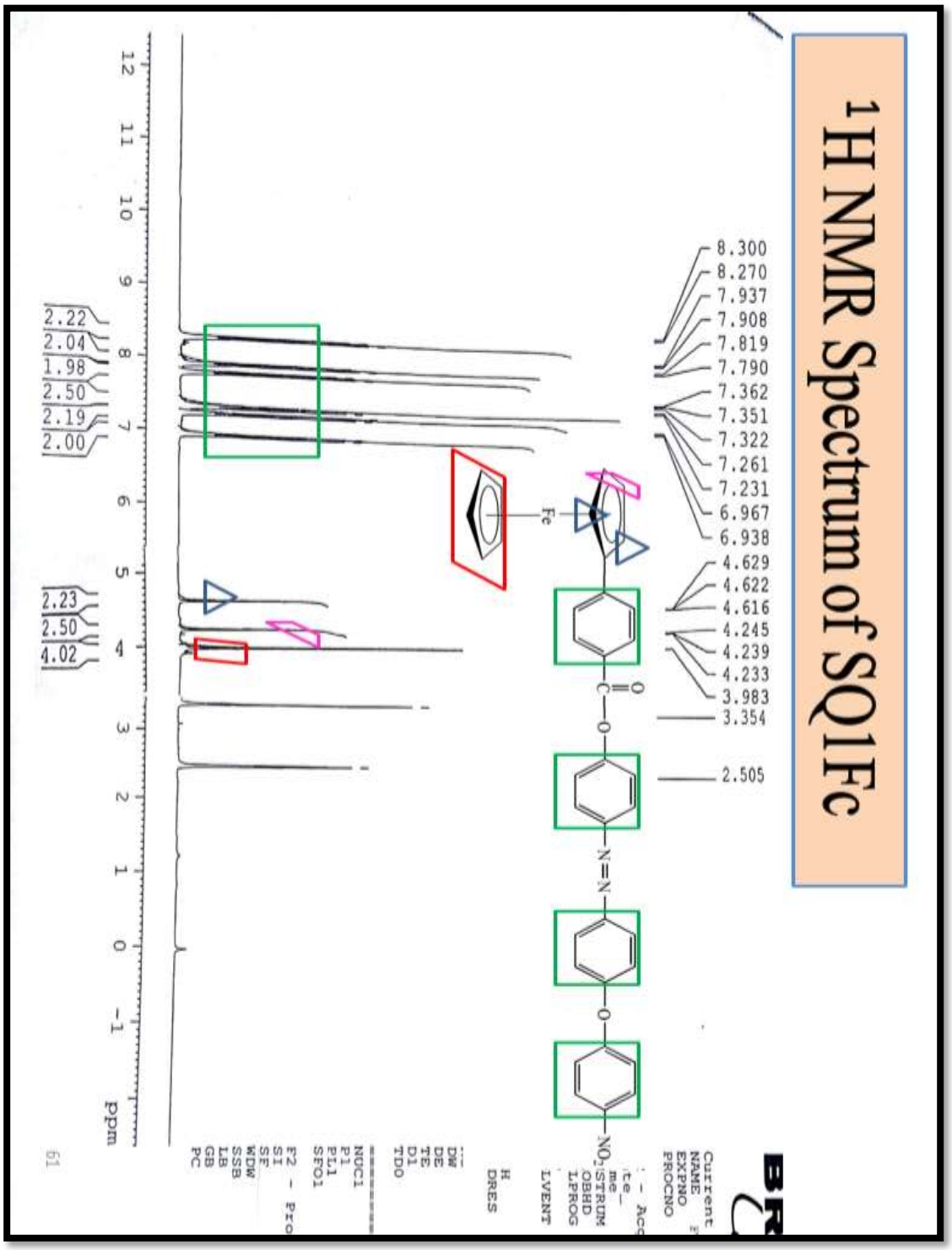
1H NMR Spectrum of SQ1Fc
8.300
8.270
7.937
7.908
7.819
7.790
7.362
7.351
7.322
7.261
7.231
6.967
6.938
4.629
4.622
4.616
4.245
4.239
4.233
3.983
3.354
2.505
2.22
2.04
1.98
2.50
2.19
2.00
2.23
2.50
4.02
Fe
N=N
O
C
ppm